Aus dem Institut für Veterinär-Anatomie
des Fachbereichs Veterinärmedizin
der Freien Universität Berlin
und
dem Robert Koch Institut Berlin

Establishment and application of CRISPR/Cas Technology in Non-Tuberculous Mycobacteria (NTM)

Inaugural-Dissertation
zur Erlangung des Grades einer
Doktorin der Veterinärmedizin
an der
Freien Universität Berlin

vorgelegt von
Suriya Akter
Tierärztin aus Dhaka, Bangladesch

Berlin 2024
Journal-Nr.: 4425

mbvberlin | mensch und buch verlag

Aus dem Institut für Veterinär-Anatomie
des Fachbereichs Veterinärmedizin
der Freien Universität Berlin
und
dem Robert Koch Institut Berlin

Establishment and application of CRISPR/Cas Technology in Non-Tuberculous Mycobacteria (NTM)

Inaugural-Dissertation
zur Erlangung des Grades
einer Doktorin der Veterinärmedizin
an der
Freien Universität Berlin

vorgelegt von
Suriya Akter
Tierärztin aus Dhaka, Bangladesch

Berlin 2024
Journal-Nr.: 4425

Gedruckt mit Genehmigung des Fachbereichs Veterinärmedizin
der Freien Universität Berlin

Dekan:	Herrn Univ.-Prof. Dr. Uwe Rösler
Erster Gutachter:	Prof. Dr. Lothar H. Wieler
Zweiter Gutachter:	PD Dr. Soroush Sharbati
Dritter Gutachter:	Univ.-Prof. Dr. Thomas Alter

Deskriptoren (nach CAB-Thesaurus):
mycobacterium, molecular biology, CRISPR-Cas9, molecular genetics techniques, genome editing

Tag der Promotion: 12.01.2024

Bibliografische Information der *Deutschen Nationalbibliothek*
Die Deutsche Nationalbibliothek verzeichnet diese Publikation in der Deutschen Nationalbibliografie; detaillierte bibliografische Daten sind im Internet über <http://dnb.ddb.de> abrufbar.

ISBN: 978-3-96729-237-4
Zugl.: Berlin, Freie Univ., Diss., 2024
Dissertation, Freie Universität Berlin
D188

Dieses Werk ist urheberrechtlich geschützt.
Alle Rechte, auch die der Übersetzung, des Nachdruckes und der Vervielfältigung des Buches, oder Teilen daraus, vorbehalten. Kein Teil des Werkes darf ohne schriftliche Genehmigung des Verlages in irgendeiner Form reproduziert oder unter Verwendung elektronischer Systeme verarbeitet, vervielfältigt oder verbreitet werden.

Die Wiedergabe von Gebrauchsnamen, Warenbezeichnungen, usw. in diesem Werk berechtigt auch ohne besondere Kennzeichnung nicht zu der Annahme, dass solche Namen im Sinne der Warenzeichen- und Markenschutz-Gesetzgebung als frei zu betrachten wären und daher von jedermann benutzt werden dürfen.

This document is protected by copyright law.
No part of this document may be reproduced in any form by any means without prior written authorization of the publisher.

alle Rechte vorbehalten | all rights reserved
© Mensch und Buch Verlag 2024
Choriner Str. 85 - 10119 Berlin
verlag@menschundbuch.de – www.menschundbuch.de

Table of Contents

1 Introduction 1

2 Literature Review 3

2.1 Mycobacterial cell wall 4

2.2 The Mycobacterium genus 5

2.3 The *Mycobacterium tuberculosis* complex (MTBC) 6

2.4 Nontuberculous mycobacteria (NTM) 7

2.5 *Mycobacterium avium* subsp. *hominissuis* (MAH) 8

2.6 *Mycobacterium abscessus* (MABS) 8

2.7 Genome editing methods 9

2.8 CRISPR/Cas9 10

2.8.1 Natural immune system in bacteria 10

2.8.2 CRISPR Type II System 12

2.8.3 CRISPR/Cas9 orthologs for gene editing 14

2.8.4 CRISPR/Cas9 editing in Mycobacteria 15

2.9 CRISPR/Cas9 editing in MABS 17

2.9.1 *mps1* gene 17

2.9.2 Other four endogenous genes (*porin*, *ppiA*, *erm-41*, and *whiB7*) in MABS 18

3 Materials and Method 23

3.1 Bacterial Strains, plasmids, and growth conditions 23

3.2 Generation of reporter NTM strains for CRISPRi /dCas9 28

3.2.1 Vectors pLJR962 and pLJR9765 29

3.2.2 Design of CRISPR-sites in *eGFP* gene and cloning for vector construction 30

3.2.3 Measurement of the fluorescence of strains with down-regulation of *eGFP* gene by flow cytometry 33

3.3 Generation of nuclease active CRISPR/Cas9 system 33

3.4 Cloning of sgRNA sequences into pSAK14 for gene mutation 34

3.5 Molecular Biological Methods 34
3.5.1 Preparation of competent *E. coli* and transformation 34
3.5.2 Plasmid isolation 35
3.5.3 Preparation of electrocompetent MAH cells and electroporation 35
3.5.4 Preparation of electrocompetent MABS and Msmeg and electroporation 36
3.5.5 Genomic DNA preparation from Mycobacteria 36
3.5.6 Polymerase chain reaction (PCR) 37
3.5.7 Quantitative real-time PCR 38
3.5.8 Agarose gel electrophoresis and product purification 39
3.6 Sanger sequencing 40
3.6.1 Whole-genome sequencing (WGS) and genome analysis 41
3.7 Glycopeptidolipid (GPL) extraction and TLC analysis 41
3.8 Methods for quantification of mycobacteria in broth culture 42
3.8.1 OD600 measurement 42
3.9 Measurement of relative light units depending on ATP amount 42
3.10 Antibiotic susceptibility testing by sensititre 43
3.11 Screening for MABS virulence-mutants 43
3.11.1 The growth rate in broth cultures under pH stress 43
3.12 H_2O_2 and NO Stress resistance tests 43
3.12.1 Induction of cytokine expression in THP-1 cells 44
3.12.2 Infection of THP-1 cell lines and intracellular growth measurement 44
3.13 Bioinformatic tools and analysis 45
3.14 Computer software and programs used 45
3.15 Statistical Analysis 46

4 Results 47
4.1 Generation of reporter NTM strains 47
4.2 Gene silencing with CRISPRi in reporter NTM 47
4.2.1 *eGFP* gene silencing by CRISPRi/dCas9 in reporter *M. smegmatis* 48
4.2.2 *eGFP* gene silencing by CRISPRi/dCas9 in reporter *Mycobacterium avium hominissuis* 50
4.2.3 *eGFP* gene silencing by CRISPRi/dCas9 in reporter *M. abscessus* 53

4.3 Generation of CRISPR plasmid pSAK14 ... 56
4.3.1 Generation of plasmid pSAK12 for *eGFP* gene knockout ... 56
4.4 CRISPR-mediated knock-out mutagenesis in reporter in NTM ... 56
4.4.1 CRISPR-mediated gene knock-out in *M. smegmatis* ... 56
4.4.2 CRISPR- gene knock-out in *Mycobacterium avium* subsp. *hominissuis* ... 58
4.4.3 CRISPR-mediated gene knock-out in *M. abscessus* ... 59
4.5 Testing the performance and specificity of the CRISPR knock-out system with an endogenous gene from *M. abscessus* ... 60
4.5.1 Analysis of the off-target activity of CRISPR in *M. abscessus* ... 62
4.5.2 Phenotypic Characterization of *M. abscessus mps1* gene mutants ... 63
4.6 The knockout of additional four endogenous genes (*porin*, *ppiA*, *erm-41*, and *whiB7*) in *M. abscessus* by CRISPR/Cas9 ... 65
4.6.1 Knockout of the *porin* gene (Mab_1080) in isolate MABS 40/14-3 ... 66
4.6.2 CRISPR/Cas9-mediated knockout of the *ppiA* gene in MABS 40/14-3 strain ... 68
4.6.3 CRISPR/Cas9-mediated knockout of the *erm-41* and *whiB7* genes in MABS 40/14-3 strain ... 69
4.7 Phenotypic characterisation of selected *porin* and *ppiA* gene mutants ... 69
4.7.1 Investigating pH resistance through porin KO and PpiA KO *M. abscessus* ... 70
4.7.2 Effect of H_2O_2 on the growth and viability of Porin KO and PpiA KO in *M. abscessus* ... 72
4.7.3 Effect of DETA/NO on the growth and viability of Porin KO and PpiA KO mutants in *M. abscessus* ... 73
4.7.4 Antibiotic Sensitivity test of Porin KO and PpiA KO mutants in *M. abscessus* using Sensititre™ ... 74
4.7.5 Cytokine responses of THP-1 cell line infected with Porin KO and PpiA KO mutants in *M. abscessus* ... 75
4.7.6 Intracellular survival in THP-1 cell line of Porin KO and PpiA KO mutants in *M. abscessus* ... 76

5 Discussion and Outlook ... 79
5.1 Discussion ... 79
5.2 Outlook ... 87

6 Zusammenfassung ... 89

7 Summary ... 90

8 References ... 91

9 Annex 99

9.1 List of publication 99

9.1.1 Scientific articles 99

9.1.2 Poster presentations at conferences 99

9.1.3 Scientific presentations at conferences 99

9.2 Acknowledgment 100

9.3 Sources of funding-Funding Sources 102

9.4 Conflicts of Interest 102

10 Declaration of Independence 103

List of Figures

Figure 1 The cell wall of mycobacteria

Figure 2 An overview of the classification of human pathogenic Mycobacteria. 6

Figure 3 A cluster of genes is responsible for the synthesis and transport of the GPL. 9

Figure 4 A prokaryotic cell's CRISPR system..11

Figure 5 Model of the CRISPR Cas defensive mechanism in prokaryotic cells...........12

Figure 6 Diagram of the CRISPR/Cas9 system's components. 13

Figure 7 Map of plasmid pMN437. 28

Figure 8 pLJR965 is the M. tuberculosis-optimized and pLJR962 is the *M. smegmatis* -optimized CRISPRi backbone. 29

Figure 9 The dCas9Sth1 PAM variants are shown. 30

Figure 10 *eGFP* gene in the plasmid pMN437 is the target of a single guide RNA template. 31

Figure 11 Down-regulation of *eGFP* expression in *M. smegmatis* mc^{2}155 broth cultures. 48

Figure 12 Expression of the *eGFP* gene in reporter *M. smegmatis* broth cultures with induction by ATc. 49

Figure 13 Down-regulation of *eGFP* expression in *Mycobacterium avium* subsp. *hominissuis* broth cultures. 51

Figure 14 Expression of the eGFP gene in reporter *Mycobacterium avium* subsp. *hominissuis* broth cultures with induction by ATc. 52

Figure 15 Down-regulation of *eGFP* expression in *M. abscessus* broth cultures. 54

Figure 16 Expression of the eGFP gene in reporter *M. abscessus* broth cultures with induction by ATc. 55

Figure 17 Site-directed mutagenesis was validated by PCR and sanger sequencing. 56

Figure 18 Sanger sequencing of mutations of *eGFP* mutants in *M. smegmatis* (pMN437) (pSAK12). 57

Figure 19 Sanger sequencing of mutations of *eGFP* mutants in *Mycobacterium avium* subsp. *hominissuis* (pMN437) (pSAK12). 59

Figure 20 Target region of *mps1* for knockout by CRISPR/Cas9. 60

FIGURE 21 CHANGE OF MORPHOLOGY BY *MPS1* MUTATION. 63

FIGURE 22 GPL EXPRESSION OF *M. ABSCESSUS* STRAINS. 64

FIGURE 23 RESISTANCE TOWARDS LOW PH OF MUTANT MABS 40/14-3 (PLH1) PORIN KO AS COMPARED TO CONTROL MABS 40/14-3 (PSAK14). 70

FIGURE 24 RESISTANCE TOWARDS LOW PH OF MUTANT MABS 40/14-3 (PSAK43) PPIA KO AS COMPARED TO CONTROL MABS 40/14-3 (PSAK14) 71

FIGURE 25 EFFECT OF H_2O_2 STRESS ON SURVIVAL OF THE *M. ABSCESSUS* STRAINS. 72

FIGURE 26 EFFECT OF NO STRESS ON SURVIVAL OF THE *M. ABSCESSUS* STRAINS....................73

FIGURE 27 INDUCTION OF CYTOKINE SECRETION BY THP1 MACROPHAGE AFTER INFECTION WITH THE PORIN KO MABS STRAIN AND THE CONTROL *M. ABSCESSUS* STRAIN. 75

FIGURE 28 INDUCTION OF CYTOKINE SECRETION BY THP1 MACROPHAGE AFTER INFECTION WITH THE PPIA KO *M. ABSCESSUS* STRAINS...76

FIGURE 29 INTRACELLULAR SURVIVAL OF *M. ABSCESSUS* MUTANTS COMPARED TO WILD-TYPE IN THP-1 CELL LINE. 77

List of Tables

TABLE 1 LISTS THE VARIOUS CAS PROTEIN SUBTYPES AND THE CORRESPONDING PAM SEQUENCES.(TABLE MODIFIED FROM (HTTP://CRISPOR.TEFOR.NET/). 15

TABLE 2 LIST OF STRAINS 23

TABLE 3 LIST OF THE PLASMIDS USED IN THIS STUDY 24

TABLE 4 A LIST OF THE OLIGONUCLEOTIDES USED IN THIS STUDY AND THE PAM-SEQUENCE OF THE TARGET GENES 26

TABLE 5 PRIMER PAIRS FOR PCR AND SANGER SEQUENCING USED IN THIS STUDY 27

TABLE 6 THE CONSTRUCTED PLASMIDS PSAK6, PSAK7, PSAK8, PSAK9. 32

TABLE 7 COMPONENTS OF A CONVENTIONAL PCR (THERMOFISHER SCIENTIFIC). 37

TABLE 8 CYCLER PROGRAM OF A CONVENTIONAL PCR. 38

TABLE 9 COMPONENTS OF A QUANTITATIVE REAL-TIME POLYMERASE CHAIN REACTION 38

TABLE 10 CYCLER PROGRAM OF A QUANTITATIVE REAL TIME POLYMERASE CHAIN REACTION 39

TABLE 11 SANGER SEQUENCING REACTION PROTOCOL USING BIGDYE^{TM} KIT. 40

TABLE 12 BIGDYE^{TM} SEQUENCING REACTION CYCLER CONDITIONS 40

TABLE 13 DNA QUANTITY IN SEQUENCING REACTIONS ACCORDING TO DNA SAMPLE 41

TABLE 14 LIST OF SOFTWARE USED IN THIS STUDY. 46

TABLE 15 NAME OF REPORTER STRAINS 47

TABLE 16 MUTATION RATE OF THE *EGFP* GENE IN *M. SMEGMATIS* (PMN437) (PSAK12) 57

TABLE 17 MUTATION RATE OF THE *EGFP* GENE IN *MYCOBACTERIUM AVIUM* SUBSP. *HOMINISSUIS* (PMN437) (PSAK12) 58

TABLE 18 TOTAL NUMBER OF ROUGH COLONIES AFTER ELECTROPORATION WITH PSAK33 61

TABLE 19 CRISPR/CAS9-MEDIATED KNOCKOUT OF *MPS1* GENE (MAB_4099C) IN MABS 09/13-3 61

TABLE 20 SPECIFICITY OF KNOCKOUT MUTAGENESIS OF *MPS1* GENE 62

TABLE 21 LIST OF *M. ABSCESSUS* STRAINS USED FOR PHENOTYPIC CHARACTERIZATION 63

TABLE 22 ANTIBIOTIC SUSCEPTIBILITY OF THE MABS 09/13-3 STRAINS CONTROL MABS 09/13-3 (PSAK14), AND *MPS1* MUTANT MABS 09/13-3 (PSAK33) MPS1 KO. THREE TESTS WERE CONDUCTED, AND THIS ONE PROVIDED A REPRESENTATIVE OUTCOME 65

TABLE 23 ADDITIONAL FOUR ENDOGENOUS GENES IN *M. ABSCESSUS* SELECTED FOR APPLICATION OF THE CRISPR/CAS9 METHOD 66

TABLE 24 CRISPR/CAS9-MEDIATED KNOCKOUT OF *PORIN* GENE IN MABS 40/14-3 STRAIN....... 67

TABLE 25 TYPE OF MUTATION IS LISTED AS FOLLOWS: TYPE OF MUTATION (DELETION OR INSERTION), SITE OF MUTATION.. 68

TABLE 26 TYPE OF MUTATION IN MABS 40/14-3 STRAIN.. 69

TABLE 27 THE STRAINS USED FOR PHENOTYPIC CHARACTERIZATION IN *M. ABSCESSUS* 70

TABLE 28 SENSITITRE^{TM} RESULTS OF MABS 40/14-3 (PSAK14) (CONTROL) WITH MUTATED MABS 40/14-3 (PLH1) PORIN KO AND MABS 40/14-3 (PSAK43) PPIA KO AFTER 5 DAYS OF INCUBATION FROM TWO INDEPENDENT EXPERIMENTS................................ 74

List of Abbreviations

°C	degree Celsius
A	Adenine
AA	Amino acid
ABC	ATP-binding-cassette
AIDS	Acquired immune deficiency syndrome
ATc	Anhydrotetracycline
ATP	Adenosine triphosphate
bp	Base pairs
C	Cytosine
CF	Cystic fibrosis
CFTR	Cystic fibrosis conductance regulator
CFU	Colony forming units
CRISPR	Clustered regularly interspaced short palindromic repeats
crRNA	CRISPR ribonucleic acid
dCas9	Dead Cas9 (nuclease-inactive CRISPR-associated endonuclease)
DEPC H2O	Diethylpyrocarbonate-treated water
DETA/NO	Diethylenetriamine/nitric oxide adduct
DNA	Desoxyribonucleic acid
dNTP	Deoxyribonucleotide triphosphate
DSB	Double strand break
E. coli	*Escherichia coli*
ECM	Extracellular matrix
ELISA	Enzyme-linked immunosorbent assay
EtOH	Ethanol

G	Guanine
GPL	Glycopeptidolipids
HygR	Hygromycin resistance
Indel	Insertion/deletion
KanR	Kanamycin resistance
kb	Kilobase
M. abscessus / MABS	*Mycobacterium abscessus*
mADC	Modified albumin dextrose catalase supplement
MAH	*Mycobacterium avium* subsp. *homissuis*
MB	Middlebrook (growth medium)
MH	Mueller-Hinton II (growth medium)
MIC	Minimum inhibitory concentration
MOI	Multiplicity of infection
Msmeg	*Mycobacterium smegmatis*
MTB	*Mycobacterium tuberculosis*
MTBC	*Mycobacterium tuberculosis* Complex
NTM	Nontuberculous mycobacteria
OADC	Oleic acid albumin dextrose
OD	Optical density
PAM	Protospacer adjacent motif
PBS	Phosphate buffered saline
PMA	Phorbol-12-myristat-13-acetate
PCR	Polymerase chain reaction
qPCR	Quantitative real-time polymerase chain reaction
RE	Restriction enzyme
RGM	Rapidly growing mycobacteria
RLU	Relative light unit
RT	Room temperature

SDS	Sodium dodecyl sulfate
SGM	Slowly growing mycobacteria
sgRNA	Single guide ribonucleic acid
SNV	Small nucleotide variant
SOC	Super Optimal broth with Catabolite repression
T	Thymine
Ta	annealing temperature
TAE	TRIS-acetat-EDTA
TB	tuberculosis
TE	TRIS-EDTA
TetR	Tet repressor
TLC	Thin-layer chromatography
tracrRNA	transactivating CRISPR ribonucleic acid
U	Unit
WHO	World Health Organization
µ	Micro

1 Introduction

Non-tuberculous mycobacteria (NTM) are a wide range of microorganisms that can infect people and lead to disseminated infections, skin infections, and persistent lung infections, especially in those with impaired immune systems. The treatment of NTM infections is challenging due to their intrinsic resistance to antibiotics and the absence of effective treatments. The rate of patients being successfully cured of infections caused by *Mycobacterium abscessus* (MABS) is still only around 30 % (Degiacomi *et al.* 2019). Hence, there is an urgent need to develop new and improve currently available treatment strategies (Quang and Jang 2021). For this, it is fundamental to understand the underlying molecular mechanisms of virulence and resistance. By determining the role of genes in mechanisms contributing to pathogenicity, new targets for therapeutic approaches can be discovered. In general, to determine the role of genes in phenotypic properties, it is necessary to test and validate methods for gene knockdown or knockout. Therefore, there is an urgent need to develop new tools and strategies for genetic modification of NTM.

The powerful genetic tools CRISPRi and CRISPR/Cas9 have caused a revolution in the area of molecular biology in recent years. CRISPRi is a gene silencing technology that uses a deactivated Cas9 (dCas9) protein to repress gene expression, while CRISPR/Cas9 is a genome editing technology that uses a Cas9 protein guided by a single guide RNA (sgRNA) to introduce precise stable changes in the genome. These tools have been successfully applied to many bacterial species, including *Mycobacterium tuberculosis* (MTB) and *Mycobacterium smegmatis* (Msmeg).

The aim of this research project is to establish and optimize CRISPRi and CRISPR/Cas9 technology in NTM *Mycobacterium avium hominissuis* (MAH) and *Mycobacterium abscessus* (MABS) and to apply these tools for the study of gene function. The system should further be modified to perform loss-of-function studies in MABS. Proof of functionality of the knock-out system was to be obtained by mutating interesting genes and investigating the effects on certain virulence properties.

Research question: Can CRISPRi and CRISPR/Cas9 technology in Non-Tuberculous Mycobacteria (NTM) improve understanding of their pathogenicity and potential for developing new therapies?

Hypothesis: The establishment of CRISPRi and CRISPR/Cas9 technology in Non-Tuberculous Mycobacteria (NTM) will allow for efficient gene knockdown and knockout, leading to an improved understanding of the role of specific genes in NTM pathogenicity and virulence. This will make it easier to find possible targets for the creation of new treatments for NTM infections.

Aim: The aim of this thesis is to establish and apply CRISPRi and CRISPR/Cas technology in NTM, with a particular focus on *M. abscessus* (MABS). Specifically, this thesis has the objectives:

1. To establish CRISPRi technology in clinically relevant NTM species, including MAH and MABS
2. To generate a knockout system by CRISPR/Cas9
3. To evaluate the knockout system by CRISPR/Cas9 and testing the specificity by an endogenous gene
4. To apply CRISPR/Cas9 system for several genes in MABS to investigate the role of pathogenicity and virulence

2 Literature Review

Other *Mycobacterium* species except *M. leprae* and *M. tuberculosis complex* (MTBC) are known as Non-tuberculous mycobacteria (NTM) (Porvaznik et al., 2017). NTMs include animal and human opportunistic pathogens found in the environment (Yu et al., 2014). Many NTMs cause pulmonary disease, usually manifesting as underlying structural airway disease such as bronchiectasis and chronic lung disease (Daley et al., 2020). In recent years, the rate of NTM isolation from respiratory tract samples and the number of patients infected with NTM have increased rapidly in many countries (Lai et al., 2010), (Marras et al., 2013), (Brode et al., 2017). Importantly, most NTMs (with the exception of *M. kansasii*) are resistant to all major antituberculous drugs or sensitive to only a few (Gopinath & Singh, 2010; Tortoli et al., 2003). The importance of NTM diagnosis in the management of lung disease is increasingly recognized (Tortoli et al., 2003). Thus, it is essential to identify NTM species in airway samples in order to choose successful treatments. Only a few of the known NTM species cause lung disease in humans. The most common slow-growing opportunistic mycobacteria (SGM) are members of the *M. avium* complex (MAC) (van Ingen et al., 2018), which includes *M. avium* and *M. intracellulare*. Among the rapid-growing mycobacteria (RGM), the *M. abscessus* complex (MABC) is a common pathogen of lung disease. The virulence of NTM varies greatly between species. For example, *M. gordonae* is considered a rare human disease, but *M. kansasii* is often associated with disease symptoms (van Ingen et al., 2009). Determining the presence of a positive culture and significant clinical and radiological signs of illness within a few months is crucial. Multiple checks must be conducted to establish whether the sickness could be attributed to low-pathogenic species such as *M. gordonae*. On the other hand, a positive culture for *M. kansasii* isolates may be sufficient to support the start of antibiotic therapy (Jankovic et al., 2016).

Since the clinical signs of lung infections brought on by NTM resemble those of tuberculosis and other pulmonary diseases, diagnosing them can be exceedingly difficult, and in underdeveloped nations, they are typically underreported (Gopinath & Singh, 2010).

As a result, there is still a lack of knowledge regarding the epidemiology and prevalence of NTM instances. Additionally, because NTMs are frequently resistant to drugs used in tuberculosis therapy (Griffith et al., 2007), they are frequently mistaken for multidrug-resistant (MDR) tuberculosis, particularly in nations where TB and AIDS are the main focus of the healthcare system. A survey revealed that in Iran, approximately 12 % of patients with chronic and MDR TB were actually confirmed to have NTM infection (Tabarsi et al., 2009). However, the prevalence of lung disease brought on by NTM is rising globally, making it a new hazard to the global health (Prevots & Marras, 2015). According to reports from affluent nations with access to specialist medical care, the burden of NTM diseases has surpassed that of tuberculosis (TB) in nations like the US, Canada, Japan, Korea, Australia, and the United Kingdom (Adjemian et al., 2012; Koh et al., 2013; Shah et al., 2016; Thomson, 2010), (Namkoong et al., 2016). For instance, in England and Ireland, the yearly incidence rates increased from 5.6/100,000 in 2007 to 7.6/100,000 in 2012 (Shah et al., 2016). Similar findings were made by the US National Institutes of Health, which discovered an increase in pulmonary NTM diseases among those 65 and older nationwide from 1997 to 2007, significantly increased from 20 to 47 cases/100,000 persons, or 8.2 % per year, with a total of 181,037 cases.

Therefore, the lack of understanding regarding NTM is a burning issue, as inaccurate diagnosis and inefficient treatment doses contribute to the progression of the disease and the deterioration of the patient's health (Sousa et al., 2019). NTM are inherently resistant bacteria that exhibit a persistent nature, making them difficult to defeat (Wu et al., 2018). Therefore, the necessity to research and create new, improved NTM therapy methods is essential. Understanding how hosts and pathogens interact as well as how NTM can survive by influencing host defense mechanisms is crucial for achieving the objective. The current state of NTM drug discovery, according to one source, "is reminiscent of the TB situation 20 years ago" (Wu et al., 2018). Effective genetic modification techniques are essential for the identification and characterisation of drug targets (Ding et al., 2021). Mycobacteria are difficult to genetically manipulate, mostly because of their slow development, the pathogenicity of some species, their GC-rich genomes, and their durable cell walls.

Mycobacteria have recently benefited from the development of many genetic engineering tools (Chhotaray et al., 2018; Murphy et al., 2018), particularly thanks to the CRISPR-Cas system (Rock et al., 2017; Yan et al., 2020; Yan et al., 2017).

2.1 Mycobacterial cell wall

Mycobacteria are distinguished from other bacteria by having thick, hydrophobic cell walls that are abundant in long-chain fatty acids known as mycolic acids (Figure 1) (Kaneda, Naito et al. 1986; Zuber, Chami et al. 2008; Marrakchi, Lanéelle et al. 2014; Nataraj, Varela et al. 2015). The mycobacterial cell membrane prevents gram-colored mycobacteria from staining them enough (Hinson, Bradsher et al. 1981, Trifiro, Bourgault et al. 1990). They are a member of the class of bacteria known as acid-fast bacteria that can be stained by the Ziehl-Neelsen stain. The structure of the mycobacterial cell wall is what causes this staining behavior. Its primary constituents are long-chained mycolic acids, arabinogalactan, and peptidoglycan, which are covered in a capsule of polysaccharides and proteins (Jankute, Cox et al. 2015). The hydrophobic structure of the mycobacterial cell membrane provides various benefits, including strong resistance to medicines and stress-inducing environmental factors.

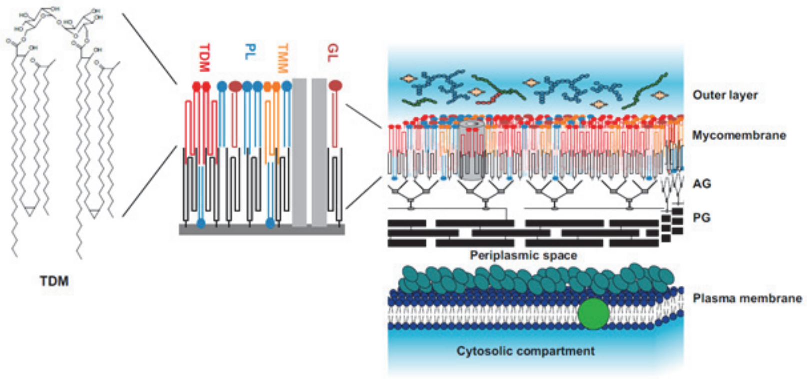

Figure 1 The cell wall of Mycobacteria.

The outer layer is made up of glucans, different lipids, and proteins. The permeability barrier is represented by the mycomembrane. The inner leaflet of the mycomembrane is apparently made up of free lipids such as trehalose dimycolates (TMD) in red, Trehalose monomycolates (TMM) in orange, different glycolipids (GL) in brown, and phospholipids (PL), in blue. The inner leaflet of the cell envelope is composed of a parallel arrangement of mycolic acid (MA) chains (depicted in black) that are coupled to arabinogalactan (AG). This AG-MA complex is further covalently attached to peptidoglycan (PG), forming a structural framework in the cell envelope. The standard lipid bilayer plasma membrane comprising phospholipids(blue) and proteins (green) is separated from the cell wall by a periplasmic space and has a thickness that is unexpectedly close to that of mycomembrane, around 7-8 nm, despite the absence of the extremely long chain mycolic acids. Source (Marrakchi et al. 2014).

2.2 The *Mycobacterium* genus

Mycobacteria are Gram-Positive aerobe, rod-shaped bacteria (Conn & Dimmick, 1947; Forbes et al., 2018). They are remarkable for having cell walls that contain mycolic acid, being acid-fast, and having a high percentage of guanine + cytosine in their genomes (61 % to 71 %) (Lévy-Frébault & Portaels, 1992). The genus *Mycobacterium* has more than 200 species

(Parte, 2020), which are largely divided into three groups: *M. leprae*, nontuberculous mycobacteria, and *M. tuberculosis* complex (Figure 2).

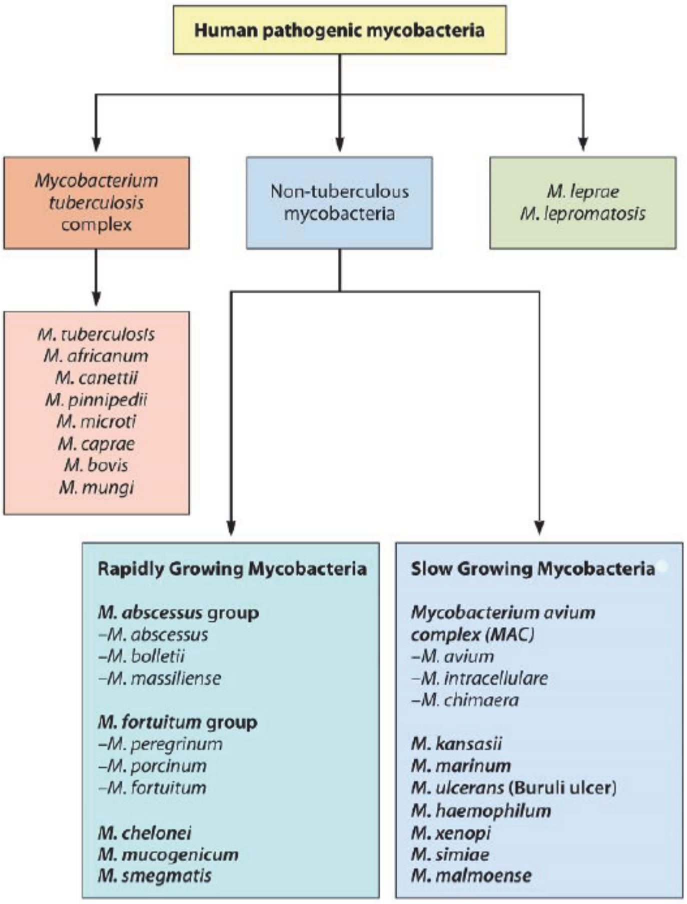
Human pathogenic mycobacteria
Mycobacterium tuberculosis complex
Non-tuberculous mycobacteria
M. leprae
M. lepromatosis
M. tuberculosis
M. africanum
M. canettii
M. pinnipedii
M. microti
M. caprae
M. bovis
M. mungi
Rapidly Growing Mycobacteria
M. abscessus group
–M. abscessus
–M. bolletii
–M. massiliense
M. fortuitum group
–M. peregrinum
–M. porcinum
–M. fortuitum
M. chelonei
M. mucogenicum
M. smegmatis
Slow Growing Mycobacteria
Mycobacterium avium complex (MAC)
–M. avium
–M. intracellulare
–M. chimaera
M. kansasii
M. marinum
M. ulcerans (Buruli ulcer)
M. haemophilum
M. xenopi
M. simiae
M. malmoense

Figure 2 An overview of the classification of human pathogenic Mycobacteria.

Mycobacteria are typically divided into three groups: those that cause leprosy, those causing tuberculosis (*M. tuberculosis* complex), and nontuberculous mycobacteria (NTM). NTM distinguish between rapid and slow growers. Source (Franco-Paredes et al., 2018)**.**

2.3 The *Mycobacterium tuberculosis* complex (MTBC)

The MTBC species *M. tuberculosis, M. bovis, M. africanum, M. microti, M. canetti, M. caprae,* and *M. pinnipedii* cause human tuberculosis (LoBue et al., 2010). Airborne transmission of MTBC occurs from infected humans and animals. The sickness can be brought on by a dose of 10 bacilli inhaled, and it has a long latent period (Chedore et al., 2002). Since the attenuated live vaccine (*M. bovis* Bacillus Calmette-Guérin: BCG) provides only a modest level of protection, the disease is typically treated with antibiotic therapy or, in rare circumstances, surgery. Even yet, *M. tuberculosis* affects one-third of the world's population and causes more than a million deaths each year, according to the World Health Organization (WHO, 2022).

2.4 Nontuberculous mycobacteria (NTM)

NTM can be found all over the natural environment, including in freshwater and soil (Falkinham, 1996). They can also be found in household dust, tap water, and water pipes in addition to the biofilms seen in sanitary facilities (Falkinham, 2016; Lahiri et al., 2014; Taylor et al., 2000). Some NTM, like *M. avium*, can even grow in low-nutrient settings, making them perfect for growth in potable water systems (Williams et al., 2009). They were found in even amoebae. It is problematic that they also occur in hospital water networks (Ovrutsky et al., 2013). NTM infections can be acquired through a variety of means. Typically, they are picked up through soil or water, or disseminated via aerosols. Additionally, they might be acquired post-surgery or transmitted via medical devices (Falkinham, 2009; Fowler & Mahlen, 2014; Franco-Paredes et al., 2018; Heifets, 2004), and also person-to-person transmission of *M. abscessus* is observed in CF patients (Bryant et al., 2016).

NTM are, as previously mentioned, opportunistic pathogens. On a few rare occasions, immunocompetent persons developed NTM infections (Fowler & Mahlen, 2014). However, as was already mentioned, those who have immunodeficiencies are particularly vulnerable to the effects of NTM infections. Humans with HIV infections or those who already have lung illnesses like cystic fibrosis are examples of susceptible hosts. The risk group also includes those whose immune systems have been weakened because of therapy. Additionally, it is believed that close contact or intense environmental exposure, such as farming, increases the risk of infection (Falkinham, 1996; Heifets, 2004; van Ingen et al., 2012). NTM are challenging to treat for several reasons. They are invulnerable to standard antibiotics (Heifets, 2004; Jarlier & Nikaido, 1994; Porvaznik et al., 2017). The cell walls of NTM are thick, lipid-rich, and hydrophobic. The mycolic acids are a significant part of cell walls. They support the slow development and hydrophobicity of the outer membrane (Falkinham, 2009; Jarlier & Nikaido, 1994). The thick cell walls explain the resistance to antibiotics, cleaning agents, and heavy metals (Falkinham, 2009; Jarlier & Nikaido, 1994; Porvaznik et al., 2017; Rodgers et al., 1999).

It is oftenly impossible to treat infections with traditional antibiotics, and single-drug therapies frequently cause mycobacteria to develop acquired resistance (Falkinham, 1996). Multi-drug therapy using three or four different antibiotics has occasionally been found to be more effective (Fowler & Mahlen, 2014) (Heifets, 2004). The interval between pathogen detection and treatment is another significant element. Most of the time, this time frame is excessive (Porvaznik et al., 2017). Another issue is the variation in clinical manifestation among mycobacteria of the same species. Patients with NTM illnesses frequently require individualized rehabilitative care.

2.5 *Mycobacterium avium* subsp. *hominissuis* (MAH)

The MAC includes the *M. avium* subsp. *hominissuis* (MAH) subspecies. The most often isolated NTM species group globally is known as MAC (Hoefsloot et al., 2013). In addition to MAH, *M. avium* contains three further subspecies: *M. avium* subsp. *avium*, *M. avium* subsp. *silvaticum*, and *M. avium* subsp. p*aratuberculosis* (Mijs et al., 2002; Thorel, Krichevsky, and Lévy-Fréb, 2002). MAH and *M. avium* subsp. *paratuberculosis* can be identified by a distinct IS1245 insertion element (Paustian et al., 2005). In order to distinguish MAH from the other subspecies, additionally variations in growth temperature and the 16S-23S rDNA internal transcribed spacer (ITS) can be applied (Mijs et al., 2002).

In particular, MAH can be seperated from isolates found in birds that were given the name *M. avium* subsp. *avium*. Interesting research showed that the subspecies *hominissuis* and the "bird-type" have different genetic make-ups (Mijs et al., 2002). According to studies by Van Coppenraet, de Haas, Lindeboom, Kuijper, and van Solingen (2008), MAH is frequently associated with childhood cervical lymphadenitis and cystic fibrosis (Sanchini et al., 2016). Although it seems unlikely that birds will spread the disease, environmental transmission is very likely (Lahiri, Kneisel, et al., 2014; Van Coppenraet et al., 2008). Common sources of MAH include potting soil, garden and pot dirt, and house dust (Kaevska et al., 2011; Lahiri, Kneisel, et al., 2014; Sanchini et al., 2016).

2.6 *Mycobacterium abscessus* (MABS)

Mycobacterium abscessus (MABS), one of the rapidly growing NTMs, is becoming more significant in medicine due to the potential skin problems and to lung infections it can cause in persons with CF. It can also cause illnesses such as lymphadenitis and infections of the lungs, skin, bones, and soft tissues as an opportunistic pathogen (Lewin and Schäfer 2019). The inherent high resistance to chemotherapeutics and antibiotics makes treating an infection with MABS very difficult (Brown-Elliott et al., 2012), (Rominski et al., 2017). These mycobacteria's distinctive cell wall, which includes complex lipids like glycopeptidolipids (GPL) (Gutiérrez et al., 2018) among other things, is how they acquire both resistance and pathogenicity. On agar plates, MABS isolates from human samples can display two distinct morphologies. Colonies isolated from patients might appear both smooth and rough at the same time. The rough morphology reveals dry, the smooth softly wet colonies (Howard et al., 2006). Infection with MABS most likely occurs after coming into contact with infected individuals, contaminated water sources, biofilms, or fomites, though the transmission paths are rarely recognized (Johansen et al., 2020).

The different morphological types depend on the levels of trehalose dimycolate (TDM) (Rüger et al., 2014) and GPL, respectively. When there is much GPL and minimal TDM, mycobacteria appear smooth (Catherinot et al., 2009). The lack of GPL expression and high levels of TDM are the primary characteristics of the rough morphology. The increased presence of GLP on the surface of mycobacteria leads to their ability to create biofilms and is associated with lower levels of virulence. Humans are more vulnerable to the rough variants (Degiacomi et al., 2019). Smooth colonies may turn transiently rough due to factors like high antibiotic concentrations (Gutiérrez et al., 2018). Sugar and a tetrapeptide-linked acyl chain make up the GPL. The production of GPL involves more than fifteen genes (Gokhale et al., 2007; Ripoll et al., 2007). A number of genes, particularly *mps1*-*mps2*-*gap* or *mmpL4b*, are responsible for producing and transporting the peptidyl core of the GPLs (Biet et al., 2008).

In Figure 3 members of the non-ribosomal protein synthesis family (nrp) include *mps1* and *mps2* (nrp). When these genes are mutated or missing, MABS develops rough morphologies instead of smooth ones due to the loss of GPL synthesis or transport (Pawlik et al., 2013).

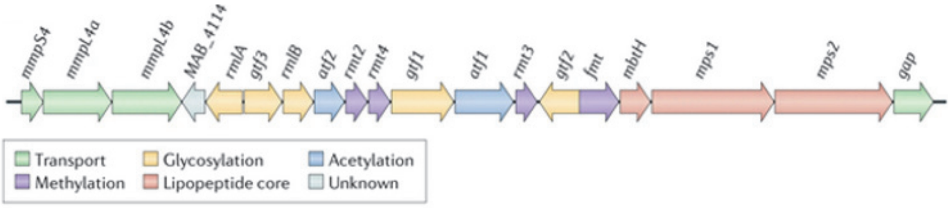

Figure 3 A cluster of genes is responsible for the synthesis and transport of the GPL.
Source (Johansen et al., 2020)

2.7 Genome editing methods

To exploit the potential of targeted mutagenesis, new approaches have been quickly expanding. Methods of genome editing were developed based on Mega nucleases, zinc finger nucleases (ZFNs), and transcription activator-like effector nucleases (TALENs), (Yin et al., 2017). These techniques execute in vitro or in vivo random mutagenesis using inverse genetics. By improving the efficiency of homologous recombination, programmable nucleases like ZFNs, and TALENs, may improve genome processing. Both methods require optimization and present a number of difficulties (Ma et al., 2016). ZFNs were the first generation of sequence-specific programmable nucleases (SSNs), which represented a significant advancement in the field of genome editing. SSNs at particular chromosomal loci can result in double-strand breaks (DSBs), which can be repaired either by the error-prone non-homologous end joining mechanism (NHEJ) or the homologous directed repair (HDR) mechanism (Symington & Gautier, 2011). ZFNs, for example, have been used to modify plant genomes, although this approach is limited due to issues with manipulating various species and the expense (Ramirez et al., 2008). The expertise acquired from investigating *Xanthomonas* led to the development of the other genome processing tool, TALENs (Moscou & Bogdanove, 2009). In essence, when engaging with a foreign agent like viruses, *Xanthomonas* bacteria release TAL effector enzymes through the stage III secretion system. The bacteria alter the pathogen's genes to withstand the attack (Malzahn et al. 2017). Despite being simpler to employ than ZFNs, this method still requires challenging TAL protein tandem repeat domain building (Ma et al., 2016). On the other hand, CRISPR-Cas9 technology has recently drawn interest from a wide range of industries. It has been found that using this method significantly increases the ability to alter the genes of many different species. (Kanchiswamy, 2016).

2.8 CRISPR/Cas9

2.8.1 Natural immune system in bacteria

The innate immune system of bacteria and archaea is the basis of the CRISPR/Cas9 technology, which uses short RNA to direct the breakdown of foreign nucleic acids. In 1987 CRISPR has been identified for the first time in the *Escherichia coli* population (Ishino et al., 1987). This system, which protects those organisms from plasmids and other mobile elements like phages, is shared by most archaea and many bacterial species (Sorek et al., 2008). The CRISPR/Cas method, which was first introduced in 2012 by (Jinek et al., 2012) as a very efficient tool for genetic modification in bacteria, has since been identified in a wide range of organisms (Jiang & Doudna, 2017). Key components of the bacterial immune system are CRISPR chains. They are made up of brief palindromic DNA clusters with so-called spacers between each loop. The *cas* genes are a collection of genes related to CRISPR and used to produce Cas proteins (Jinek et al., 2012; Wiedenheft et al., 2012). These act as DNA-cutting nucleases as well as DNA-unwinding helicases. When a bacterial phage attacks the bacteria, there will be a number of responses in this framework. (Figure 4) (Lab TD 2012) shows how this system operates. The spacers will serve as the bacterial phage's acknowledgment or activation mechanism, acting as the genetic memory for earlier bacterial attacks. If the spacer is activated, the foreign DNA will be added to the CRISPR framework. This will produce a library of short CRISPR-derived RNA (crRNAs) that have the attacking nucleic acid's extra structure (Jinek et al., 2012; Wiedenheft et al., 2012).

Three different CRISPR/Cas systems exist. There are some common elements between type I and type III systems: Pre-crRNAs are processed by specialized Cas endonucleases, and once mature, each crRNA forms a substantial multi-Cas protein complex that can recognize and cleave nucleic acids that are complementary to the crRNA. However, type II systems use a different mechanism to process pre-crRNAs. In these systems, the trans-activating crRNA (tracrRNA), which is complementary to the repeat sequences in the pre-crRNA, initiates processing before the Cas9 (formerly Csn1) protein, which is present, induces processing by the double-stranded (ds) RNA-specific ribonuclease RNase III. Cas9 is the only protein that is believed to be involved in the crRNA-guided silencing of foreign DNA (Jinek et al., 2012).

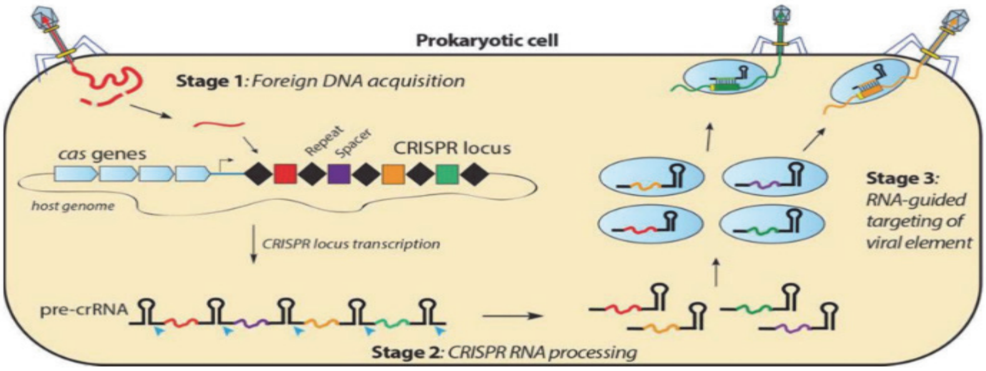
Prokaryotic cell
Stage 1: Foreign DNA acquisition
cas genes
Repeat
Spacer
CRISPR locus
host genome
CRISPR locus transcription
Stage 3: RNA-guided targeting of viral element
pre-crRNA
Stage 2: CRISPR RNA processing

Figure 4 A prokaryotic cell's CRISPR system.

When a bacterium is attacked by a bacterial phage, the CRISPR mechanism responds. Brief palindrome DNA repetitions make up CRISPR, and there are so-called separators between each repetition. These spacers are unique. They recognise or activate the bacterial phage and serve as the genetic memory of earlier bacterial attacks. When the spacer is activated, that foreign DNA will be replicated into the CRISPR. As a result, several short CRISPR-derived RNAs (crRNAs) are produced, adding to the attacking nucleic acid sequences. The genes that make Cas proteins are several CRISPR-related genes. Source (Reis A, 2014; TD, 2012).

2.8.2 CRISPR Type II System

The acquisition of foreign DNA at the CRISPR loci is the first stage of CRISPR-mediated protection (Wiedenheft et al., 2012). The CRISPR RNA (crRNA) and trans-activating crRNA attach to the Cas9 endonuclease, which then becomes activated (tracrRNA).
The first 20 or so nucleotides of the crRNA determine the target specificity complementary to the target DNA sequence, and the tracrRNA serves as a scaffold for Cas9 binding complementary to the crRNA sequence. Depending on the specific CRISPR ortholog, the trans-activating CRISPR RNA (tracrRNA) undergoes a folding process that results in the formation of two to three stem-loop structures. Furthermore, the tracrRNA and crRNA can form an RNA duplex that is referred to as chimeric single guide RNA (sgRNA) which can simulate the natural crRNA-tracrRNA hybrid and make the experimental setup of this system easier (Figure 5). The most popular genome-editing technology is the CRISPR-Cas9 system because of its great efficiency and simplicity. One of the most important targeting elements is the protospacer-adjacent motif (PAM), which varies among many Type II systems.

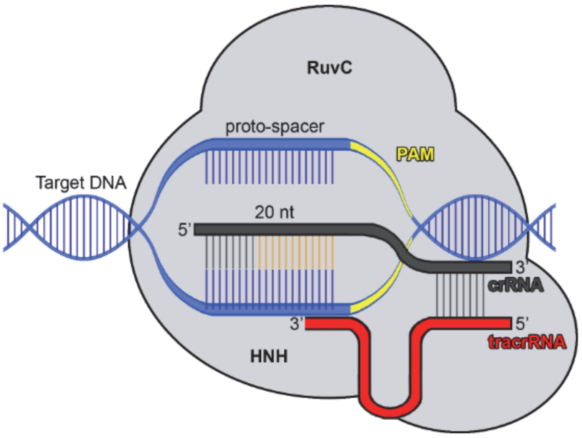

Figure 5 Model of the CRISPR Cas defensive mechanism in prokaryotic cells.

Cas9 protein (grey) is activated by the base pairing of crRNA (black) and tracrRNA (red). The base pairing of crRNA and the proto-spacer DNA in the presence of an adjacent PAM sequence then directs the Cas9 protein to a particular cleavage site in the invasive nucleic acid (yellow). The Cas9 protein will cleave the dsDNA and so destroy the foreign nucleic acid thanks to the HNH and RuvC domains. The figure is modified from (Bortesi & Fischer, 2015; Jinek et al., 2012).

CRISPR/SpCas9 (from *Streptococcus pyogenes*), the most widely used modified system, requires a PAM of the sequence 5'-NGG-3', where N can be any nucleotide. The only part of the system that needs to be modified in order to point Cas9 at a particular location on a double-stranded DNA substrate, is the crRNA sequence (Jinek et al., 2012). As Cas9 is turned on, it is guided to the predetermined target sequence and locks onto an adjacent protospacer pattern (PAM), as illustrated in (Figure 5). Two different active sites, the RuvC and HNH domains, then cause a DSB. According to (Jinek et al., 2012), the Cas9 enzyme's HNH nuclease domain cleaves the complementary strand of the target DNA at sites that are complementary to the guide sequence carried by the crRNA. Simultaneously, the Cas9 RuvC-like domain cleaves the noncomplementary strand. This dual cleavage activity results in the generation of blunt ends when the target DNA is sliced approximately 3-5 bases upstream of the protospacer adjacent motif (PAM) sequence.

Both the Non-homologous end joining (NHEJ) and homology-directed repair (HDR) processes can be used to restore DSB. NHEJ is the most common approach but is prone to error. This approach typically contributes to specific alterations such as a small deletion, insertion, or frameshift (Wyman & Kanaar, 2006). These modifications may cause the virus to become inactive. DSB repair by HDR results in the introduction of certain desired mutations or inserts (Figure 6) (Thurtle-Schmidt & Lo, 2018).

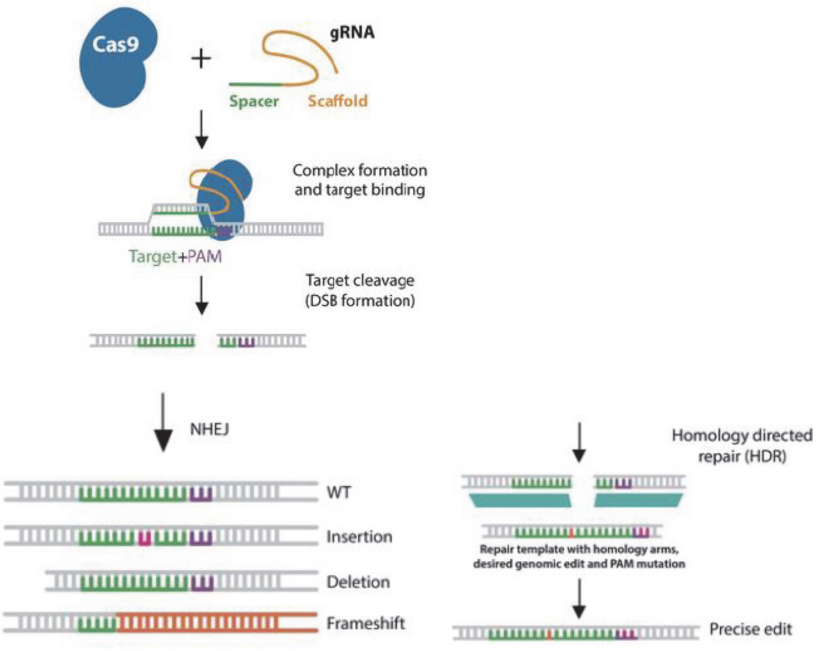
Cas9
gRNA
Spacer
Scaffold
Complex formation and target binding
Target+PAM
Target cleavage (DSB formation)
NHEJ
WT
Insertion
Deletion
Frameshift
Homology directed repair (HDR)
Repair template with homology arms, desired genomic edit and PAM mutation
Precise edit

Figure 6 Diagram of the CRISPR/Cas9 system's components.

The Cas9 protein and gRNA combine to produce a ribonucleoprotein complex that binds to the genome's target sequence. Sequences complementary to the PAM sequence and spacer can identify targets within the genome. Double-stranded breaks caused by CRISPR/Cas9 can be fixed by inserting "indels" through the NHEJ pathway or by utilizing the HDR mechanism. (Figure from (https://www.addgene.org/guides/crispr/)).

It is possible to evaluate a gene's function and how it impacts phenotypic traits using methods for genetic modification (Nyaradzai Mitchell Chimukuche & Monique J. Williams, 2021). In comparison to other genome editing methods, CRISPR/Cas9 has the advantages of being inexpensive, simple to employ, and resistant to off-target change (Doudna & Charpentier, 2014). Genes in bacteria can be silenced using CRISPR/Cas9 systems delivered via a vector plasmid, which has a cloning site for inserting the sgRNA template and can thus be customized to target the proper genomic area (Zhang et al., 2018). Editing genes in numerous species, including bacteria, yeast, crops, cattle, and even collections of animal cells, has been done in this way (Cho et al., 2013; Cong et al., 2013; DiCarlo et al., 2013; Friedland et al., 2013; Lemay et al., 2017; Woo et al., 2015)

2.8.3 CRISPR/Cas9 orthologs for gene editing

The DNA region that the CRISPR system, such as CRISPR-Cas9, is meant to break is followed by the DNA sequence known as PAM, which is typically 2 to 6 base pairs in length. In order to cut, a Cas nuclease needs the PAM, which is normally found 3–4 nucleotides downstream of the cut site (Table1) (http://crispor.tefor.net) (Ding et al., 2016; Jamal et al., 2016). Identification of the appropriate PAM sequences on the DNA strand for the chosen enzyme is therefore very crucial. The protein SpCas9, whose PAM sequence is 5'-NGG-3' and whose guide RNA is 20 nucleotides long, has been utilized most commonly. N can be any base. In addition to SpCas9 *Streptococcus pyogenes* (*S. pyogenes*), a number of Cas9 orthologs with unique characteristics have been found from various origins. Hundreds of Cas9 orthologs are now available. A few of them, SaCas9 *Staphylococcus aureus* (*S. aureus*), SthCas9- CRISPR1 *Streptococcus thermophilus* (*S. thermophilus*), and SthCas9- CRISPR3 (*S. thermophilus*) are currently available that have been designed for in vivo mycobacterial genome engineering. These Cas9 orthologs differ from one another in terms of editing efficiency, PAM requirements, Cas endonuclease size, crystal structure, etc. The key Cas endonucleases used by mycobacteria for in vivo genome editing is compared in Table 1.

Table 1 lists the various Cas protein subtypes and the corresponding PAM sequences. (Table modified from (http://crispor.tefor.net/).

Name	Cas orthologs	PAM (5'-3')	Origin	Size of protein (kb)	Type
Spy	SpCas9	NGG	*S. pyogenes*	1368	II A
Sth1	SthCas9-CRISPR1	NNAGAA(A/T)	*S. thermophilus*	1121	II A
Sth3	SthCas9-CRISPR3	NGGNG	*S. thermophilus*	1388	II A
Sau	SaCas9	NNGRRT (R = A or G)	*S. aureus*	1053	II A
Spa	SpaCas9		*S. pasteurianus*	1130	II A
Cas12a (Cpf1)	Cas12a (Cpf1)	TTTN	*Acidaminococcus*	~3.9 (AsCpf1)	V

2.8.4 CRISPR/Cas9 editing in Mycobacteria

The CRISPRi system was well characterized in *E. coli* and *Bacillus subtilis* (Peters et al., 2016; Qi et al., 2013). A good way to analyze the functions of genes is genome editing, for example, generating gene deletions by homologous recombination. But many techniques including common approaches have turned out to be inefficient for mycobacteria (Choudhary et al., 2015). Another general problem is proteotoxicity, triggered by overexpression of Cas9 (Nielsen & Voigt, 2014). A Type III CRSIPR/Cas locus was found in mycobacteria, but type II systems were absent.

Mycobacteria have recently been the subject of various genetic engineering techniques (Chhotaray et al., 2018; Murphy et al., 2018), greatly aided by the development of the CRISPR-Cas system (Rock et al., 2017); Yan et al., 2020; Yan et al., 2017). (Yan et al., 2017) described a highly effective method for producing point mutations, deletions, and insertions in *M. smegmatis* that relies on recombination and CRISPR-Cas12a-mediated counter selection (Msmeg).

In recent years the CRISPR interference (CRISPRi) system was established for mycobacteria. This strategy has shown effectiveness in repressing genes in Msmeg and MTB complex bacteria (Choudhary et al., 2015). (Choudhary et al., 2015) optimized the dCas9 from *S. pyogenes* and implemented the system in Msmeg mc^{2}155, *M. bovis* BCG Pasteur (BCG) and in the H37Rv strain of MTB. They observed downregulation of genes, but also partially no significant change in expression level. The repression level of gene expression could be increased by extending the length of the target-specific complementary sgRNA region and by expressing of multiple sgRNAs in parallel, targeting the same gene (Choudhary et al., 2015). Despite that, the downregulation was rather low compared to other bacteria.

In order to examine essential gene functions in MTB (Singh et al., 2016), optimized CRISPR interference presented a quick method. This method may be especially helpful in identifying genes with unknown functions and identifying prospective targets for new small chemical inhibitors. CRISPRi has the potential to overcome some of the limitations to allow a more facile analysis of essential genes in the MTB (Qi et al., 2013).

(Rock et al., 2017) argued that for an examination of essential gene functions a higher knockdown level is required. They developed an optimized CRISPRi system by using a more efficient Cas9 orthologue, the CRISPR1 Cas9 from *Streptococcus thermophilus* (dCas9Sth1) (Rock et al., 2017). With this optimized system they observed a robust knockdown of targets in Msmeg and MTB*.* The dCas9Sth1 contains point mutations within HNH and RuvC, nuclease domains which are homologous to D10A and H840A of the Cas9 of *S. pyogenes* (Bikard et al., 2013) (Qi et al., 2013). The nuclease-dead enzyme is controlled by an anhydrotetracycline (ATc) inducible promotor like in (Choudhary et al., 2015), but an optimizing of the ATc-regulated promotor was essential for both Msmeg and MTB (Rock et al., 2017). The known PAM sequence of the *S. thermophilus* system (5 ´NNAGAAW (Rock et al., 2017)3´) differs from the one of *S. pyogenes* (5´NGG-3´). (Rock et al., 2017) found several PAM sequence variants, differing in bases, which still produce target knockdowns. The more different the variant is from the original sequence, the less efficient the downregulation is. 24 PAM variants were tested, and they determined gene knockdowns spanning 2.7–216.7 fold. This increases the number of possible targets and shows an opportunity for “tuning” or rather specifically regulated repression. It should also be mentioned that the system was observed to be very specific: Two mismatches between sgRNA and target sequence were enough to prevent binding and gene silencing. So far, the CRISPRi/dCas9 system was established for Msmeg, MTB, and *M. bovis*.

According to a study by Klepina et al. (2022), CRISPRi provides an experimental method to study drug-target interactions in MABS (Kurepina et al., 2022). The silencing of numerous target genes was demonstrated by (Gupta & Rohde, 2022) and for the first time established ftsZMab as a crucial gene and promising therapeutic target.

Most prokaryotic cells lack the NHEJ system (Bikard et al., 2013). There are some bacteria, such as Msemg, MTB, and *Bacillus subtilis*, that have a simplified NHEJ mechanism that just requires Ku and ligase D (LigD), two essential proteins (Gong et al., 2005). More crucially, it has been demonstrated that other bacteria, such as Msmeg and *E. coli*, can function using the MTB NHEJ system (Tong et al., 2015). Three bacterial (Msemg, MTB, and *Bacillus subtilis*) NHEJ systems in *E. coli* were investigated by (Zheng et al., 2017), and the Msmeg NHEJ system was determined to have the highest activity. The *glnALG* pathway (4.2 Kb) and two sizable segments (67 and 123 Kb) were successfully removed in *E coli* using the MsmNHEJ system and Cas9.

The *Streptococcus thermophilus* (*S. thermophilus)* CRISPR1-Cas9 (Sth1Cas9) gene is functional in *Mycobacterium marinum* and MTB, allowing for highly efficient and exact DNA breaks and indel creation without any off-target effects (Meijers et al., 2020). Moreover, this technique can be employed with dual sgRNAs to simultaneously produce two indels or to make particular deletions. (Yan et al., 2020) created a CRISPR-Cas-mediated NHEJ genome editing tool that allowed for the rapid generation of point mutations, deletions, and insertions in Msmeg. This tool enabled for marker-less deletions in Msmeg and MTB. (Yan et al., 2017) described a highly effective method for producing point mutations, deletions, and insertions in Msmeg that relies on recombination and CRISPR-Cas12a-mediated counter-selection.

2.9 CRISPR/Cas9 editing in MABS

Molecular biology has undergone a revolution thanks to the breakthrough CRISPR-Cas9 genome editing method. One of its applications is the ability to perform gene knockout, where a specific gene can be completely inactivated or deleted from the genome. This technique has now been used to study the function of genes in MABS.

2.9.1 *mps1* gene

In the present thesis, CRISPR-Cas9 has been used to perform a knockout of the *mps1* gene from MABS also known as MAB_4099c, which has been shown to play a critical role in the glycopeptidolipid (GPL) production and antibiotic sensitivity of MABS. A study by (Bernut et al., 2016) showed that deletion of the *mps1* gene in MABS resulted in a significant decrease in GPL production. This decrease in GPL production was also associated with increased susceptibility to several antibiotics, including clarithromycin, tigecycline, and imipenem.

The loss of Mps1 function led to altered cell wall structure and reduced antibiotic susceptibility (Bernut et al., 2016). The study also found that deletion of *mps1* gene resulted in increased sensitivity to vancomycin, which targets cell wall biosynthesis. The *mps1* gene is involved in the regulation of GPL biosynthesis at the transcriptional level. The study showed that the *mps1* gene product interacts with the transcription factor MpsR to modulate GPL production in MABS (Dubée V, 2017). The *mps1* gene has also been demonstrated to be involved in colony morphotype and GPL (Glycopeptidolipid) synthesis. GPL is a complex molecule that is involved in the virulence and pathogenesis of MABS, and it has been shown that the production of GPL is regulated by *mps1*. Additionally, the colony morphotype of MABS is dependent on the presence and activity of the *mps1* gene.
The study of the role of the mps1 gene in GPL production and colony morphotype is crucial for understanding the mechanisms of pathogenesis and virulence in MABS. This information can be used to develop new therapeutic strategies against this bacterium and to improve our understanding of the role of this gene in the survival and persistence of MABS in the host.

Overall, the mps1 gene plays a crucial role in the regulation of GPL production and antibiotic sensitivity in MABS. In order to create more potent treatments for MABS infections, it may be useful to understand the molecular mechanisms behind these processes in order to find new targets.

2.9.2 Other four endogenous genes (*porin*, *ppiA*, *erm-41*, and *whiB7*) in MABS

2.9.2.1 The *porin* gene

The *porin* genes of MABS encode for a type of outer membrane protein known as a porin. Porins play a critical role in the permeability of the cell membrane and are involved in the transport of nutrients and other molecules into and out of the cell.

A variety of pore proteins known as porins are crucial for the movement of hydrophilic substances inside bacterial cells. Porins are abundantly expressed in various gram-positive and gram-negative bacteria (Achouak et al., 2001). Porins play a wide range of roles in the virulence of various kinds of pathogenic bacteria, including promoting cell adhesion, triggering apoptosis in host cells, and transporting virulence-related surface proteins (Müller et al., 1999; Azghani et al., 2002; Brunson et al., 2019).Two Msp-type porins are encoded in the genome of MABS, which are MAB_1080 and MAB_1081.The gene MAB 1080 has a length of 672 bp and is located between 1,096,492 and 1,097,163 of the MABS 09/13-3 genome, accession ERS4791737.

Msmeg possesses four pore-forming proteins called MspA, MspB, MspC, and MspD that control nutrient inflow, which is crucial for preserving normal growth rates (Stephan et al., 2005). MABS porins are present in a monophyletic group that includes the Msmeg porin MspD, suggesting that they have a common ancestor. The gene MAB_1080 produces a protein that is annotated in the literature as either MspA (Li et al. 2020) or MspD (Lewin et al., 2021). However, the gene MAB_1080 in the MABS subspecies massiliense is designated as *mmpA* (de Moura et al. 2021).

When MspA, MspC, and MspD are removed, Msmeg survives longer in macrophages by strengthening its resistance to nitric oxide produced by the host (Fabrino et al., 2009; Sharbati-Tehrani et al., 2005). Similar to this, in a study conducted by de Moura et al. in 2021, it was found that the deletion of porins in MABS, had a positive impact on bacterial persistence in SCID mice and their ability to survive within phagocytic cells. (de Moura et al., 2021). Nevertheless, mutants did not show varied macrophage glucose uptake, NO susceptibility, or cell cytotoxicity. Porin MmpA knockout strain showed reduced glucose absorption. It is noteworthy that CF patients' sequential samples from various early and late MABS infections display alterations within the *mmp* porin genes (Lewin et al., 2021). Phylogenetic analysis was unable to determine if *porin* mutations contributed to the increased virulence or spread of dominant clinical MABS isolates (de Moura et al., 2021). This shows that even while this family of proteins is important for virulence in other species, porins, including those found in MABS, may serve purposes unrelated to virulence.

Understanding the function of porins in MABS is crucial for the development of novel therapeutic strategies against this pathogen as well as for understanding the processes of resistance and virulence in mycobacterial infections.

2.9.2.2 The *ppiA* gene

Peptidyl-prolyl isomerase A, also known as PpiA, is an enzyme that catalyzes the cis-trans isomerization of proline-containing peptide bonds. In mycobacteria, PpiA has been implicated in multiple cellular processes, including protein folding and stability, stress response, virulence, and antibiotic resistance.

(Pandey et al., 2017) demonstrated the ability of recombinant rPpiA and rPpiB to bind to foreign proteins in vitro and inhibit their aggregation. Gel filtration chromatography has proven that oligomeric rPpiA and rPpiB exist in purified form. Compared to plasmid vector controls, *E. coli* cells overexpressing MTB PpiA and PpiB could withstand temperature stress. Transient expression of MTB PpiA and PpiB proteins in HEK293T cells results in enhanced cell survival compared to control cells when exposed to oxidative stress (induced by H_2O_2) and hypoxic conditions induced by Cobalt-chloride ($CoCl_2$) (Pandey et al., 2016). This observation suggests that the presence of these proteins likely plays a role in the adaptation of MTB to oxidative stress and hypoxic conditions that occur within the host. This MTB cyclophilins' chaperone-like role may serve as a stress responder and subsequently contribute to tuberculosis.

Dubey et al. (2021) investigated the role of PpiA in MTB. The study aimed to understand the function of PpiA in MTB survival and virulence, as well as to evaluate its potential as a drug target. The researchers used a combination of genetic, biochemical, and in vitro and in vivo assays to study the effects of PPiA deletion and inhibition in MTB. They found that PpiA deletion led to a significant reduction in MTB survival under oxidative stress and nutrient starvation conditions, as well as in macrophages and mice. They also showed that PpiA inhibition led to a reduction in MTB growth and survival *in vitro*. In addition, the study revealed that PpiA interacts with multiple MTB proteins, including several virulence factors and components of the oxidative stress response. The researchers suggested that PpiA may be involved in controlling the function of these proteins as well as in modifying host immunity and MTB response to stress. Studies in other mycobacterial species suggest that PpiA may play a similar role in MABS as it does in other mycobacteria.

2.9.2.3 The *erm-41* gene

The *erm-41* gene in MABS is a key determinant of inducible macrolide resistance in this pathogen. The MABS infection treatment regimen typically includes the use of macrolides, for instance, clarithromycin. However, the presence of the *erm-41* gene can confer resistance to macrolides and lead to treatment failure.

The *erm-41* gene encodes a protein, which belongs to the ribosomal RNA methyltransferase family. It has been demonstrated that Erm-41 alters the bacterial ribosome's 23S rRNA component, which is the target of macrolide antibiotics. This modification prevents macrolides from binding to the ribosome and inhibiting protein synthesis, leading to resistance. The *erm-41* gene in MABS is inducible, which means that its expression only occurs under specific circumstances, such as when a person is exposed to macrolide antibiotics. This allows MABS to conserve energy and resources by not expressing the resistance gene unless it is needed (Nash et al., 2009).

The presence of the *erm-41* gene has been associated with poor treatment outcomes in patients with MABS infections, particularly those caused by the subspecies MABS subsp. *abscessus* and subsp. *bolletii*. In the subsp. *massiliense* the gene is truncated and therefore

inactive. There are few effective treatments for macrolide-resistant MABS infections, and research is ongoing to discover novel antibiotics and treatment regimens.
In conclusion, the *erm-41* gene is crucial for the emergence of macrolide resistance in MABS and has significant effects on the management of this challenging disease.

2.9.2.4 The *whiB7* gene

The MABS *whiB7* gene is a transcriptional regulator that helps the bacterium adapt to various environmental circumstances. Specifically, WhiB7 has been implicated in the bacterium's response to oxidative stress and adaptation to hypoxic conditions. WhiB7 has also been implicated in virulence and stress response in mycobacteria. For example, in MTB, WhiB7 was found to be necessary for survival under hypoxic conditions, which are encountered during infection in the host. Additionally, WhiB7 was found to be required for the full virulence of MTB in a mouse model of the infection (Voskuil et al., 2011). It was discovered that the gene MAB_ 3508c, which shares 75 % of its sequence with the *whiB7* genes of Msmeg and MTB, is involved in the intrinsic resistance of MABS to different antibiotics (Burian et al., 2012; Hurst-Hess et al., 2017). WhiB7 activates genes linked to drug resistance and redox balance in MTB via interacting with domain 4 of the key sigma factor in the RNA polymerase holoenzyme (Wan et al., 2021).

WhiB7, showing effects on intrinsic antibiotic resistance, is strongly induced upon exposure to clinically relevant ribosome-targeting antibiotics (erythromycin, clarithromycin, amikacin, tetracycline, and spectinomycin). Deletion of the *whiB7* gene in MABS leads to susceptibility to all antibiotics mentioned above (Burian et al., 2012; Hurst-Hess et al., 2017). Therefore, it appears that the MABS *whiB7* gene is crucial for both the development of antibiotic resistance in the bacteria and its ability to adapt to various environmental situations. Further research is needed to fully understand the mechanisms underlying the role of *whiB7* in MABS biology.

3 Materials and Method

3.1 Bacterial Strains, plasmids, and growth conditions

All bacterial strains and plasmids used in this study and their characteristics are listed in Table 2 and Table 3.

The mycobacterial strains (Table 2) were grown at 37°C with or without shaking in Middlebrook (MB) 7H9 broth (BD Biosciences, Heidelberg, Germany) supplemented with 10 % modified ADC (mADC) (2 g Glucose, 5 g Bovine Serum Albumin (BSA) fraction V, 0.85 g NaCl in 100 ml water) (cultivation of MABS and Msmeg) or 10 % OADC (Sigma-Aldrich GmbH) (cultivation of MAH and 0.05 % Tween 80 (Roth, Karlsruhe, Germany). To grow colonies on agar, MB 7H11 agar (BD Biosciences, Heidelberg, Germany) supplemented with mADC or OADC was used. For the purpose of selecting recombinant mycobacteria, 100 µg/ml kanamycin (Roth, Karlsruhe, Germany) or/and 100 µg/ml hygromycin B was added (Roth, Karlsruhe, Germany) to the media. Luria-Bertani (LB) broth (10 g Peptone 140, 5 g Sodium Chloride, 5 g Yeast Extract, in 1L water) and Luria-Bertani (LB) agar (12 g Agar, 10 g Peptone 140, 5 g Sodium Chloride, 5 g Yeast Extract in 1L MilliQ water) were used to cultivate *Escherichia (E.) coli* Stellar at 37°C. When necessary, medium was supplemented with 100 µg/ml kanamycin or 100 µg/ml hygromycin B for the selection of recombinant *E. coli*. To induce the expression of Cas9 protein and sgRNA, MB7H9 broth and MB7H11 agar medium were supplemented with anhydrotetracycline (ATc) (50, 100 or 500 ng/ml).

Table 2 List of Strains.

Bacterial species	Isolate Name	Origin/Description	References
Mycobacterium avium subsp. hominissuis (MAH)	MAH-P-09/13	Pulmonary infection, CF patient	(Sanchini et al., 2017)
Mycobacterium abscessus (MABS)	MABS-P-09/13	Pulmonary infection, CF patient	(Lewin et al., 2021)
Mycobacterium abscessus (MABS)	MABS-P-40/14-3	Pulmonary infection, CF patient	(Lewin et al., 2021)
Mycobacterium smegmatis (Msmeg)	*M. smegmatis* mc^2 155		(Snapper et al., 1990)
Escherichia (E.) coli	*E. coli* Stellar (HST08)	lacZα, Δ(mrr-hsdRMS-mcrBC), ΔmcrA	Takara Bio

Table 3 List of the plasmids used in this study.

Plasmid	Relevant Characteristics	References
pLJR965	Integrative CRISPR/dCas9 interference backbone vector (8631 bp) for gene knockdown in mycobacteria; coding for a dead Cas9Sth1 endonuclease; a anhydrotetracycline resistance gene is present as a selective marker	(Rock et al., 2017)
pLJR962	Integrative CRISPR/dCas9 interference backbone vector (8881 bp) for gene knockdown in mycobacteria; coding for a dead Cas9Sth1 endonuclease; a kanamycin resistance gene is present as a selective marker	(Rock et al., 2017)
pMN437	*eGFP* gene and a hygromycin resistance gene (*hygR*) are both present in the 6235-bp plasmid, which was incorporated into the reporter strains' genomes.	pMN437 was a gift from Michael Niederweis
pSAK6	pLJR965 with the sequence for the sgRNA GFP 1 oligo (20 nt, binding 211 bp downstream from the start codon of *eGFP*) for downregulation of *eGFP* gene	This study
pSAK7	pLJR965 with the sequence for the sgRNA GFP 2 oligo (20 nt, binding 79 bp downstream from the start codon of *eGFP*) for downregulation of *eGFP* gene	This study
pSAK8	pLJR962 with the sequence for the sgRNA GFP 1 oligo (20 nt, binding 211 bp downstream from the start codon of *eGFP*) for downregulation of *eGFP*	This study
pSAK9	pLJR965 with the sequence for the sgRNA GFP 2 oligo (20 nt, binding 79 bp downstream from the start codon of *eGFP*) for downregulation of *eGFP*	This study
pSAK14	Integrative CRISPR/Cas9 backbone vector based on pLJR965 for gene knock-out in MABS; coding for a functional Cas9Sth1 endonuclease; a kanamycin resistance gene is present as a selective marker	This study
pSAK32	pSAK14 with the sequence for the sgRNA mps1 oligo (20 nt, binding 2956 bp downstream from the start codon of *mps1*) knockout of *mps1* gene	This study
pSAK33	pSAK14 with the sequence for the sgRNA mps1 oligo (21 nt, binding 6885 bp downstream from the start codon of *mps1*) knockout of *mps1* gene	This study
pLH1	pSAK14 with the sequence for the sgRNA porin oligo (20 nt, binding 513 bp downstream from the start codon of *porin)* knockout of *porin* gene	This study

pSAK43	pSAK14 with the sequence for the sgRNA *ppiA* oligo (20 nt, binding 204 bp downstream from the start codon of *PpiA)* knockout of *ppiA* gene	This study
pSAK44	pSAK14 with the sequence for the sgRNA *erm-41* oligo (20 nt, binding 475 bp downstream from the start codon of *erm-41 gene)* knockout of *ppiA* gene	This study
pSAK45	pSAK14 with the sequence for the sgRNA *erm-41* oligo (20 nt, binding 365 bp downstream from the start codon of *erm-41 gene)* knockout of *PpiA*	This study
pSAK46	pSAK14 with the sequence for the sgRNA *whiB7* oligo (20 nt, binding 200 bp downstream from the start codon of *erm-41 gene)* knockout of *whiB7*	This study

Table 4 A list of the oligonucleotides used in this study and the PAM-sequence of the target genes.

Plasmid name	Oligo name	Sequence (5´-3´)	PAM-sequence (5´-3´)
pSAK6/pSAK8	FW_ oligo gfp1	GGGAATTCATGTGGTCCGGGTAGCG	NNAGAAG
	RV_ oligo gfp1	AAACCGCTACCCGGACCACATGAA	
pSAK7/pSAK9/pSAK12	FW_ oligo gfp2	GGGAGCCCTCACCCTCGCCGGAGAC	NNAGAAC
	RV_ oligo gfp2	AAACGTCTCCGGCGAGGGTGAGGGC	
pSAK33	FW_ oligo mps1	GGGAGGAGCCAACCGTCGAGCAC	NNAGAAG
	RV_ oligo mps1	AAACGTGCTCGACGGTTGGCTCC	
pSAK32	FW_ oligo mps1-2	GGGAATGCTGTCCCCGCCCAGGTC	NNAGAAG
	RV_ oligo mps1-2	AAACGACCTGGGCGGGGACAGCAT	
pLH1	FW_ oligo porin	GGGATTCGGACCGGCAACCGCTAC	NNAGAAG
	RV_ oligo porin	AAACGTAGCGGTTGCCGGTCCGAA	
pSAK43	FW_ oligo ppiA	GGGAGATCATGAATCCGTCGATGACCCG	NNGGAAG
	RV_ oligo ppiA	AAACCGGGTCATCGACGGATTCATGATC	
pSAK44	FW_ oligo erm-41-1	GGGAGAATCCACCTGCGGTGGATG	NNGGAAA
	RV_ oligo erm-41-1	AAACCATCCACCGCAGGTGGATTC	
pSAK45	FW_ oligo erm-41-2	GGGAGCTGCAGCACCAGGTCGGCAG	NNAGCAG
	RV_ oligo erm-41-2	AAACCTGCCGACCTGGTGCTGCAGC	
pSAK46	FW_ oligo whiB7	GGGAGCGCCACAATGGTCCCCTGCT	NNAGAAT
	RV_ oligo whiB7	AAACAGCAGGGGACCATTGTGGCGC	

Table 5 Primer pairs for PCR and Sanger Sequencing used in this study.

Target	Primers	Sequence 5' --> 3'	Ann. Temp	Product size
KanR	Tn903/S1	CGAGGCCGCGATTAAATTCCAAC	60°C	600 bp
	Tn903/AS1	TGAGTGACGACTGAATCCGGTGAGA		
dCas9	FW_Rock_dCas9	AACCGCTACCTGGAGATCCT	57.5°C	512 bp
	RV_Rock_dCas9	GTGTTCAGGGTCAGCACGTA		
codon 9 of dCas9	Q5SDM_9	CTGGGCCTGGaCATCGGCATC	70°c	
		CACCAGGTCCGACATATCGATACC		
codon 599 of dCas9	Q5SDM_599	CGAGGTGGACcaCATCCTGCCG	70°c	
		CGAGGTGGACcaCATCCTGCCG		
eGFP	FW-GFP-cas9	CGAGGAGCTGTTCACCGG	57.5°C	697 bp
	BW-GFP-cas9	TTGTACAGCTCGTCCATGCC		
	FW_GFP_1	CGAATCCAACTGGCTTGTCC	57.5°c	1500 bp
	RV-GFP_1	TCTTTCCTGCGTTATCCCCTG		
	FW_GFP_2	TTGTACAGCTCGTCCATGCC	57.5°c	1200 bp
	RV-GFP_2	AGTGAGCGAGGAAGCGGAAG		
	FW_ClaI_Gfp_pMN437	ACGTTCTCGGCTCGATGATC	57.5°c	2490 bp
	RV_ClaI_Gfp_pMN437	CAGGCTCGCGTAGGAATCAT		
Hyg	FW-Hyg-2	AGTCGTGCAGGAAGGTGAAG	57.5°c	901 bp
	FW-Hyg-2	GCGGACCTCTATTCACAGGG		
	FW-Hyg-3	AGTCGTGCAGGAAGGTGAAG	57.5°c	1056 bp
	FW-Hyg-3	GCGGACCTCTATTCACAGGG		
mps1	FW-msp1	GTTGTCCGCTCACCAGAAGA	56.5°c	810 bp
	RV-msp1	CGGCAAAGCATCCAAAACCA		
	FW-msp1-2	GAACACGACCGGTTGGACAA	57.5°c	2000bp
	RV-msp1-2	AGTGTGGCATGCCTATCCAG		
porin	FW_mspA	GCGCTCTGCTCATGACTCTT	57.5°c	563 bp
	RV_mspA	GATCAAACGCGCGTAAGGAC		
ppiA	FW-ppiA-2	ACTTCACCGATCCAGACAGC	57.5°c	511 bp
	RV-ppiA-2	ACTTCACCGATCCAGACAGC		

erm-41	FW-erm-41	GACCGGGGCCTTCTTCGTGAT	62°c	700 bp
	RV-erm-41	GACTTCCCCGCACCGATTCC		
whiB7	FW-WhiB_7	CGGACCGATTCAAATTGGCG	57.5°c	866 bp
	RV-WhiB_7	CTTTGTCGTGTTGCCGATCG		
rpoB	Mab rpoB-FW	CGATAGAGGACTTCGCCTAACC	60°c	76 bp
	Mab_rpoB_RV	TCGAGCACGTAAACTCCCTTTC		
	Mab_rpoB_probe	[FAM]CCACTGACCGAACATCTATCCCGC [TAMRA]		
Sequencing primers	seq sg pLJR962	TTCCTGTGAAGAGCCATTGATAATG	57.5°c	
cas9	Cas9Seq_ 9_F	GGATTTGACTTCCCTATCAGTGA		
	cas9Seq_ 599_F	CCAACCAGTACAACGGCAAG		

3.2 Generation of reporter NTM strains for CRISPRi /dCas9

pMN437 (Figure 7) is a vector with a codon-optimized *eGFP* gene encoding an improved GFP (enhanced fluorescence, faster folding, more stable) and *Hyg*R gene that can replicate both in *E. coli* and mycobacteria. The plasmid pMN437 was electroporated into suitable NTM strains. Here we used Msmeg strain mc^{2}155, MAH clinical strain MAH P-09/13, and MABS clinical strain MABS P-09/13 for reporter strain generation. The proof of the successful transformation with the plasmid was done with the help of blue light applied to the agar plates, fluorescence microscopy and PCR.

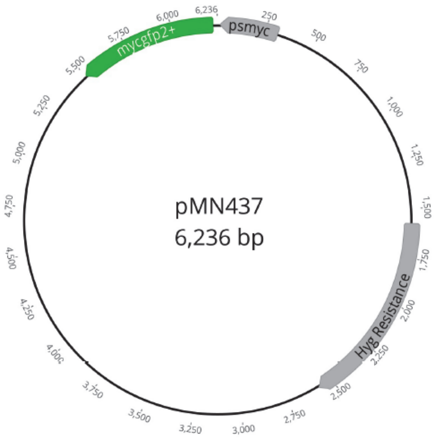
mycgfp2+
psmyc
Hyg Resistance
pMN437
6,236 bp
6,236
250
500
750
1,000
1,250
1,500
1,750
2,000
2,250
2,500
2,750
3,000
3,250
3,500
3,750
4,000
4,250
4,500
4,750
5,000
5,250
5,500
5,750
6,000

Figure 7 Map of plasmid pMN437.

Size of 6236 bp. The reporter gene mycogfp2+ or *eGFP* gene is highlighted in green. The *eGFP* fragment is around 716 bp in size. The gene is regulated by the promotor psmyc. The plasmid carries a hygromycin (hyg) resistance gene.

3.2.1 Vectors pLJR962 and pLJR9765

The CRISPRi/dCas system for Msmeg and MTB was improved by the Jeremy Rock group by creating and using various CRISPRi backbone variants. These variants vary, for instance, in the Cas9 promoter, sgRNA, and Tet repressor's expression level. pLJR965 with a size of 8,631 bp and pLJR962 with a size of 8881 bp (Figure 8) are the backbones for MTB and Msmeg, respectively. A TetR-regulated promotor is responsible for regulating the dCas9Sth1 gene. The plasmid contains two BsmB I restriction sites 5' to the sgRNA scaffold sequence and the selection marker *KanR* gene for kanamycin resistance.

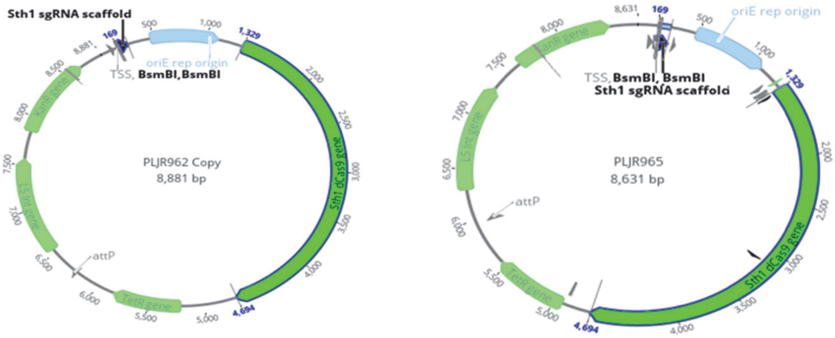
Sth1 sgRNA scaffold
169
8,881
500
1,000
1,329
oriE rep origin
TSS, BsmBI,BsmBI
8,500
KanR gene
8,000
7,500
L5 Int gene
7,000
6,500
attP
6,000
TetR gene
5,500
5,000
4,694
4,000
3,500
3,000
2,500
2,000
Sth1 dCas9 gene
PLJR962 Copy
8,881 bp
8,631
169
500
oriE rep origin
1,000
1,329
8,000
KanR gene
7,500
TSS, BsmBI, BsmBI
Sth1 sgRNA scaffold
7,000
L5 Int gene
6,500
PLJR965
8,631 bp
attP
6,000
5,500
TetR gene
5,000
4,694
4,000
3,500
3,000
2,500
2,000
Sth1 dCas9 gene

Figure 8 pLJR965 is the *M. tuberculosis*-optimized and pLJR962 is the *M. smegmatis* - optimized CRISPRi backbone.

The dCas9 from *Streptococcus thermophilus* (dCas9sth$_1$) is present in the plasmids. Tet repressor (TetR)-regulated promotor is in charge of controlling dCas9 and sgRNA expression. Additionally, the plasmid has a L5-intergration site, an OriE-derived *E. coli* replication origin from pBR322, and a kanamycin-selectable marker (KanR). The sgRNA scaffold is positioned upstream of OriE. Two distinct BsmBI restriction sites are located 5' to the sgRNA scaffold sequence and can be used to ligate a sequence that is complementary to a target of choice. (Rock et al., 2017) and Rock's Cloning Guide are references.

3.2.2 Design of CRISPR-sites in *eGFP* gene and cloning for vector construction

The sgRNAs were cloned into the BsmB1 restriction sites upstream of the Sth1 sgRNA scaffold in pLJR962 and pLJR965 for the knockdown of the *eGFP* gene. sgRNA sequence, which is complementary to the target gene, makes up the binding domain of the sgRNA. The guidelines of the cloning guide from (Rock et al., 2017) were followed in order to locate an appropriate sequence in the gene. The protospacer adjacent motif (PAM) sites selected are important for making CRISPRi/dCas9 effective in mycobacteria (Figure 9). Two sgRNA sequences that target the non-template (NT) strand of the *eGFP* gene's open reading frame (ORF) were created to silence the gene. First, two strong PAM sequences (5' NNAGAAC 3' and 5' NNAGAAG 3') (Figure 9) within the template strand (non-coding) were found to specifically target the NT strand of the *eGFP* gene (Figure 10). The 20 nucleotides immediately 5' to the PAM were selected to obtain the sgRNA once the PAM in the template strand had been located.

A sgRNA target sequence was ligated into the BsmB I cloning sites of pLJR965 and pLJR962. The more the sequence deviates from the sequence 5'-NNAGAAG-3', the less is the fold repression of the target. First, the genomic sequence of the *eGFP* gene was searched for these PAM sequences (Figure 10).

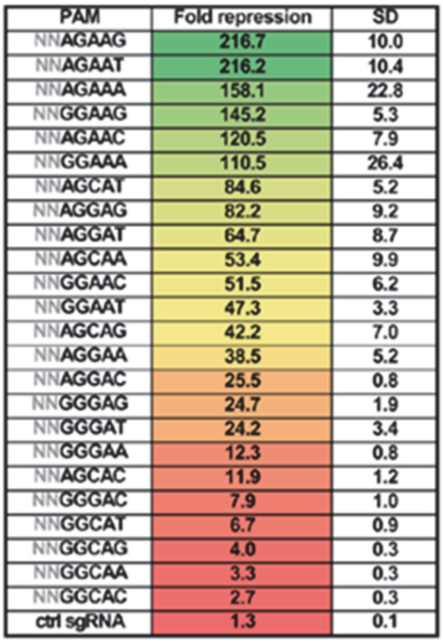

PAM	Fold repression	SD
NNAGAAG	216.7	10.0
NNAGAAT	216.2	10.4
NNAGAAA	158.1	22.8
NNGGAAG	145.2	5.3
NNAGAAC	120.5	7.9
NNGGAAA	110.5	26.4
NNAGCAT	84.6	5.2
NNAGGAG	82.2	9.2
NNAGGAT	64.7	8.7
NNAGCAA	53.4	9.9
NNGGAAC	51.5	6.2
NNGGAAT	47.3	3.3
NNAGCAG	42.2	7.0
NNAGGAA	38.5	5.2
NNAGGAC	25.5	0.8
NNGGGAG	24.7	1.9
NNGGGAT	24.2	3.4
NNGGGAA	12.3	0.8
NNAGCAC	11.9	1.2
NNGGGAC	7.9	1.0
NNGGCAT	6.7	0.9
NNGGCAG	4.0	0.3
NNGGCAA	3.3	0.3
NNGGCAC	2.7	0.3
ctrl sgRNA	1.3	0.1

Figure 9 The dCas9Sth1 PAM variants are shown.

Cas9Sth1 tolerates the reported PAM sequence 5'-NNAGAAW-3' as well as variant PAM consensus sequences. luciferase test was used to identify the degree of fold repression. SD: Standard deviation Figure from (Rock et al., 2017).

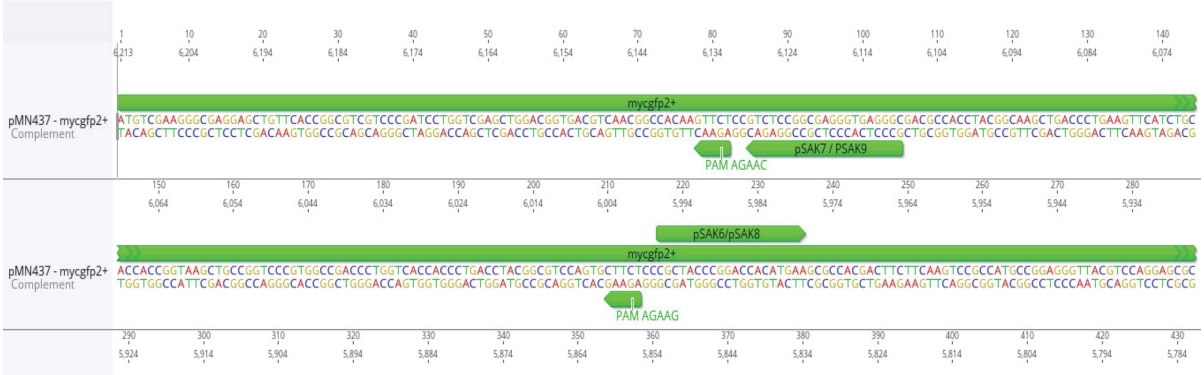
1
10
20
30
40
50
60
70
80
90
100
110
120
130
140
6,213
6,204
6,194
6,184
6,174
6,164
6,154
6,144
6,134
6,124
6,114
6,104
6,094
6,084
6,074
mycgfp2+
pMN437 - mycgfp2+
Complement
ATGTCGAAGGGCGAGGAGCTGTTCACCGGCGTCGTCCCGATCCTGGTCGAGCTGGACGGTGACGTCAACGGCCACAAGTTCTCCGTCTCCGGCGAGGGTGAGGGCGACGCCACCTACGGCAAGCTGACCCTGAAGTTCATCTGC
TACAGCTTCCCGCTCCTCGACAAGTGGCCGCAGCAGGGCTAGGACCAGCTCGACCTGCCACTGCAGTTGCCGGTGTTCAAGAGGCAGAGGCCGCTCCCACTCCCGCTGCGGTGGATGCCGTTCGACTGGGACTTCAAGTAGACG
pSAK7 / PSAK9
PAM AGAAC
150
160
170
180
190
200
210
220
230
240
250
260
270
280
6,064
6,054
6,044
6,034
6,024
6,014
6,004
5,994
5,984
5,974
5,964
5,954
5,944
5,934
pSAK6/pSAK8
mycgfp2+
pMN437 - mycgfp2+
Complement
ACCACCGGTAAGCTGCCGGTCCCGTGGCCGACCCTGGTCACCACCCTGACCTACGGCGTCCAGTGCTTCTCCCGCTACCCGGACCACATGAAGCGCCACGACTTCTTCAAGTCCGCCATGCCGGAGGGTTACGTCCAGGAGCGC
TGGTGGCCATTCGACGGCCAGGGCACCGGCTGGGACCAGTGGTGGGACTGGATGCCGCAGGTCACGAAGAGGGCGATGGGCCTGGTGTACTTCGCGGTGCTGAAGAAGTTCAGGCGGTACGGCCTCCCAATGCAGGTCCTCGCG
PAM AGAAG
290
300
310
320
330
340
350
360
370
380
390
400
410
420
430
5,924
5,914
5,904
5,894
5,884
5,874
5,864
5,854
5,844
5,834
5,824
5,814
5,804
5,794
5,784

Figure 10 *eGFP* gene in the plasmid pMN437 is the target of a single guide RNA template.

The sequences 5'-NNAGAAC-3' and 5'-NNAGAAG-3' inside the gene were employed as PAM sequences. Following a two-nucleotide gap between the 3' end of the single guide RNA template and the 5' end of the sequence-specific PAM site, 20 base pairs within the *eGFP* gene were created as a single guide RNA (sgRNA) template starting from the 5' end of the PAM sequence. Geneious Prime was used to demonstrate the selection and location of the sgRNA sequences. pSAK6/pSAK8/pSAK7/pSAK9 indicate the presence of specific sgRNAs in the different plasmids.

The sgRNA was designed by extracting at least 20 nucleotides adjacent (with a gap of 2 bases) to the PAM sequence and ending them with an adenine (A) or guanine (G). Since an "A" or "G" efficiently initiates mycobacterial transcription. If the 20th nucleotide was not an "A" or a "G", the oligo size was moved to 21 nucleotides, the reverse (RV) oligo represents the reverse complement, while the forward (FW) oligo corresponds to the transcribed sequence of sgRNA. It was necessary to add the sequences 5'-GGGA-3' to forward oligo and 5'-AAAC-3' to reverse oligo in order to regenerate the sgRNA promoter and dCas9 handling sequences (Table 4). By incubating 4 µl of each oligonucleotide (100 µM) in 42 µl of annealing buffer (50 mM TRIS pH 7.5, 50 mM NaCl, 1 mM EDTA) for 2 min at 95°C, both oligonucleotides were annealed. Then, annealed oligonucleotides were cooled to room temperature. In this way, the insert was prepared. 3 µg of the pLJR965 and pLJR962 plasmid was digested using the restriction enzyme BsmBI. 3 µg of plasmid DNA, 1 U BsmB I per µg DNA, and 5 µl of 10x

NEB3.1 buffer were all present in one reaction (50 µl). To complete the total volume of 50 µl, water was added to fill the remaining space. The reaction mixture was initially subjected to incubation at 55 °C for a duration of two hours. Following this step, the enzyme was inactivated by exposing the mixture to a temperature of 80 °C for 20 minutes. A review of the results was done using agarose gel electrophoresis. The Wizard® SV Gel and PCR Clean-Up System Kit (Promega, Germany) were used to purify the digested vector. The T4 DNA ligase technique from New England Biolabs was used to carry out the ligation at room temperature for 3 hours. Heat shock was used to convert the ligation mix and controls into *E. coli* Stellar after incubation. 50 ng of digested pLJR965 was employed as an extra control to verify the plasmid's relegation rate. A preculture was created the following day after the developed colonies were transferred to fresh agar plates. With the use of the BigDye Terminator v3.1 Cycle Sequencing Kit (Thermofisher, Germany), the region around the cloning sites of the plasmids of various clones was sequenced using the primer seq sg pLJR962 (Table 5) that binds near the cloning site of the vector and 300 ng of plasmid for sequencing. The annealing temperature in the sequencing reaction was 58°C. The correctly ligated plasmids were transformed into reporter NTM strains containing the plasmid pMN437 after the sequencing results were evaluated. The constructed plasmids pSAK6, pSAK7, pSAK8, and pSAK9 are described and the respective PAM sites are shown in (Table 3) and (Table 6).

Table 6 The constructed plasmids pSAK6, pSAK7, pSAK8, pSAK9.

Oligo Name	Distance to Start codon	PAM	Vector	Name of constructed Plasmid	Recipient strains
GFP1	211 bp	5' NNAGAAG 3'	pLJR962	pSAK8	Msmeg (pMN437) MABS 0913-3 (pMN437)
			pLJR965	pSAK6	MAH 0913-3 (pMN437)
GFP2	79 bp	5' NNAGAAC 3'	pLJR962	pSAK9	Msmeg (pMN437) MABS 0913-3 (pMN437)
			pLJR965	pSAK7	MAH 0913-3 (pMN437)

To confirm the presence of the plasmids, PCR for the *KanR* gene and the *dCas9* gene was applied (primers and annealing temperatures in Table 5) and the PCR products were visualized by agarose gel electrophoresis.

3.2.3 Measurement of the fluorescence of strains with down-regulation of *eGFP* gene by flow cytometry

Precultures of the reporter strains, the down-regulated strains and control strains without a plasmid were grown to OD_{600} between 1.0-1.5. From these cultures, 500 µl were pipetted into 60 ml of fresh medium, if necessary, with antibiotics (100 µg/ml kanamycin and 100 µg/ml hygromycin) and allowed to grow for four days to OD_{600} ~1.5 for MABS and Msmeg and ten days for MAH. For MABS and Msmeg, ATc concentrations of 0, 50, and 100 ng/ml for induction and incubation times of 1, 4, and 8 days were tested. For MAH, ATc concentrations of 0, 100, and 500 ng/ml and incubation times of 4, 8, and 12 days were tested. To induce the dCas9 gene and expression of sgRNA, MABS and Msmeg cultures were supplemented with desired ATc concentrations every 24 h, whereas MAH cultures were treated with ATc at every 96 h. 20 ml of each sample was transferred to a 50 ml cell culture bottle and appropriate concentration of ATc was added. The reporter strain was included as a control. The tubes were shaken at 37°C and 180 rpm. After the incubation times had expired, the tubes were centrifuged at 10,000 g for 5 min. The supernatants were discarded, and the pellets were washed with 5 ml of PBS. Then, they were centrifuged again, and the pellets were resuspended in 1 ml of CellFIX (diluted 1:10) (Becton Dickinson Benelux NV, Belgium) to fix the mycobacteria and incubated for one day at room temperature (RT). The samples were then stored at 4°C in the dark until measurement. On the day of the measurement, the samples were resuspended and 200 µl pipetted into a 96 round-bottom well plate and measured on the CytoFLEX (Beckman Coulter, USA) FACS device. The forward scatter (FSC), side scatters (SSC), and fluorescein isothiocyanate (FITC) were measured. Only the first 100,000 events were registered, and the flow rate was set to 30 µl/min. P1 median FITC-A fluorescence was calculated from 10,000 cells per sample using a minimum of three samples. It was measured with the FITC-A ray, which allows for the analysis of fluorescence at 530 nm. Based on their forward (FSC) and side scatter (SSC) profiles, cells that may have clumped together were gated out.

3.3 Generation of nuclease active CRISPR/Cas9 system

(Rock et al., 2017) developed and published a CRISPR interference system to silence genes, which served as the backbone for the CRISPR/Cas9 method for producing knockout mutants constructed in this study. To restore the catalytically active $Cas9Sth_1$, the vector pLJR965 was used as a template. The alanine at position 9 (GCC) (A) was changed into aspartic acid (GAC) (D) and the alanine at position 599 (GCC) (A) was changed into a histidine (CAC) (H), transforming $dCas9Sth_1$ into a nuclease-active form $Cas9Sth_1$ using the Q5® site-directed mutagenesis kit from New England Biolabs, USA. Site-directed mutagenesis was validated by PCR and DNA sequencing.

3.4 Cloning of sgRNA sequences into pSAK14 for gene mutation

Different top-scoring PAM sites described by (Rock et al., 2017) were selected for insertion into pSAK14 to inactivate the target genes in NTM. The procedure presented by (Rock et al., 2017) was adhered to. Table 4 contains a list of each sgRNA scaffold sequence employed in this investigation. The cloning procedure and confirmation of recombinant plasmids were done as described in Chapter 3.2.2.

3.5 Molecular Biological Methods

3.5.1 Preparation of competent E. coli and transformation

E. coli Stellar TM (Table 1) was used for generation of competent cells. The *E. coli* Stellar TM cells were cultured at 37°C overnight in 10 ml of LB. 1 ml of the overnight culture were added to 100 mL LB media within a 500 mL flask. The culture was shaken and allowed to grow at 37 °C until the OD_{600} reached 0.25–0.3. After being placed on ice, the culture was chilled for fifteen minutes. The chilled culture was then transfered to two 50 ml falcon tubes. To collect the cells, the culture was centrifuged at 10,000 g for 10 min at 4°C. The supernatant was discarded, and the pellet was resuspended in 40 ml of ice-cold, 0.1 M $CaCl_2$ solution. The cells were then allowed to cool for 30 minutes and centrifuged once more at 10,000 g for 10 min at 4°C. Then, the pellet was reconstituted in 2.5 ml of ice-cold 15 % glycerol containing $CaCl_2$ and aliquoted into 200 µl stocks. The aliquots were either instantly frozen in liquid nitrogen and then at -70°C or immediately used for heat shock transformation.

100 ng of plasmid DNA (Table 2) was added to 100 µl of competent *E. coli* Stellar^{TM} cell suspension and incubated on ice for 30 min. For negative controls, 10 µl of water instead of plasmid DNA were used. The next phase involved a 45-second heat shock at 42°C, which was followed by a second 2-minute incubation period on ice. The mixture was transferred to a 10 ml tube containing 1 ml of sterile, pre-warmed SOC broth (1 % Bacto tryptone, 0.25 % Bacto yeast extract, 4.28 mM NaCl, 1.25 mM KCl, 5 mM MgCl2, 20 mM Glucose), and incubated at 37°C for one hour. After centrifuging the cells at 13,000 g for 2 minutes, 150 µl of fresh SOC medium was added to the cell pellet. After that, the pellet was resuspended. A selective antibiotic (either kanamycin 100 µg/ml, hygromycin 100 µg/ml, or both antibiotics) was then

added to 100 µl and 50 µl of cell suspension before being plated on LB agar for selection. The plates were incubated at 37°C overnight.

3.5.2 Plasmid isolation

In order to isolate a plasmid, *E. coli* cells were grown at 37°C for overnight in 5 ml of LB containing an antibiotic for selection. The cells were collected by centrifuging for 30 seconds at 11,000 rpm, and the pellet was resuspended in 100 µl of cold solution 1 (50 mM Glucose, 25 mM TRIS-HCl, pH 8.0, 10 mM Na_2EDTA, 100 mg/ml RNase A). Then, 200 µl of solution 2 (0.2 mM NaOH, 1 % SDS) was added and the content of the tube was carefully mixed. Once 150 µl of 3 M NaOAc (pH 4,8) were added, the solution was thoroughly blended by carefully inverting the tubes. The probes were centrifuged at 10,000 g for 10 min. 400 µl of the supernatant was transferred to a 1.5 ml Eppendorf tube. One ml of ice-cold, 99.9 % ethanol was then added. After a gentle re-mixing, the samples were incubated at -20°C for 30 minutes. Thereafter, the samples were centrifuged at 4°C for 10 min at 6,000 g. After discarding the supernatant, the pellet was washed with 500 µl of 70% ethanol. The supernatant was carefully removed after the pellet was centrifuged at 10,000 g for 5 minutes at 4°C. After being dried at RT, the pellet was dissolved in 50 µl of water. The Quantus^{TM} Fluorometer (Promega, USA) was used to measure the amount of plasmid DNA present in accordance with the manufacturer's instructions.

3.5.3 Preparation of electrocompetent MAH cells and electroporation

3 ml of the MAH preculture was added to 100 ml of the electroporation growth media (8.7 g Middlebrook 7H9, 171.5 g Sucrose, 0.1 g Tween 80, 100 ml OADC, in 1 l water) and incubated at 37 °C. 10 ml of 15% glycine was added two days before electroporation, when the OD_{600} was at 0.5. The cells were then centrifuged for 10 minutes at RT at 10,000 g. The cell pellet was carefully washed three times with the electroporation buffer (100 ml Glycerol, 171.5 g Sucrose in 1l MilliQ water). In this way, the resuspended cells were gathered in a single tube. The pellet was dissolved in 1 ml of electroporation buffer after centrifuging the cells again. Competent cells were kept at -70°C. For electroporation, 300 µl of competent MAH cells and 1 µg of plasmid DNA were mixed. For negative controls, 10 µl of water instead of plasmid DNA was used. Each sample was transferred into a 2 mm electroporation cuvette (Carl Roth, Karlsruhe, GER). The electroporation was carried out by Gene Pulser Xcell™ Electroporation Systems, Bio-Rad Laboratories, Inc. at 2.5 KV, 25 µF, and 1,000 Ω. After that, the sample was added to 1 ml of the electroporation growth medium. The cells were incubated at 37°C overnight. The samples were centrifuged at 13,000 g for 5 minutes the following day, and the

pellet was resuspended in 500 µl of MB broth containing mADC. Around 100 µl of the cell mixture was plated on MB agar plates with kanamycin 100 µg/ml or hygromycin 100 µg/ml or both antibiotics for selection (see 3.1). The plates were incubated at 37 °C for approximately 2-4 weeks.

3.5.4 Preparation of electrocompetent MABS and Msmeg and electroporation

To produce highly electrocompetent MABS and Msmeg cells, a single colony was used to inoculate 10 ml of MB broth supplemented with mADC. This culture was grown at 37 °C with light shaking (80 rpm) up to an OD_{600} of about 2. In cell culture flasks, 1 ml of this culture was then introduced into 200 ml of MB broth supplemented with mADC. It was shaken overnight at 100 rpm at 37°C until an OD_{600} of roughly 1.5 was achieved. The bacteria were then placed in ice for one to two hours, collected by centrifugation (10,000 g, 15 min, 4°C), and washed four times with decreasing volumes (50, 25, 10, and 5 ml each time) of ice-cold wash solution (10% glycerol). Electrocompetent bacteria were suspended in 1 ml of wash solution and directly used for electroporation. 200 µl of electrocompetent MABS or Msmeg cell suspension with 500 ng of plasmid DNA were used. This combination was then transferred into an electroporation cuvette with a 2 mm electrode gap (Carl Roth, Karlsruhe, Germany). The cuvette was electroporated using an electroporator (Gene Pulser Xcell Electroporation system, Bio-Rad Laboratories Inc.), and a pulse was activated using 2500 V, 25 F, and 1000 Ω. The cells were then put into a 15 ml centrifuge tube with 1 ml of the MB media with mADC and gently shaken at 37°C for 4 hours. Then, the samples were centrifuged for 5 minutes at 13,000 g. The pellet was resuspended in 500 µl of MB broth with mADC, and around 100 µl of that mixture was plated on MB agar plates with the proper antibiotics for selection (see 2.1). The plates were incubated at 37 °C for approximately 5-7 days.

3.5.5 Genomic DNA preparation from Mycobacteria

Mycobacterial cultures were centrifuged at 6000 x g at 4°C for 10 minutes once they reached an OD_{600} 2. Following resuspension of the pellet in 400 µl of TE8 buffer (0,01 M Tris-HCl, 0,001 M EDTA, pH 8), mycobacteria were heated at 80°C for 30 minutes. Samples were cooled to room temperature before being incubated at 37°C overnight with 5 µl of lysozyme (150 mg /ml) added to the solution. The following day, the lysate was added to 70 µl of 10 % SDS and 5 µl Proteinase K (20 mg /ml) before being incubated at 65°C for 2 hours. 100 µl of 5 M NaCl and 100 µl of cetyl-trimethyl-ammonium-bromid (CTAB: 10% CTAB (SIGMA, Germany) in 0.7 M NaCl (Carl Roth, Germany) were then added to the sample, and incubated again at 65 °C for 10 min. The mixture was then centrifuged for 10 min at 4° C and 13,000 rpm using 300 µl of phenol, chloroform, and isoamyl alcohol (25:24:1, pH 7,5-8,0) (Carl Roth, Karlsruhe, Germany). 200 µl of the upper aqueous phase was transferred to a fresh tube, mixed with 200 µl of chloroform/isoamyl alcohol (24:1) (Carl Roth, Germany), and then centrifugation was done as before. 100 µl of the upper phase was again transferred to a fresh tube, 10 µl of sodium acetate pH 5.2 and 100 µl of pure isopropanol were added, and the mixture was mixed and incubated at -20 °C overnight. The mixture was centrifuged for 30 minutes at 4 °C at 10,000 g. The pellet was centrifuged, with 500 µl of 70 % ethanol for washing, left to dry for 30 to 60 minutes at room temperature, and then resuspended in 100 µl of water. DNA was quantified using the Quantus fluorometer (Promega, Germany) in accordance with the manufacturer's recommendations.

3.5.6 Polymerase chain reaction (PCR)

Purified DNA, cell material from agar plates (colony PCR), or broth were used in PCR reactions. (Table 7) lists the main components for one reaction (50 µl), and (Table 8) lists the cycler program, with the annealing temperature customized to the primers used. 100 ng of DNA was added if using it as a template, and the remaining space was filled with water. When using cells, the cell material was resuspended in water, heated for 30 minutes at 96°C, and then 15 µl was added to the master mix. When the reaction was finished, the samples were mixed with 6x loading dye, and further analysed by agarose gel electrophoresis.

Table 7 Components of a conventional PCR (*ThermoFisher Scientific)*.

Component	Concentration	Volume for one reaction (µl)
10x Dream Taq buffer	10x	5
dNTP	10 mM	1
$MgCl_2$	25 mM	1,6
Forward Primer	10 pmol/µl	1
Reverse Primer	10 pmol/µl	1
Dream Taq Polymerase	5 Units/µl	0.25
Template (100 ng DNA)		X
DEPC water		Ad 50 µl

Table 8 Cycler program of a conventional PCR.

Step	Cycles	Temperature	Time
Initial denaturation	1x	96°C	5 min
Denaturation	35 x	96°C	30 sec
Annealing		X°C	30 sec
Elongation		72°C	60 sec
Final Elongation	1x	72°C	7 min
	1x	4°C	Hold

3.5.7 Quantitative real-time PCR

Quantitative real-time PCR (qPCR) was used to amplify and measure the amount of DNA only from MABS samples. Using a qPCR, the genome equivalents in a MABS culture were calculated by calculating the abundance of the gene encoding the sigma factor σB (*rpo*B). As standard, previously quantified DNA of isolate MABS 09/13-3 was used in dilution steps from 10^{-2} to 10^{-6}. The measured amount of DNA within the sample was calculated to the genome equivalents, based on the weight of approximately 5.5×10^{-3} pg per MABS genome equivalent. The reaction mix (Table 9) was prepared in a nucleic acid-free box to prevent contamination

Table 9 Components of a quantitative real-time polymerase chain reaction.

Component	Stock Concentration	Volume for one reaction (µl)
10x Dream Taq buffer	10x	2,5
dNTP	10 mM	0,5
$MgCl_2$	25 mM	0,8
Forward Primer	10µM	1,25
Reverse Primer	10µM	1,25
probe	10µM	0,5
DreamTaq Polymerase	5 Units/µl	0.125
Template	Variable	
DEPC water	Variable	Total volume 25 µl

while using a cooling rack. Reactions were placed in a thermocycler applying settings as listed in (Table 10) with an annealing temperature for respective primers (Table 5).

Table 10 Cycler program of a Quantitative real time polymerase chain reaction.

Step	Cycles	Temperature	Time
Initial denaturation	1x	95°C	3 min
Denaturation	35 x	95°C	30 sec
Annealing		X°C	30 sec
Elongation		72°C	60 sec /kb
	1x	4°C	Hold

3.5.8 Agarose gel electrophoresis and product purification

3.5.8.1 Agarose gel electrophoresis

Agarose was melted in 1 x TAE (40 mM Tris base, pH 7.5, 20 mM acetic acid, 1 mM EDTA) buffer at a concentration based on the desired product size (0.8-1.5 %) and then placed onto an electrophoresis sled. The gel was placed on the chamber that contained 1 x TAE buffer and was utilized for electrophoresis. Samples were combined with 6 x loading dye (1:6 loading dye: sample; Carl Roth, Karlsruhe, GER) and run together with a DNA ladder (Thermo Fisher Scientific, USA) with a scale based on the anticipated product size at 100-110 volts for 60-80 min. GelRed or GelGreen (Biotium, Fremont, CA, USA) were used to stain the gel while being shaken. Vilber Fusion FX (Vilber Lourmat, Eberhardzell, GER) with the Evolution-Capt Edge software was used to document the gel.

3.5.8.2 Product purification using the Wizard® SV gel and PCR clean-up system

DNA fragments visible in the GelGreen-stained agarose gels were removed from gels and purified using the Wizzard® SV gel and PCR clean-up system (Promega, Germany) in accordance with the manufacturer's instructions. As described in section 4.5, DNA was quantified using the Quantus^{TM} Fluorometer after being eluted in 25 µl of DEPC water and stored at 4°C.

3.6 Sanger sequencing

The BigDye™ sequencing kit from Thermo Fisher Scientific, Waltham, Massachusetts, USA, was used for Sanger DNA sequencing. Prior to the sequencing procedure, 5 µl of the PCR product were incubated for 15 min at 37°C, then 15 min at 85°C with 0.5 µl of exonuclease I (10 U) and 1 µl of alkaline phosphatase (1 U) for cleanup (Thermo Fisher Scientific, Waltham, MA, USA). After that, the Sanger sequencing reaction mixture took place (Table 11).

Table 11 Sanger sequencing reaction protocol using BigDye™ kit.

Component	Stock concentration	Volume per sample in µl
BigDye™		0.5 µl
BigDyeTM buffer	5×	2 µl
Primer	10 µM	0.5 µM
DNA	variable	variable
DEPC	variable	Total volume 10 µl

The sequencing reaction was carried out in a thermocycler using the procedure described in (Table 12), with the appropriate primer's annealing temperature (Table 5). The DNA sample was added at a concentration based on fragment size (Table 13).

Table 12 BigDye™ sequencing reaction cycler conditions.

Step	Cycles	Temperature	Time
Initial denaturation	1x	96°C	1 min
Denaturation	25x	96°C	10 sec
Annealing		X°C	5 sec
Elongation		72°C	4 min
Final elongation	1x	72°C	5 min

Table 13 DNA quantity in sequencing reactions according to DNA sample.

DNA Sample	Size	DNA quantity
PCR product	100-200 bp	1-3 ng
PCR product	200-500 bp	3-10 ng
PCR product	500-1000 bp	10-20 ng
Plasmid		150-300 ng

3.6.1 Whole-genome sequencing (WGS) and genome analysis

Genomic DNA was isolated from MABS P09/13-3 WT (parent strain), MABS P09/13-3(pSAK14) (control strain) and different MABS P09/13-3(pSAK 33) *msp1* mutants. Samples were delivered to the Robert Koch Institute's unit MF2 (Genomsequenzierung und Genomische Epidemiologie) for Illumina next-generation sequencing (paired-end, 150 bp). Genome assembly was performed by the RKI’s unit MF1 (Bioinformatik und Systembiologie). The Geneious Prime workflow "Map reads then discover variations/SNPs" was used to find SNPs and Indels in the mutants and control strain compared to the wild type using the settings "coverage 20" and "variation frequency 0.9".

3.7 Glycopeptidolipid (GPL) extraction and TLC analysis

MABS P09/13-3 WT (parent strain), MABS P09/13-3 (pSAK14) (control strain), and MABS P09/13-3 (pSAK 33) *msp1* mutant No 318, were grown at 37°C in Middlebrook 7H9 broth with 0.05 % Tween 80 and mADC enrichment. The bacteria were heat-killed once they reached an OD_{600} 1.8-2.0 (log phase), and the GPL was then extracted from the dried bacterial pellets from 50 ml cultures. In order to extract the dried pellets, 10 ml of chloroform-methanol (2:1, V: V) was used, and 1 minute of 100% power ultrasonication (Branson Sonifier-450 D, G. Heinemann). The liquid phases were hydrolyzed with 3 ml of 0.2 N sodium hydroxide in methanol to remove the alkali-labile lipids. The pH of the lipid extracts neutralized them to pH 7 with 6 N HCl. Following that, 6 ml of chloroform and 5 ml of water were added, and the mixture was centrifuged at 8000 g for 10 minutes. The organic solvent-containing bottom phase was pipetted into a fresh tube and then totally evaporated. The resulting pellet was now dissolved in 1 ml of chloroform/methanol (2:1, V: V) and used for Thin Layer Chromatography (TLC).

TLC silica gel $_{60}$ TLC plate ((aluminum sheet, silica gel coated with fluorescent indicator F254) (Merck, Germany)) with roughly 7x7 cm in dimensions was used for TLC. On the TLC plate, probes were placed at least 1 cm apart and 0.5 cm above the lower edge. The TLC plate was then allowed to dry for 10 minutes at room temperature. A 500 ml beaker was filled with a pleated filter and 10 ml of the solvent chloroform/methanol (9:1, V: V). The chamber was then sealed off to allow the atmosphere to be fully saturated. The pleated filter guaranteed fast and even saturation of the whole chamber. The TLC Plate was put inside the chamber with the probes facing down as soon as the chamber was saturated (after about 30 minutes). Until the solvent reached the top edge of the chamber, the TLC was incubated there. The TLC was then removed and left to dry for 20 minutes at room temperature. After being evenly wetted with 20 % H_2SO_4, the dried TLC plate was once again dried at room temperature. The TLC plate was gently heated with a hot air dryer for an additional 20 minutes until all bands were visible.

3.8 Methods for quantification of mycobacteria in broth culture

3.8.1 OD600 measurement

To measure the growth rate of mycobacteria, 100 µl of liquid culture was diluted in 900 µl of MB medium and the OD600 was measured in disposable cuvettes in a Spectrometer Ultrospec 100 (Pharmacia Biotech).

3.9 Measurement of relative light units depending on ATP amount

Measurement of relative light units (RLU) depending on the ATP amount within a bacterial suspension was used as a reference value for growth. To this end, the BacTiter-GloTM (Promega, USA) microbial cell viability assay kit was used. To protect the reagents, every step was carried out in darkness. 50 µl of a culture that previously was diluted 1:10 with sterile MilliQ water was mixed with 50 µl of luciferase solution from the kit in a white 96-well microtiter plate. After sealing the plate and incubating for 5 min at RT, the plate was shaken on a plate shaker for 1 min at 400 rpm and subsequently incubated for another 10 min at RT. Afterwards, the bioluminescence was measured with the Mithras Microplate Reader from Berthold Technologies GmbH & Co. KG using the software MicroWin 2010.

3.10 Antibiotic susceptibility testing by sensititre

A cotton swab was used to sweep transfer the densely grown bacterial cultures from MB 7H11 agar plates to a centrifuge tube containing 3–4 ml of sterile water. By vortexing, the bacteria were resuspended. The optical density was then changed to an OD_{600} range of 0.10 to 0.11. Thereafter, 50 µl of the bacterial dilution was put into a 10 ml Müller-Hinton broth (ThermoFisher Scientific/Oxoid/Remel) after it had been corrected for cations. 100 µl of the suspension was added to each well of a sensititre plate (SensititreTM RAPMYCOI susceptibility testing Plate, TREK Diagnostic Systems, ThermoFisher) containing several antibiotics at various concentrations after the suspension had been thoroughly mixed. The plates were incubated at 30 °C. After five days, the MABS' growth was assessed. The Sensititre Vizion System (Thermo Scientific, TREK Diagnostic, UK) and a mirror were both used to visually read the growth and for each strain the minimal inhibitory concentration (MIC), which is defined as the lowest concentration at which no growth is observed, was computed.

3.11 Screening for MABS virulence-mutants

3.11.1 The growth rate in broth cultures under pH stress

All of the transformed mycobacteria and wild type were compared in terms of growth rates in MB 7H9 broth supplemented with mADC at neutral pH (7) and under pH stress (pH 5). Cultures were inoculated to an initial OD_{600} range of 0.02 to 0.03 and allowed to develop at 37°C for two weeks without shaking in neutral pH (pH 7) and under pH stress (pH 5). There were three inoculations for each strain. By quantifying ATP using the BacTiter-GloTM Microbial Cell Viability Assay kit (Promega Corporation, WI, USA) in accordance with manufacturer's instructions, the growth of cultures was evaluated. Using the microplate luminometer Tecan Infinite 200pro (Tecan, Germany), the luminescence was measured as relative light units (RLU).

3.12 H2O2 and NO Stress resistance tests

96-well microplate tests were used to assess the mycobacterial strains' tolerance to stress caused by H_2O_2 (reactive oxygen species) and NO stress. Microplate wells were filled with log-phase bacterial cultures (OD_{600} nm of 1.8) grown in MB7H9 broth containing mADC at 37 °C. The bacterial cultures were then exposed to H_2O_2 at two different concentrations (20 mM and 100 mM). After 4 hours following exposure to H_2O_2 stress, the amount of ATP was measured (chapter 2.6.2) to determine the sensitivity to H_2O_2. To calculate the percentage survival for each strain, the bacterial viability was assessed both with and without stress treatment.

The bacterial strains were also incubated for 4 hours in a medium with 25 mM of DETA/NO (diethylenetriamine/nitric oxide adduct), a NO donor. The difference in % survival was calculated in the same way as for the H_2O_2 susceptibility test.

3.12.1 Induction of cytokine expression in THP-1 cells

The THP-1 cell line was infected in 24-well cell culture plates (TPP, Switzerland) with three wells per sample. THP-1 cells were cultivated in a total of 250,000 cells per well and then given phorbol-12-myristat-13-acetate (PMA, 10 ng/ml). THP-1 cells were then allowed to adhere to the well surface for 3 days at 37°C and 5 % CO2. The cells were then infected with MABS mutants and control (pSAK14) at a MOI 1 based on MABS qPCR units. After 24 hours, the supernatants were collected, and ELISA determined cytokine concentrations using the Human ELISA Ready Set Go kits (Natutec, Germany).

3.12.2 Infection of THP-1 cell lines and intracellular growth measurement

THP-1 cells were PMA treated, seeded, and infected as mentioned before. After 3 hours, the supernatants were collected, and cells were washed twice with RPMI 1640. After that, the cells were treated with 200 µg/ml amikacin for two hours in order to eradicate the mycobacteria in the supernatant. Then, each well received 1 ml of media supplemented with 5 µg/ml amikacin after being washed twice with RPMI medium. Following the removal and eradication of extracellular bacteria, samples were quantified at the end of the infection period of 3 hours, 1, 2, 3, and 4 days late. For this, the cells were lysed in 1 ml sterile water at 37°C for 20 minutes. Quantitative real-time PCR with the Aria System were used to measure the amount of mycobacterial DNA present in sample lysates in order to determine the intracellular survival (Agilent Technologies, USA). 200 µl of the sample lysate, 100 µl of TE-9 2 x buffer (1 M Tris, 40 mM EDTA, 20 mM NaCl pH 9, and 2 % SDS), and 6 µl of Proteinase K (50 mg/ml) were used to extract the DNA. The mixture was incubated at 58°C for 60 minutes and then at 97°C for 30 minutes. Phenol/chloroform/isoamyl alcohol (25:24:1, pH 7,5-8,0) and chloroform/isoamyl alcohol (24:1) (Carl Roth, Karlsruhe, Germany) were used to extract the DNA after bringing the mixture to room temperature. The DNA was then precipitated with 12.5 µl 3 M sodium acetate pH 5 and 300 µl ice cold 100 % ethanol. The pellet was air dried and resuspended in 50 µl MilliQ-water. The MABS DNA was quantified by amplifying an amplicon in the *rpo*B gene of MABS using primers Mab_rpoB_FW and Mab_rpoB_RV and a FAM-labelled detector probe Mab_rpoB_probe (Table 5). Thermo Scientific Dream Taq PCR kit was used for MABS DNA amplification. The PCR reaction (final volume of 25 µl) was done by following (Table 10). Real-time PCR was used to estimate sample DNA concentrations using a standard made up of six dilutions of genomic MABS DNA at known concentrations.

3.13 Bioinformatic tools and analysis

DNA sequences were analyzed using the software Geneious Prime from Biomatters (Table 14). Sequenced genomes of the used isolates were obtained from (Lewin et al., 2021). Further sequence analysis was done by MF1 at the Robert Koch Institute, Berlin, Germany, and comparative analyses were conducted with Geneious Prime. Primers were designed using the software Geneious Prime from Biomatters (Table 14). The coefficients primer and product length, melting temperature, secondary structure formation, and specificity were respected according to the suggestions of Geneious Prime. For some primers, extensions were attached to, for example, generate overhangs complementary to RE digestion sites to serve desired purposes.

3.14 Computer software and programs used

The software utilized in this investigation is listed below in (Table 14).

Table 14 List of software used in this study.

Name	Company/Reference
Aria real-time PCR software	Agilent Technologies, Santa Clara, CA, USA
Geneious Prime (version 2021 and 2022)	Biomatters, Ltd., Auckland, LZD
GraphPad Prism 8.4.0	GraphPad Software, Inc., San Diego, CA, USA
Microsoft Office 365 (version 2022)	Microsoft Corporation, Redmond, WA, USA
MicroWIn (2010)	Berthold Technologies, Bad Wildbad, GER
NEBcloner® (Version 1.10.0)	New England Biolabs, Ipswich, MA, USA
NEBioCalculator® (version 1.15.0)	New England Biolabs, Ipswich, MA, USA
SWIN® (version 3.3)	Thermo Fisher Scientific, Waltham, MA, USA
Vizion	Thermo Fisher Scientific, Waltham, MA, USA
Tecan i-control 3.9.1.0	Tecan Trading AG
NCBI (BLAST)	https://blast.ncbi.nlm.nih.gov/Blast.cgi)
CytExpert 2.3.1.22	Beckman Coulter CytoFLEX

3.15 Statistical Analysis

GraphPad Prism 8.4.0 was used for statistical analysis and graphing (Graph pad Software, Inc.). Each experiment was performed at least in three independent experiments. The student’s t-test and two-way ANOVA test were used to assess the significance of the results between the experimental and control groups. Only for intracellular survival and cytokine secretion in THP-1 cells two independent experiments with three technical repetitions were performed and means ± standard deviation was determined by Mann-Whitney U test. Significant data were defined as those with *P < 0.05; **P < 0.01; ***P < 0.001; ****P < 0.0001.

4 Results

The system for down-regulation and mutagenesis in *M. avium* and *M. abscessus* is based on the one-plasmid CRISPRi system developed by Rock (Rock et al., 2017). This system is based on plasmids pLJR965 and pLJR962, kanamycin-resistant plasmids, allowing for the ATc inducible expression of dCas9 and the sgRNA. The results are presented in five sections. The first section deals with developing and installing CRISPRi/dCas9 in reporter NTM strains (section 4.1). The second section deals with the *eGFP* gene knockdown by CRISPRi/dCas9 in NTM; the downregulation of e*GFP* was determined by flow cytometry (section 4.2). The third section deals with the e*GFP* gene knockout by CRISPR/Cas9 in NTM and the genotypic characterisation of the generated mutant strains PCR and sequencing (section 4.3). The fourth section deals with the performance and specificity of CRISPR/Cas9 in an endogenous gene - the *mps1* gene - in MABS and the phenotypic characterisation of the generated *mps1* mutant strains (section 4.4), and the last section deals with the knockout mutagenesis by CRISPR/Cas9 of additional four endogenous genes (*porin, ppiA, erm-41 and whiB7*) in MABS and the phenotypic characterisation of the generated mutant strains (section 4.5).

4.1 Generation of reporter NTM strains

Reporter plasmid pMN437, which harbours the *eGFP* gene, was introduced into Msmeg, MABS and MAH by electroporation to generate the reporter strains listed in Table 15.

Table 15 Name of reporter strains.

Name of Strains	Reporter plasmid	Reporter strains
MABS	pMN437	MABS (pMN437)
MAH P-09/13	pMN437	MAH P-09/13 (pMN437)
MABS P-09/13	pMN437	MABS P-09/13 (pMN437)

4.2 Gene silencing with CRISPRi in reporter NTM

The experiments described above aimed at confirming the functioning of the mechanism of CRISPRi in NTM by measurement of fluorescence as an indicator for *eGFP* expression using flow cytometry. The reduction in expression was calculated by determining the percentage of fluorescence from the samples with ATc compared to the sample without ATc.

4.2.1 *eGFP* gene silencing by CRISPRi/dCas9 in reporter *M. smegmatis*

We first tested the CRISPRi vectors pSAK8 and pSAK9 targeting different sites in the *eGFP* gene for their ability to inhibit gene expression in the reporter strain Msmeg (pMN437). Within groups, the reduction was calculated by determining the percentage of fluorescence from the samples with ATc compared to the sample without ATc. The negative control wild type Msmeg (WT) had the lowest fluorescence, and the positive control reporter strain Msmeg (pMN437) had the highest fluorescence. Furthermore, it was evident, that transformation with the plasmids pLJR962, pSAK8, and pSAK9 already slightly influenced the gene expression even without ATc induction. Noticeably, the fluorescence intensity of the positive control increased with longer incubation times. The three plasmids pLJR962, pSAK8, and pSAK9, sharing the identical plasmid backbone, had effects on *eGFP* gene expression (pLJR962 with induction only after eight days). In contrast with pLJR962, greater reductions in fluorescence intensities could be achieved with the other plasmids pSAK8 and pSAK9. With pSAK8 and pSAK9, a downregulation of more than 50 % was detected with 50 ng/ml ATc and 100 ng/ml ATc after eight days (Figure 11).

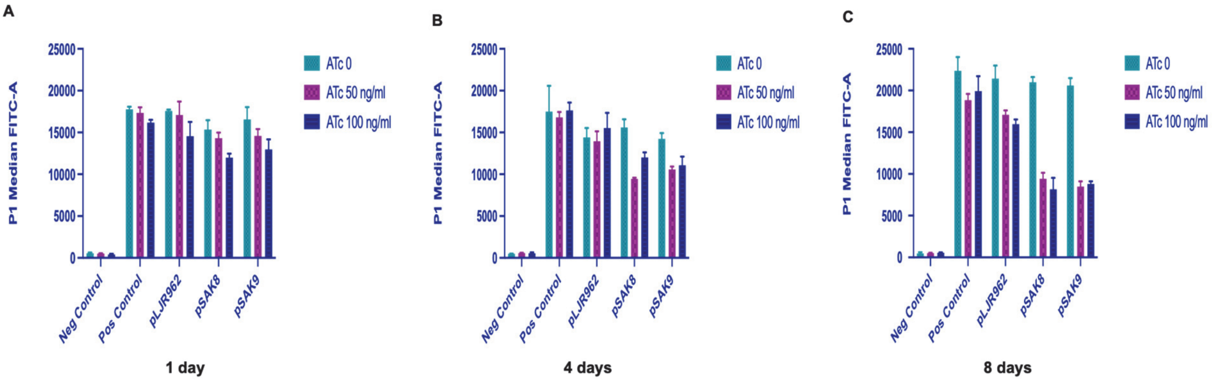

Figure 11 Down-regulation of e*GFP* expression in *M. smegmatis* mc^{2}155 broth cultures.

Except for the negative control, all strains contained the reporter plasmid pMN437. Additional plasmids present in Msmeg are shown on the x-axis; fluorescence intensity is displayed on the y-axis. ATc 0, ATc 50 ng/ml, and ATc 100 ng/ml indicate the amount of Anhydrotetracycline added to the cultures every 24 hours. The negative control was the Msmeg without reporter plasmid pMN437. The positive control was the Msmeg with reporter plasmid pMN437. The pLJR962 was the Msmeg with the reporter plasmid pMN437 with the *eGFP* gene and with pLJR962 (without sgRNA oligo). A) FACS results from 1-day incubation, B) from 4 days, and C) from 8 days. The reporter strain Msmeg with the plasmids pSAK8 and pSAK9 showed greater effects on fluorescence after 4 and 8 days compared to pLJR962. Data are means ± standard deviation of the results from three independent experiments with three technical repetitions.

Figure 12 demonstrates that electroporation with plasmid pLJR962 results in 97.24 % of the *eGFP* gene being expressed at 50 ng/ml ATc and 82.90 % at 100 ng/ml ATc after a single day. *eGFP* gene expression achieved after four days with an ATc concentration of 50 ng/ml was 97.67 % and 108.77 % with a concentration of 100 ng/ml ATc. After eight days, the expression of *eGFP* gene of 79.98 % was measured with 50 ng/mL Atc and 74.81 % expression was seen at ATc 100 ng/ml.

For the plasmid, pSAK8, after 1 day, the expression of *eGFP* gene of 93.54 % was measured with 50 ng/ml ATc and 78.30 % at ATc 100 ng/ml. *eGFP* gene expression achieved after four days with an ATc concentration of 50 ng/ml was 60.77 % and 77.10 % with a concentration of 100 ng/ml ATc. After eight days, the expression of *eGFP* gene of 44.93 % was measured with 50 ng/mL Atc and 38.77 % expression was seen at ATc 100 ng/ml.

And for the plasmid, pSAK9, after 1 day, the expression of the *eGFP* gene of 88.33 % was measured with 50 ng/ml ATc and 78.35 % at ATc 100 ng/ml. *eGFP* gene expression achieved after four days with an ATc concentration of 50 ng/ml was 74.25 % and 77.95 % at a concentration of 100 ng/ml ATc. After eight days, the expression of the *eGFP* gene 41.31 % was measured with 50 ng/ml Atc and 42.80 % expression was seen at ATc 100 ng/ml.

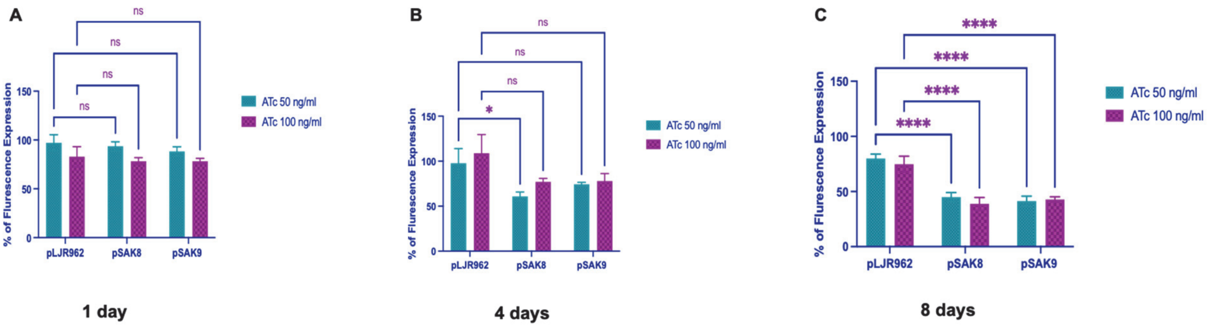

Figure 12 Expression of the *eGFP* gene in reporter *M. smegmatis* broth cultures with induction by ATc.

Expression of the *eGFP* gene in reporter Msmeg broth cultures with incubation by ATc for (A) 1 day, (B) 4 days, and (C) 8 days compared to uninduced cultures and shown as “% of Fluorescence Expression” by the y-axis. ATc 50 ng/ml, and ATc 100 ng/ml indicate the amount of anhydrotetracycline added to the cultures every 24 hours. The greatest downregulation was achieved with plasmid pSAK8 and pSAK9. Highly significant downregulation by the plasmids with sgRNA compared to the vector control with pLJR962 was only obtained after 8 days. The fluorescence expression of *eGFP* at two different ATc concentrations of 50 ng/ml and 100 ng/ml using pSAK8 was 93.54 and 78.30 % after 1 day, 60.77 and 77.10 % after 4 days, and 44.93 and 38.77 % after 8 days. At two different ATc concentrations of ATc 50 ng/ml and ATc 100 ng/ml, fluorescence expression in pSAK9 was 88.33 and 78.35 % after 1 day, 74.25 and 77.95 % after 4 days, and 41.31 and 42.80 % after 8 days. Data are means ± standard deviation of the results from three independent experiments with three technical repetitions each using Two-way Anova *P < 0.05; **P < 0.01; ***P < 0.001; ****P < 0.0001. each using Two-way Anova *P < 0.05; **P < 0.01; ***P < 0.001; ****P < 0.0001.

As seen in Figure 12, plasmids pLJR962, pSAK8, and pSAK9 in Msmeg had little or no effect on *eGFP* gene expression in induced cultures after one day of cultivation. After four days of incubation, in bar graph B, a significant effect was only seen in the pSAK8 with 50 ng/ml ATc and with 100 ng/ml ATc no significant effect. For pSAK9 *eGFP* gene expression was not significant for both ATc concentrations of 50 ng/ml and 100 ng/ml. The results after eight days showed that 50 ng/ml and 100 ng/ml ATc produced a similar effect for both pSAK8 and pSAK9, which was highly significant (P < 0.0001). According to these results, both plasmids and ATc concentrations performed equally well. A concentration of 50 ng/ml ATc is sufficient to reduce *eGFP* gene expression by these CRISPRi plasmids and 8 days is enough for the highest reduction.

4.2.2 *eGFP* gene silencing by CRISPRi/dCas9 in reporter *Mycobacterium avium hominissuis*

Based on these successful pilot experiments with the Msmeg reporter strain, this e*GFP* gene expression reduction system was investigated in depth in the NTM pathogen MAH. The same two sequences in the coding sequence from the e*GFP* gene were targeted as used for the down-regulation experiments with Msmeg. Down-regulation of e*GFP* in MAH P-09/13 (pSAK6) and MAH P-09-13 (pSAK7) was determined by Flow cytometry at serial time points (four, eight, and twelve days) in cultures induced with different ATC concentrations (100 ng/ml and 500 ng/ml) and in control cultures to which no inducer was added. The effects were assessed by comparing to the vector pLJR965 that did not include a sgRNA gene-specific targeting sequence. The positive control carried only the reporter plasmid pMN437 which has e*GFP* gene and showed the highest fluorescence intensity (Figure 13). Noticeable, the introduction of the plasmid pLJR965 without sgRNA already had a great effect on e*GFP* expression.

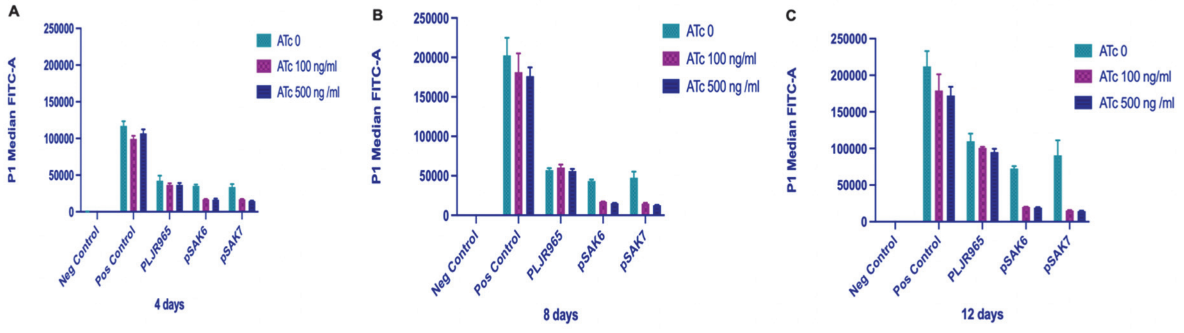

Figure 13 Down-regulation of e*GFP* expression in *Mycobacterium avium* subsp. *hominissuis* broth cultures.

Except for the Neg Control, all strains contained the reporter plasmid pMN437. Additional plasmids present in MAH are shown on the x-axis and the fluorescence intensity is on the y-axis. ATc 0, ATc 100 ng/ml, and ATc 500 ng/ml indicate the amount of anhydrotetracycline added to the cultures every 4 days. The Neg control was the MAH without reporter plasmid pMN437. The positive control was the MAH with reporter plasmid pMN437. Further strains were the reporter strain MAH with the plasmids pLJR965 (without sgRNA oligo) the reporter strain MAH with the plasmids pSAK6 or pSAK7 (with sgRNA oligo of the *eGFP* gene) A) FACS results from 4-day incubation, B) from 8 days and C) from 12 days. The reporter strain MAH with the plasmids pSAK6 and pSAK7 showed greater effects on fluorescence after 8 and 12 days compared to pLJR965. Data are means ± standard deviation of the results from three independent experiments with three technical repetitions.

Unfortunately, the problem with MAH and pLJR965 is mainly that even without induction the plasmid reduced expression.

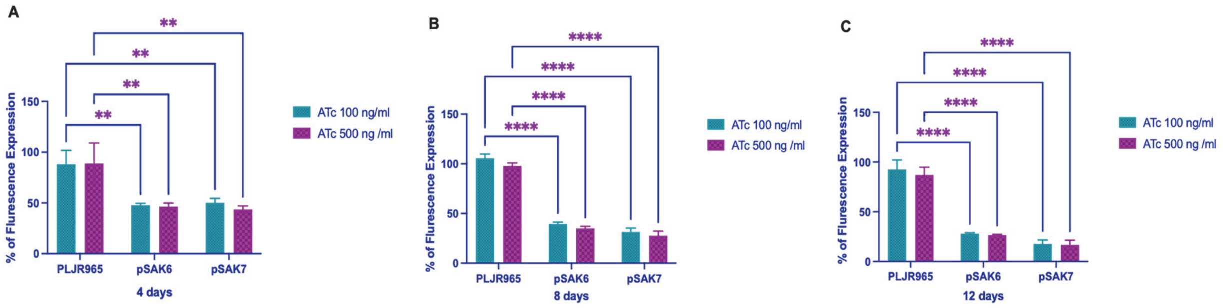

Figure 14 Expression of the *eGFP* gene in reporter *Mycobacterium avium* subsp. *hominissuis* broth cultures with induction by ATc.

Expression of the *eGFP* gene in reporter MAH broth cultures with induction by ATc for (A) 4 days, (B) 8 days, and (C) 12 days compared to uninduced cultures and shown as “% of Fluorescence Expression” by the y-axis. ATc 100 ng/ml, and ATc 500 ng/ml indicate the amount of anhydrotetracycline added to the cultures every 4 days. The greatest downregulation was achieved with plasmids pSAK6 and pSAK7. Highly significant downregulation by the plasmids with sgRNA compared to the vector control with pLJR965 was only obtained after 8 days. The fluorescence expression of *eGFP* at two different ATc doses of 100 ng/ml and 500 ng/ml using pSAK6 was 47.84 and 46.49 % after 4 days, 39.37 and 35.07 % after 8 days, and 27.33 and 26.50 % after 12 days. At two different ATc concentrations of ATc 100 ng/ml and ATc 500 ng/ml, fluorescence expression in pSAK7 was 50.19 and 43.74 % after 4 days, 31.45 and 27,64 % after 8 days, and 17.52 and 16.71 % after 12 days. Data are means ± standard deviation of the results from three independent experiments with three technical repetitions each using Two-way Anova *$P < 0.05$; **$P < 0.01$; ***$P < 0.001$; ****$P < 0.0001$.

According to Figure 14, electroporation with the plasmid pLJR965 causes the *eGFP* gene to fluorescence expressed at levels of 88.24 % at 100 ng/ml ATc and 88.93 % at 500 ng/ml ATc compared to uninduced cultures after four days, which is a nearly identical effect. After eight days, the *eGFP* gene fluorescence expressed was 105.69 % at an ATc concentration of 100 ng/ml and 97.93 % at a concentration of 500 ng/ml ATc. After twelve days, the fluorescence expression of *eGFP* gene 92.53 % was measured with 100 ng/ml ATc and 87.10 % fluorescence expression was seen at ATc 500 ng/ml.

After four days, the fluorescence expression of the *eGFP* gene in the plasmid pSAK6 amounted to 47.84 % with 100 ng/ml ATc and 46.49 % with 500 ng/ml ATc. After eight days, the *eGFP* gene fluorescence expression was 39.37 % at an ATc concentration of 100 ng/ml and 35.07 % at a concentration of 500 ng/ml ATc. After twelve days, the *eGFP* gene's fluorescence expression reached a maximum of 27.33 % at an ATc concentration of 100 ng/ml and 26.50 % at a concentration of 500 ng/ml ATc.

With plasmid pSAK7, the fluorescence expression of the *eGFP* gene was measured at 50.19 % at 100 ng/ml ATc and 43.74 % at 500 ng/ml ATc after four days. After eight days, *eGFP* gene expression at an ATc concentration of 100 ng/ml was 31.45 %, and it decreased to 27,64 % at a concentration of 500 ng/ml ATc. The fluorescence expression of the *eGFP* gene after twelve days was 17.52 % at an ATc concentration of 100 ng/ml and 16.71 % at a concentration of 500 ng/ml ATc.

Figure 14 shows that after four days of cultivation, the *eGFP* gene expression in induced cultures was significantly affected (**P 0.01) by the plasmids pSAK6, and pSAK7 in reporter MAH. A highly significant effect (****P 0.0001) was observed in the pSAK6 and pSAK7 with 100 ng/ml ATc and with 500 ng/ml ATc after eight days of incubation, as shown in bar graph B. Results after 12 days revealed a highly significant (****P 0.0001) comparable response to ATc at 100 ng/ml and 500 ng/ml for both pSAK6 and pSAK7. These results showed that plasmids and ATc concentrations behaved similarly. With a concentration of 100 ng/ml ATc, these CRISPRi plasmids can suppress the expression of the *eGFP* gene by around 80 %, and 12 days are needed for the highest suppression.

4.2.3 *eGFP* gene silencing by CRISPRi/dCas9 in reporter *M. abscessus*

Based on these successful pilot experiments with the Msmeg reporter strain, this e*GFP* gene expression reduction system was investigated in depth in the NTM pathogen MABS also. The same sequences in the coding sequence from the e*GFP* gene were targeted as used for the down-regulation experiments with Msmeg. Down-regulation of e*GFP* in MABS P-09/13 (pSAK9) was determined by Flow cytometry at serial time points (one, four, and eight days) in cultures induced with different ATC concentrations (50 ng/ml and 100 ng/ml) and in control cultures to which no inducer was added. The effects were assessed by comparing to the vector pLJR962 that did not include a sgRNA gene-specific targeting sequence in the reporter MABS strain with plasmid pMN437. The positive control carried only the reporter plasmid pMN437, which has e*GFP* gene and showed the highest fluorescence intensity (Figure 15). It was noticeable that the introduction of the plasmid pLJR962 without sgRNA had little effect on e*GFP* expression.

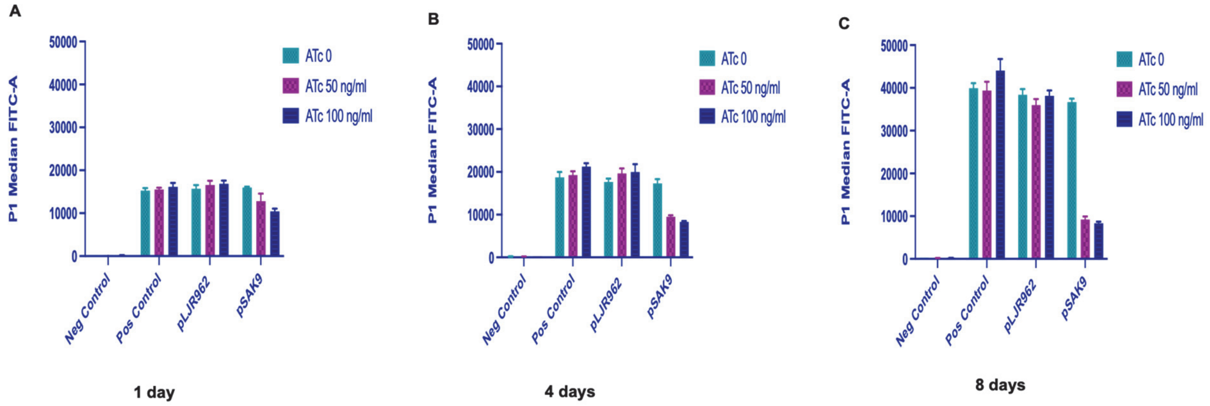

Figure 15 Down-regulation of e*GFP* expression in *M. abscessus broth* cultures.

Except for the Neg Control, all strains contained the reporter plasmid pMN437. Additional plasmids present in MABS are shown on the x-axis and the fluorescence intensity is on the y-axis. ATc 0, ATc 50 ng/ml, and ATc 100 ng/ml indicate the amount of anhydrotetracycline added to the cultures every 24 hours. The Neg control was the MABS without reporter plasmid pMN437. The positive control was the MABS with reporter plasmid pMN437. Further strains were the reporter strain MABS with the plasmid pLJR962 (without sgRNA oligo) and the reporter strain MABS with the plasmid pSAK9 (with sgRNA oligo of the *eGFP* gene). A) FACS results from 1-day incubation, B) from 4 days, and C) from 8 days. The reporter strain MABS with the plasmids pSAK9 showed greater effects on fluorescence after 4 and 8 days compared to pLJR962. Data are means ± standard deviation of the results from three independent experiments with three technical repetitions.

According to Figure 16, electroporation with the plasmid pLJR962 causes the *eGFP* gene to fluorescence expressed at levels of 106 % at 50 ng/ml ATc and 108 % at 100 ng/ml ATc after 1 day, which is a nearly identical effect. After four days, the *eGFP* gene fluorescence expressed was 111.55 % at an ATc concentration of 50 ng/ml and 113.56 % up to a concentration of 100 ng/ml ATc. After eight days, a fluorescence expression of *eGFP* gene of 93.73 % was measured with 50 ng/ml ATc and 99.5 % fluorescence expression was seen at ATc 100 ng/ml.

After one day, the fluorescence expression of the *eGFP* gene in the strain with plasmid pSAK9 was evaluated at 80 % with 50 ng/ml ATc and 65 % with 100 ng/ml ATc. After four days, the *eGFP* gene fluorescence expression was 55.03 % at an ATc concentration of 50 ng/ml and 48.03 % at a concentration of 100 ng/ml ATc. After eight days, the *eGFP* gene's fluorescence expression reached a maximum of 25.15 % at an ATc concentration of 50 ng/ml and 22.72 % at a concentration of 100 ng/ml ATc.

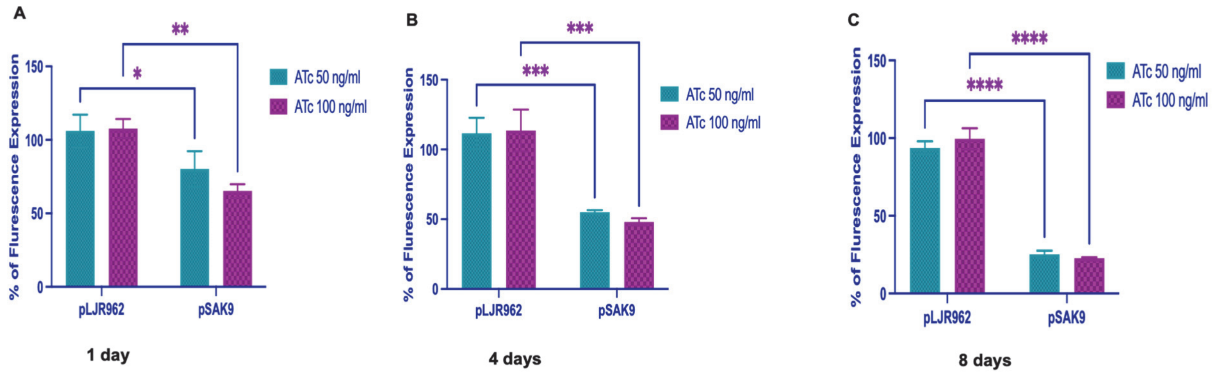

Figure 16 Expression of the *eGFP* gene in reporter *M. abscessus* broth cultures with induction by ATc.

Expression of the *eGFP* gene in reporter MABS broth cultures with induction by ATc for (A) 1 day, (B) 4 days, and (C) 8 days compared to uninduced cultures and shown as “% of Fluorescence Expression” by the y-axis. ATc 50 ng/ml and ATc 100 ng/ml indicate the amount of anhydrotetracycline added to the cultures every 24 hours. The greatest downregulation was achieved with plasmid pSAK9. Highly significant downregulation by the plasmid with sgRNA compared to the vector control with pLJR962 was only obtained after 8 days. The fluorescence expression of *eGFP* at two different ATc doses of 50 ng/ml and 100 ng/ml using pSAK9 was 80 % and 65 % after 1 day, 55 and 48 % after 4 days, and 25 and 22.70 % after 8 days. Data are means ± standard deviation of the results from three independent experiments with three technical repetitions each using Two-way Anova *P < 0.05; **P < 0.01; ***P < 0.001; ****P < 0.0001.

Figure 16 shows that after four days of cultivation, the *eGFP* gene expression in induced cultures was significantly affected (***P < 0.001) by the plasmid pSAK9 in reporter MABS. A strong significant effect (****P 0.0001) was observed in the pSAK9 with 50 ng/ml ATc and with 100 ng/ml ATc after eight days of incubation, as shown in bar graph Figure-16C. Results after 8 days revealed a highly significant (****P 0.0001) comparable response to ATc at 50 ng/ml and 100 ng/ml for pSAK9. These results showed that both ATc concentrations behaved similarly. With a concentration of 50 ng/ml ATc, the pSAK9 plasmid can suppress the expression of the *eGFP* gene, and 8 days are needed for the highest suppression.

4.3 Generation of CRISPR plasmid pSAK14

To generate CRISPR plasmid pSAK14 and to restore the catalytically active Cas9Sth$_1$, the vector pLJR965 was used as a template. The alanine at position 9 (GCC) was changed into aspartic acid (GAC) (A9D) and the alanine at position 599 (GCC) was changed into a histidine (CAC) (A599H), transforming dCas9Sth$_1$ into a nuclease-active form Cas9Sth$_1$ using the Q5® site-directed mutagenesis kit from New England Biolabs, Ipswich, MA, USA. Site-directed mutagenesis was validated by PCR and Sanger sequencing (Figure 17). The resulting plasmid was called pSAK14 and the protein has endonuclease activity encoded by Cas9.

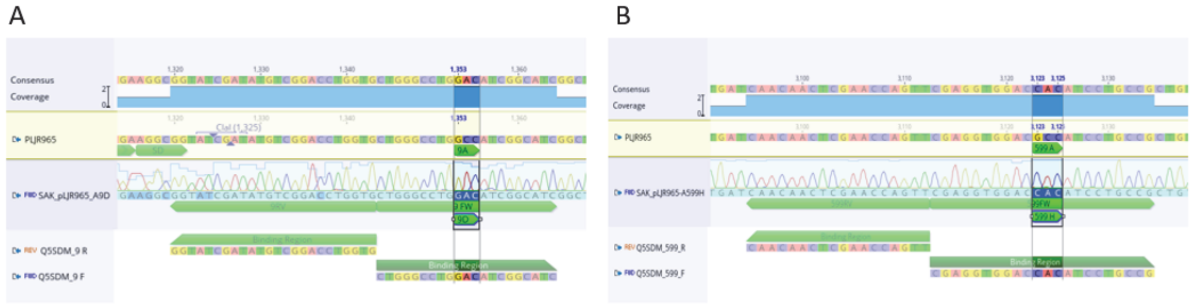

Figure 17 Site-directed mutagenesis was validated by PCR and sanger sequencing.

4.3.1 Generation of plasmid pSAK12 for *eGFP* gene knockout

A plasmid named pSAK12 was created by inserting GFP2 oligo (**Tables 3 and 4**) into the BsmBI sites of pSAK14 as a backbone vector. To target the *eGFP* gene for knockout pSAK12 was introduced by electroporation into Msmeg mc^{2}155 (pMN437), MABS 09-13-3 (pMN437), and MAH 09-13-3 (pMN437). Non-functional e*GFP* gene mutants are easily distinguished as white colonies in contrast to the green NTM containing pMN437.

4.4 CRISPR-mediated knock-out mutagenesis in reporter in NTM

4.4.1 CRISPR-mediated gene knock-out in *M. smegmatis*

The vector pSAK12 was transformed into the reporter strain Msmeg (pMN437). After the transformation, the cells were plated on MB 7H10 agar supplemented with mADC, the appropriate antibiotics, and either without ATc or with 50 ng/ml ATc or with 100 ng/ml ATc. The plates were incubated for 7 to 10 days at 37°C, and white colonies were then picked for PCR and sequencing analysis. When targeting the *eGFP* gene, the editing efficiency was calculated as the frequency of *eGFP* negative (white) transformants among all obtained colonies.

When transforming Msmeg (pMN437) with pSAK12 without the addition of ATc to the selection plates, a reduced number of transformants was obtained with only 5 white colonies and 1 green colony in comparison to transformants carrying the control vector pSAK14 containing no sgRNA (~ 45 Green colonies) (Table 16). When ATc was added to the medium, no colonies were achieved for pSAK12, while with pSAK14 the same number of colonies was achieved with and without the addition of ATc. Next, we investigated whether genome editing by deletion/insertion/base exchange had occurred in the white transformants carrying the functional CRISPR/Cas9 system with the sgRNA targeting the *eGFP* gene. Following electroporation of the pSAK12, 83 % of the white colonies showed a deletion mutation in the *eGFP* gene (Table 16) in the absence of ATc induction. In the presence of ATc induction, no white colonies occurred. indicating that gene knockout in Msmeg using a sgRNA does not require induction of the CRISPR/Cas9 system by ATc.

Table 16 Mutation rate of the *eGFP* gene in *M. smegmatis* (pMN437) (pSAK12).

Plasmid	colonies without adding ATc	Successfully mutated colonies with gene deletion in *eGFP*	Mutation rates (%)
pSAK14	~45 green col	0	0
pSAK12	1 green, 5 white col	5	100 %

The results indicate that gene editing using CRISPR/Cas9 was successful even without ATc induction, likely attributed to the leaky expression of the CRISPR/Cas9 system. So far, our strategy for identifying mutants has primarily involved the use of visual selection (white colonies in blue light) methods. We also performed PCR amplification combined with Sanger sequencing to establish what types of mutations were generated in these non-functional e*GFP* mutants. Analysis of the amplified genomic target regions revealed that 2-20 bp deletions (100%) occurred at the location of the sgRNA target site (Figure 18).

		Del (bp)	Position
WT	GACGGTGACGTCAACGGCCACAAGTTCTCCGTCTCCGGCGAGGGTGAGGGCGACGCCACCTACGGCAA	-	
Mut 1	GACGGTGACGTCAACGGCCACAAGTTCTCCGTC - - CGGCGAGGGTGAGGGCGACGCCACCTACGGCAA	2	89-90
Mut 2	GACGGTGACGTCAACGGCCACAAGTTCTCCGTC - - CGGCGAGGGTGAGGGCGACGCCACCTACGGCAA	2	89-90
Mut 3	GACGGTGACGTCAACGGCCACAAGTTCTCCGTC - - CGGCGAGGGTGAGGGCGACGCCACCTACGGCAA	2	89-90
Mut 4	GACGGTGACGTCAACGGCCACAAGTTCTCCGTC - - CGGCGAGGGTGAGGGCGACGCCACCTACGGCAA	2	89-90
Mut 5	GACGGTGACGTCAACGGCCACAAGTTCTCCGTC - GACGCCACCTACGGCAA	18	89-105

Figure 18 Sanger sequencing of mutations of e*GFP* mutants in *M. smegmatis* (pMN437) (pSAK12).

The figure shows the region of the *eGFP* gene around the PAM site next to GFP2 oligo. PAM site (red), GFP2 oligo 21 bp (yellow). WT: Msmeg (pMN437).

4.4.2 CRISPR- gene knock-out in *Mycobacterium avium* subsp. hominissuis

Since CRISPR/Cas9-mediated *eGFP* gene knock-out was efficient in Msmeg, we investigated whether the same system could be employed in a MAH reporter strain. The vector pSAK12 was transformed into the reporter strain MAH P-09/13 (pMN437). After the transformation the cells were plated on 7H10 agar supplemented with OADC, the appropriate antibiotics, and without ATc, with 100 ng/ml ATc or with 500 ng/ml ATc. The plates were incubated for 14 to 20 days at 37°C, and 254 green colonies and 10 white colonies were found on the plates without ATc, and then only white colonies were picked for PCR and sequencing analysis. Each time, all white colonies were picked for PCR and sequencing analysis.

Table 17 Mutation rate of the *eGFP* gene in *Mycobacterium avium* subsp*. Hominissuis* (pMN437) (pSAK12).

Plasmid	colonies without adding ATc	Successfully mutated colonies with gene deletion	Mutation rates in white colonies(%)	Mutation rates in all colonies(%)
pSAK14	>1000 green col no white col	0	0	0
pSAK12	254 green col 10 white col	8	(8/10) 80 %	(8/264) 3 %

For pSAK14 as a control without any *eGFP* gene oligo, we could not find any white colony, while for pSAK12 with *eGFP* gene oligo, we found 10 white colonies on plates without ATc induction. For *eGFP* gene targeted in reporter MAH, mutation rates were 80 % if related to the number of white colonies and 3 % if related to the number of all colonies obtained (Table 17). In reporter MAH, predominantly small deletion events between 2 to 13 bp occurred at the cleavage site (Figure 19).

		Del (bp)	Position
WT	GACGGTGACGTCAACGGCCACAAGTTCTCCGTCTCCGGCGAGGGTGAGGGCGACGCCACCTACGGCAA	-	
Mut 1	GACGGTGACGTCAACGGCCACAAGTTCTCCGTC--CGGCGAGGGTGAGGGCGACGCCACCTACGGCAA	2	6124-6126
Mut 2	GACGGTGACGTCAACGGCCACAAGTTCTCCGTC---------GGGTGAGGGCGACGCCACCTACGGCAA	8	6119-6126
Mut 3	GACGGTGACGTCAACGGCCACAAGTTCTCCGTC----------GGTGAGGGCGACGCCACCTACGGCAA	9	6118-6126
Mut 4	GACGGTGACGTCAACGGCCACAAGTTCTCCGTCA--------------AGGGCGACGCCACCTACGGCAA	1bp in 12 bp del	6114-6125
Mut 5	GACGGTGACGTCAACGGCCACAAGTTCTCCGTCA--------------AGGGCGACGCCACCTACGGCAA	1bp in 12 bp del	6114-6125
Mut 6	GACGGTGACGTCAACGGCCACAAGTTCTCCGTCA--------------AGGGCGACGCCACCTACGGCAA	1bp in 12 bp del	6114-6125
Mut 7	GACGGTGACGTCAACGGCCACAAGTTCTCCGTC---------------AGGGCGACGCCACCTACGGCAA	13 del	6114-6126
Mut 8	GACGGTGACGTCAACGGCCACAAGTTCTCCGTC---------------AGGGCGACGCCACCTACGGCAA	13 del	6114-6126

Figure 19 Sanger sequencing of mutations of *eGFP* mutants in *Mycobacterium avium* subsp. *hominissuis (*pMN437) (pSAK12).

The figure shows the region of the *eGFP* gene around the PAM site next to GFP2 oligo. PAM site (red), GFP2 oligo 21 bp (yellow). WT: MAH (pMN437).

This shows that CRISPR/Cas9-assisted gene editing was already effective in the absence of ATc induction, most likely as a result of the CRISPR/Cas9 system's leaky expression.

4.4.3 CRISPR-mediated gene knock-out in *M. abscessus*

Since CRISPR/Cas9-mediated *eGFP* gene knock-out was efficient in reporter Msmeg and MAH, we investigated whether the same system could be employed in the reporter strain MABS P-09/13 (pMN437). The vector pSAK12 was transformed into MABS P-09/13 (pMN437). After transformation, the cells were plated on 7H10 agar supplemented with mADC, the appropriate antibiotics, and without ATc, with 50 ng/ml ATc or with 100 ng/ml ATc. The plates were placed in an incubator and allowed to grow for a period of 7 to 10 days at a temperature of 37°C. Subsequently, white colonies were selected and picked for further analysis through PCR and sequencing. In the reporter MABS strain, we obtained only one white colony with ATc 50 ng/ml and one in ATC 100 ng/ml. After performing PCR amplification of the *eGFP* gene target regions no PCR products were found. A possible explanation is that the plasmid pMN437, which does not integrate into the genome of MABS was lost.

4.5 Testing the performance and specificity of the CRISPR knock-out system with an endogenous gene from *M. abscessus*

To further explore the performance of this CRISPR/Cas9-mediated gene knock-out system in MABS P09/13-3 (smooth), sgRNAs were designed to target the *mps1* gene. The *mps1* gene contributes to the synthesis of GPL. The loss of GPL production or transport converts smooth to rough morphologies in MABS. Therefore, non-functional *mps1* mutants are easily distinguished as rough colonies in contrast to the smooth wildtype (WT) MABS P09/13-3 colonies.

The entire length of the *mps1* gene (MAB_4099c) is 10365 base pairs. The wild-type gene version is present in the strain MABS P09/13-3 that was obtained from a respiratory sample from a patient with Cystic Fibrosis (Lewin et al. 2021). The *mps1* gene was knockout-mutated using the CRISPR/Cas9 technology in the isolate MABS P09/13-3 (smooth). As anticipated most efficient PAM site, the sequence 5´ NNAGAAG 3´ in the gene was selected, which was next to the chosen target sequence of mps1 (position 6885-6905) (Figure 20) The oligo (Figure 20) (Table 4) was cloned into the BsmBI site of pSAK14 to generate plasmid pSAK33.

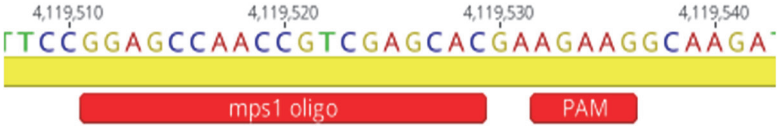

Figure 20 Target region of *mps1* for knockout by CRISPR/Cas9.

The vector pSAK33 was electroporated into MABS P09/13-3 (smooth) to knock out the gene Mab_4099c (*msp1*) using kanamycin 100 µg/ml and hygromycin 100 µg/ml for selection and with ATc (100 ng/ml) for induction and without ATc. The vector pSAK14 without oligo served as a control. All rough colonies were picked from selective plates. From those, a colony PCR using primers for the amplification of Cas9 was conducted with subsequent gel electrophoresis to check if the electroporation had been successful. From strains successfully electroporated with pSAK33, a part of the *mps1* gene was amplified by colony PCR and the PCR product was sequenced by Sanger sequencing. The reads were mapped to *mps1* gene from MABS P09/13-3 as a reference to check for mutations. The type of mutation was named by its position within the *mps1* gene followed by the type of mutation (insertion, deletion) and the affected nucleotides, respectively. As anticipated, we observed a lower number of transformants when using our targeting construct compared to transformants carrying the control vector pSAK14, which does not contain a specific guide RNA (sgRNA). This difference is likely attributable to the induction of double-stranded DNA breaks, which may lead to bacterial cell death, thereby reducing the overall number of successful transformants.

Next, we investigated whether genome editing causing knock-out mutations had occurred in the transformants carrying the functional CRISPR/Cas9 system. Following electroporation of the pSAK33, 21.05 % of the colonies showed the phenotype of *mps1* mutants (rough colony morphology) in MABS P09/13-3 without adding ATc. With the addition of 50 ng/ml ATc the number of rough colonies increased to 37.50 % and with 100 ng/ml ATc 42.85 % rough colonies were found (Table 18).

Table 18 Total number of rough colonies after electroporation with pSAK33.

MABS P09/13-3 (pSAK33)	Ratio Rough Colonies /Total Colonies	% of Rough Colonies
No ATc	4/19	21.05 %
ATc 50 ng/ml	6/16	37.50 %
ATc 100 ng/ml	9/21	42.85 %

With 50 ng/ml ATc induction, the *mps1* mutants were increased to 83 % of rough colonies, and at 100 ng/ml ATc to 100 % (Table 19). This effect was observed following ATc treatment for 10 days on plates.

Table 19 CRISPR/Cas9-mediated knockout of *mps1* gene (Mab_4099c) in MABS 09/13-3.

Plasmid	Induction medium	No. of Rough Colonies	No. of of mutant colonies	% of mutant colonies from all rough colonies
pSAK14 (Control)	No ATc	4	0	0
	ATc 50 ng/ml	5	0	0
	ATc 100 ng/ml	5	0	0
pSAK33	No ATc	4	0	0 %
	ATc 50 ng/ml	6	5	83 %
	ATc 100 ng/ml	9	9	100 %

4.5.1 Analysis of the off-target activity of CRISPR in *M. abscessus*

To test, if off-target mutations have occurred in the *mps1* knock-out mutants, we performed whole-genome sequencing by Illumina sequencing on 14 *mps1* knock-out mutants, MABS 09/13-3 (pSAK14) stock no 327 and stock no 328 as control strains and the MABS 09/13-3 WT strain (stock no 7). Among the 14 *mps1* knock-out mutants, only one (number 322 in Table 21) exhibited an additional mutation (in gene MAB_3167c), demonstrating that the CRISPR approach based on pSAK14 was very satisfying with respect to its specificity. A surprising finding was the mutation in the *rrs* gene that was found in the control strains.

Table 20 Specificity of knockout mutagenesis of *mps1* gene.

Mutations in knock-out mutants and controls (No. 327 and 328) compared to the WT (No. 7) were identified by WGS and genome comparison.

stock No.	Isolates	Mutated genes	Mutation (INDEL) in mps1
7	wild type MABS 09/13-3		
308	Wild type/Mut 308	mps1	862 bp deletion
309	Wild type/Mut 309	mps1	2164 bp deletion
311	Wild typeMut 311	mps1	12 bp deletion
312	Wild type/Mut 312	mps1	4 bp deletion
313	Wild type/Mut313	mps1, downstream of mps1	3151 bp deletion
314	Wild type/Mut314	mps1	1 bp insertion
318	Wild type/ Mut 318	mps1	55 bp deletion
319	Wild type/Mut 319	mps1	9 bp deletion
320	Wild type/Mut 320	mps1	21 bp deletion
321	Wild type/Mut 321	mps1	9 bp deletion
322	Wild type/Mut 322	mps1, MAB_3167c	1 bp deletion
323	Wild type/Mut 323	mps1	1 bp insertion
324	Wild type/Mut 324	mps1	29 bp deletion
325	Wild type/Mut 325	mps1	4757 bp deletion
327	Wild type/Control 327	rrs (16S rDNA)	No mutation in mps1
328	Wild type/Control 328	rrs (16S rDNA)	No mutation in mps1

4.5.2 Phenotypic Characterization of *M. abscessus mps1* gene mutants

Wildtype MABS P 09-13/3, MABS P09/13-3 (pSAK14) as a control strain, and MABS P09/13-3 (pSAK33) *mps1* gene mutant stock no 318 were used for further phenotypic characterization (Table 21).

Table 21 List of *M. abscessus* strains used for phenotypic characterization.

Strains Name	Description	*mps1* mutation according to WGS analysis
MABS 09/13-3	WT	No mutation
MABS 09/13-3 (pSAK33) KO	*mps1* gene mutant (318)	55 bp deletion
MABS 09/13-3 (pSAK14)	Control (328)	No mutation

4.5.2.1 Morphology pattern of *mps1* mutants

While the wild-type MABS P 09-13/3 formed smooth colonies, the *mps1* mutant MABS P09/13-3(pSAK33) exhibited rough, dry, and irregular colonies. The colonies of the MABS P09/13-3 (pSAK14) as a control strain were smoothly curved and wet (Figure 21). It was concluded that the *mps1* gene knockout affected bacterial morphology.

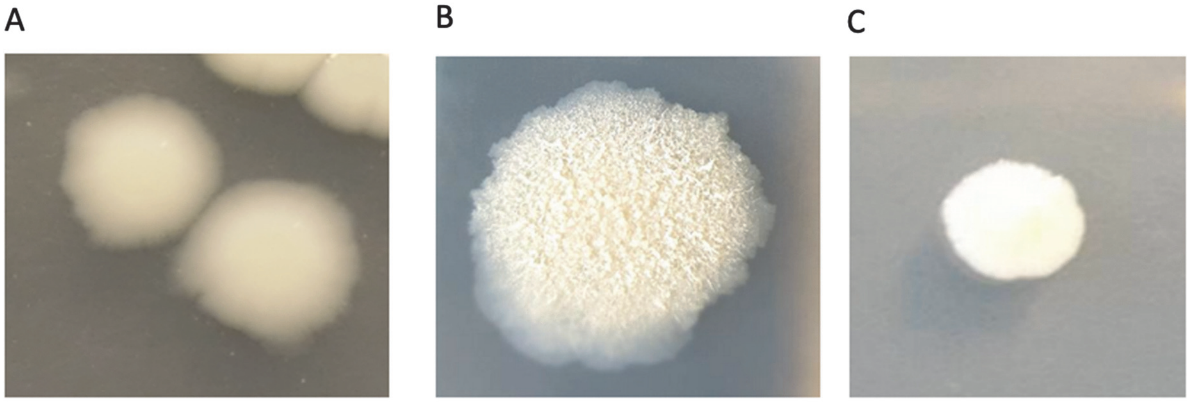

Figure 21 Change of morphology by *mps1* mutation.

(A) The MABS P09/13-3 WT formed smooth wet colonies. (B) The *mps1* mutant MABS P09/13-3(pSAK33) formed rough, dry, and irregular colonies. (C) The MABS P09/13-3(pSAK14) as a control also formed smooth and wet colonies.

4.5.2.2 GPL pattern of *mps1* mutants

To better characterize the effects of the *mps1* mutation we extracted the GPLs of the MABS strains. Thin-layer chromatography was used to visualize the different patterns of GPL expression from the wild-type, one mutant, and control strain (Figure 22). TLC analysis showed that GPLs were strongly reduced to absence only in the *mps1* mutant while they were equally abundant in the remaining strains. The mutation due to knockout in the *mps1* gene in the MABS P09/13-3 mutant thus has modified the cell wall construction. The lack of GPLs in the *mps1* mutant strain proved that the *mps1* gene product is involved in the synthesis of GPL.

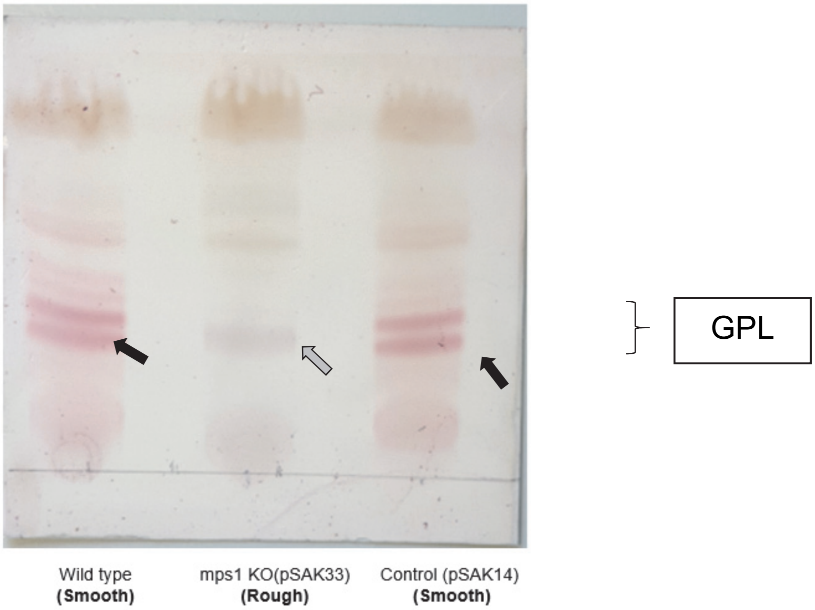

Figure 22 GPL expression of *M. abscessus* strains.

TLC of GPL extracted from MABS 09/13-3 strains. Wild type (Lane 1); *mps1* mutant (Lane 2) and control strain with MABS 09/13-3 (pSAK14) (Lane 3). Wild-type strain and control strain with pSAK14 both expressed similar GPL patterns whereas the *mps1* gene mutant did not express or expressed only very little amounts of GPL.

4.5.2.3 Antibiotic susceptibility of *mps1* mutant

The impact of the *mps1* gene mutation on the antibiotic susceptibility of the mutants was tested by measuring the MIC values for 15 clinically relevant antibiotics (Table 22). With the exception of amikacin, the susceptibility to the antibiotics was not significantly (3 dilution steps in the plate) different for the control strain and the mutant. The *mps1* mutant displayed a significant difference (3 dilution steps in the plate) in the susceptibility towards amikacin, in comparison to the control. One can hypothesize that the mutation in *mps1* could potentially cause alterations in the permeability of the cell wall, resulting in enhanced penetration of antibiotics and hypersensitivity. Another explanation may be the mutation in the *rrs* gene that was found in the control strain (Table 20).

Table 22 Antibiotic susceptibility of the MABS 09/13-3 strains control MABS 09/13-3 (pSAK14), and *mps1* mutant MABS 09/13-3 (pSAK33) mps1 KO.

Three tests were conducted, and this one provided a representative outcome.

Antibiotic	MIC (in µg/ml) of MABS 09/13-3 (pSAK14) Control	MIC (in µg/ml) of MABS 09/13-3 (pSAK33) mps1 KO
Amikacin	64	8
Amoxicillin/ Clavulanic Acid	64/32	64/32
Cefepime	32	32
Cefoxitin	32	64
Ceftriaxone	64	64
Ciprofloxacin	4	4
Clarithromycin	0,5	2
Doxycycline	16	16
Imipenem	32	64
Linezolid	16	8
Minocycline	8	8
Moxifloxacin	4	8
Tigecycline	0,5	0,5
Tobramycin	16	16
Trimethoprim/ Sulfamethoxazole	8/152	8/152

4.6 The knockout of additional four endogenous genes (*porin*, *ppiA*, *erm-41*, and *whiB7*) in *M. abscessus* by CRISPR/Cas9

After the successful knockout of the *mps1* gene in MABS P-09/13-3 by the CRISPR/Cas9 method, this same method was applied to another four endogenous genes, namely the *porin* gene MAB_1080*, ppiA, erm-41,* and *whiB7* in MABS 40/14-3 (Table 23). The oligos used for cloning of the sgRNA are listed in (Table 4).

Table 23 Additional four endogenous genes in *M. abscessus* selected for application of the CRISPR/Cas9 method.

Name of gene	Name of plasmid	Total Size (bp) of gene	PAM	Position of PAM from start codon
porin	pLH1	672	5´ AGAAG 3´	514 bp
ppiA	pSAK43	537	5´ GGAAG 3´	204 bp
erm-41	pSAK42	522	5´ GGAAA 3´ 5´ AGCAG 3´	475 bp 365 bp
whipB	pSAK46	285	5´ AGAAT 3´	200 bp

4.6.1 Knockout of the *porin* gene (Mab_1080) in isolate MABS 40/14-3

There are two *porin* genes found in MABS named *mmpA* (MAB_1080), and *mmpB* (MAB_1081). The gene *mmpA* MAB_1080 has a length of 672 bp in total. Using the CRISPR/Cas9 technology, MAB_1080 was knocked out in the isolate MABS 40/14-3. An appropriate sgRNA target sequence was designed with the highest expected PAM site efficiency. The PAM site 5’ AGAAG 3 consists of the five bases at position 507-511 followed by two spacer bases at position 512-513. The target sequence includes nucleotides at position 514-534 of the *porin* gene (Table 4). The plasmid pLH1 for *porin* gene knockout was prepared at RKI by Lena Hümmler.

The vector pLH1 was electroporated into MABS 40/14-3 to knock out the *porin* gene. The empty vector pSAK14 served as a control. Derived colonies were transferred to fresh selective agar plates supplemented with 100 µg/ml kanamycin, and 100 ng/ml ATc and only 100 µg/ml kanamycin without ATc. Thirty colonies were picked. From those, a colony PCR using primers for amplification of a part of Cas9 was conducted with subsequent gel electrophoresis to check if the electroporation was successful. From transformants successfully electroporated with pLH1, the whole *porin* gene MAB_1080 was amplified by colony PCR and sequenced by Sanger sequencing and mapped to MAB_1080 as a reference to check for mutations. The percentage of positive electroporation efficiency was high from all picked colonies, approximately 93.3 % without adding ATc and 96.6 % with adding ATc 100 ng/ml. Positive electroporation means that the plasmid pLH1 or pSAK14 successfully integrated into the genome of MABS 40/14-3 confirmed by PCR of the Cas9 gene (Table 24). Electroporation of pLH1 resulted in different rates of mutation, depending on the selective medium. Cells grown on ATc as an induction medium in addition to kanamycin showed a higher rate of compared to those without ATc of mutation (62 % compared to 39 %) as ATc induces the *cas9* promoter (Table 24).

Table 24 CRISPR/Cas9-mediated knockout of *porin* gene in MABS 40/14-3 strain.

pLH1/sgRNA-porin	**Ratio**	**% Mutants**
MABS 40/14-3	Mutants / positive Electroporant	Mutant
No ATc	11/28	39 %
ATc 100 ng/ml	18/29	62 %

From all mutations that occurred by the transformation of pLH1, a point mutation at site 515 within the *porin* gene manifesting as deletion of adenine was the most common. A deletion of guanine at site 517, a deletion of adenine and thymine at site 515-516 as well as an insertion of cytosine at site 517 occurred once, respectively. A large deletion of 403 base pairs could be found (114-517del) after plating on a selective medium containing ATc. For each type of mutation, one representative colony is exemplarily chosen in (Table 25).

To determine the impact on the protein expressed from the mutated genes MAB_1080, nucleotide sequences were translated to their Amino Acid (AA) sequence using Geneious Prime (Table 25). All mutations caused frameshifts and altered protein sequences, in the 400 bp deletion additionally a large proportion of the protein is missing.

Table 25 Type of mutation is listed as follows: type of mutation (deletion or insertion), site of mutation.

Strain	Deletion /Insertion	position of deletion/insertion
WT (MABS 40/14-8)	-	-
Mut 1	1bp (G) del	517
Mut 2	1 bp (C) insertion	517
Mut 3	2 bp (TA) del	516 -517
Mut 4	1bp (A) del	516
Mut 5	403 bp del	114-517

The 400 bp deletion mutant was used for further phenotypic analysis.

4.6.2 CRISPR/Cas9-mediated knockout of the *ppiA* gene in MABS 40/14-3 strain

The *ppiA* gene has a length of 537 bp in total. Using the CRISPR/Cas9 technology, it was knocked out in the isolate MABS 40/14-3. The PAM site 5 NNAGGAG 3´ was used for *ppiA* kockout. The target sequence includes nucleotides at positions 204-227 of the *ppiA* gene (Table 4).

The constructed vector pSAK43 was electroporated into MABS 40/14-3. All colonies (only 2 colonies) were picked from a selective plate with 100 µg/ml kanamycin and 100 ng/ml ATc. A colony PCR using primers for the amplification of a part of the *cas9* gene was conducted with subsequent gel electrophoresis to check if the electroporation was successful. After positive electroporation of pSAK43, the *ppiA* gene was compared with the WT gene by PCR and Sanger sequencing. One colony showed a deletion of 14 bp, the other of 17 bp (Table 26).

Table 26 Type of mutation in MABS 40/14-3 strain.

WT and mutant	Deletion /Insertion	position of deletion/insertion
WT (MABS 40/14-8)	-	-
Mut 1	14 bp del	14 bp del (207-220)
Mut 2	17 bp del	17 bp del (207-223)

4.6.3 CRISPR/Cas9-mediated knockout of the *erm-41* and *whiB7* genes in MABS 40/14-3 strain

For the *erm-41* gene knockout using the CRISPR/Cas9 technology in MABS 40/14-3 strain, the constructed vectors pSAK44, and pSAK45, (Table 3, Table 4) were electroporated into MABS 40/14-3. 30 colonies were picked from a selective plate with 100 µg/ml kanamycin and 100 ng/ml ATc and a colony PCR using primers for the amplification of a part of the *cas9* gene was conducted with subsequent gel electrophoresis to check if the electroporation was successful. After positive electroporation of pSAK44 and pSAK45, the *erm-41* was compared with the WT gene by PCR and Sanger sequencing. None of the colonies showed a deletion or insertion of *erm-41* gene. So, we did not get any *erm-41* gene knockout clone.

The vector pSAK46 was successfully electroporated in MABS 40/14-3 to knock down the *whiB7* gene (Table 3, Table 4) Then, we chose 30 colonies from a selective plate with 100 µg /ml kanamycin and 100 ng/ml ATc. To determine whether the electroporation was successful, a colony PCR employing primers for the amplification of a portion of the *cas9* gene was carried out, followed by gel electrophoresis. The *whiB7 g*ene was compared with the WT gene by PCR and sanger sequencing after successful electroporation of pSAK44. No colonies had insertions or deletions in the *whiB7* gene. Thus, no *whiB7* gene knockout clones were obtained.

4.7 Phenotypic characterisation of selected *porin* and *ppiA* gene mutants

Phenotypic assays were done for mutants that had been created by the CRISPR Cas9 knock-out method to discover a potential role of the genes in virulence and antibiotic resistance. Selected tests were used for phenotypic characterisation: (i) resistance towards low pH, (ii) resistance towards H_2O_2 (iii) resistance towards DETA-NO, (iv) determining antibiotic resistance/susceptibility (v) induction of cytokine secretion by infected THP-1 macrophages, and (vi) intracellular survival and growth in THP-1 macrophages. The selected MABS 40/14-3 (pLH1) Porin KO and MABS 40/14-3 (pSAK43) PpiA KO mutants underwent all phenotypic testing. The results for these mutants are reported below, in comparison to the MABS 40/14-3 (pSAK14) as a Control (Table 27).

Table 27 The strains used for phenotypic characterization in *M. abscessus.*

Name of strains	Description	Deletion
MABS 40/14-3 (pSAK14)	Control	-
MABS 40/14-3 (pLH1) Porin KO	*porin* gene KO	400 bp
MABS 40/14-3 (pSAK43) PpiA KO	*ppiA* gene KO	14 bp

4.7.1 Investigating pH resistance through Porin KO and PpiA KO *M. abscessus*

The resistance to low pH was examined by comparing the *porin* and *ppiA* mutants to the wild-type MABS strain. This assessment involved inoculating the strains into Middlebrook broth supplemented with mADC at two different pH levels, pH 5 and pH 7. The growth was measured over 10 days at 37°C by means of ATP quantification. (Figure 23 A) shows that the mutant MABS 40/14-3 (pLH1) Porin KO grew almost like the MABS 40/14-3 (pSAK14) (control) at neutral pH 7 and that there was no significant effect.

At low pH the control pSAK14 grew the same as the mutant MABS 40/14-3 (pLH1) Porin KO, there was also no significant effect (Figure 23 B).

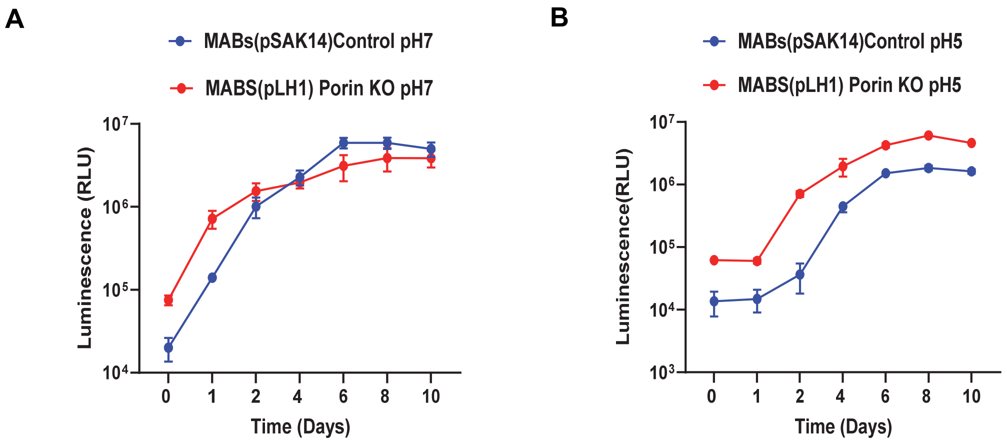

Figure 23 Resistance towards low pH of mutant MABS 40/14-3 (pLH1) Porin KO as compared to control MABS 40/14-3 (pSAK14).

A: MABS 40/14-3 pSAK14 (control) and mutant MABS 40/14-3 (pSAK43) Porin KO at neutral pH 7; B: MABS 40/14-3 pSAK14 (control) and mutant MABS 40/14-3 (pLH1) Porin KO at acidic pH 5 incubated for 10 days; the sensitivity towards the pH stresses were determined by measuring ATP production using a luminescence assay kit (BacTiter-Glo Microbial Cell Viability Assay, Promega). Data are means ± standard deviation of the results from three independent experiments, (performed in triplicates with three individual cultures per strain). No significant differences (P < 0.05, two-tailed, unpaired Student's t test) were detected.

The *ppiA* mutant MABS 40/14-3 (pSAK43) PpiA KO was analysed in the same way as the *porin* mutant. It showed a similar growth pattern as the MABS 40/14-3 (pSAK14) (control), both in neutral pH 7 and acidic pH 5 (Figure 24 A) and (Figure 24 B).

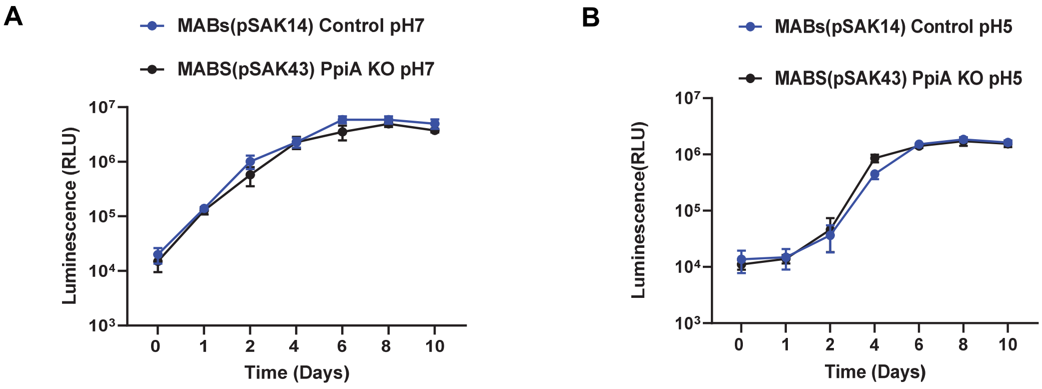

Figure 24 Resistance towards low pH of mutant MABS 40/14-3 (pSAK43) PpiA KO as compared to control MABS 40/14-3 (pSAK14).

A: MABS 40/14-3 pSAK14 (control) and mutant MABS 40/14-3 (pSAK43) PpiA KO at neutral pH 7; B: MABS 40/14-3 pSAK14 (control) and mutant MABS 40/14-3 (pSAK43) PpiA KO at acidic pH 5 incubated for 10 days; the sensitivity towards the pH stresses were determined by measuring ATP production using a luminescence assay kit (BacTiter-Glo Microbial Cell Viability Assay, Promega). Data are means ± standard deviation of the results from three independent experiments, (performed in triplicates with three individual cultures per strain). No significant differences (P < 0.05, two-tailed, unpaired Student's t test) were detected.

4.7.2 Effect of H2O2 on the growth and viability of Porin KO and PpiA KO in *M. abscessus*

The production of reactive oxygen and nitrogen intermediates by activated macrophages is a critical part of the human innate immune response during the infection process. Our MAB strains grown up to a mid-logarithmic phase were treated with hydrogen peroxide of 25 mM and 100 mM concentrations. After 4 hours of incubation, the ATP content was quantified using the BacTiter-Glo^{TM} Microbial Cell Viability Assay with reporting as relative light units (RLU). Considering the untreated to have a 100 % RLU, on the exposure to 25 mM H_2O_2 and 100 mM H_2O_2, the strain MABS 40/14-3 (pLH1) Porin KO was found to show a substantial decrease in cell viability compared to the control MABS 40/14-3 (pSAK14), which was significant for both concentrations (Figure 25 A). Considering the untreated to have a 100 % RLU, on the exposure to 25 mM H_2O_2 the control showed no reduction (108 %) but the Porin KO mutant was reduced to 69 % showing a highly significant difference in sensitivity. On the exposure to 100 mM H_2O_2, the control reduced to 86 % but the Porin KO mutant reduced to 53 % showing a significant difference in sensitivity.

On the other hand, for PpiA KO in MABS, on the exposure to 25 mM H_2O_2 and 100 mM H_2O_2 the control MABS 40/14-3(pSAK14) and MABS 40/14-3 (pSAK43) PpiA KO showed no significant difference in sensitivity (Figure 25 B). Considering the untreated to have a 100 % RLU, on the exposure to 25 mM H_2O_2 the control pSAK14 and PpiA KO mutant showed no reduction (108 % and 105 % respectively). On the exposure to 100 mM H_2O_2, the control reduced to 86 % but the Porin KO mutant reduced to 85 % showing no significant difference in sensitivity.

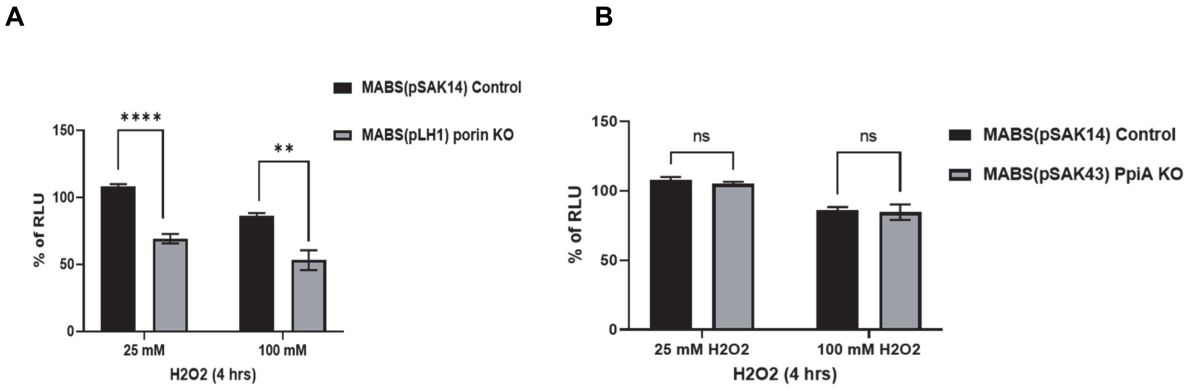

Figure 25 Effect of H_2O_2 stress on survival of the *M. abscessus* strains.

The strains used in the study, namely MABS 40/14-3(pSAK14) (Control), MABS 40/14-3 (pLH1) Porin KO, and MABS 40/14-3 (pSAK43) PpiA KO, were subjected to stress conditions by incubating them with H_2O_2 at concentrations of 25 mM and 100 mM for a duration of 4 hours. To assess their sensitivity to these stressors, the survival percentage was determined by measuring ATP production using a luminescence assay kit (BacTiter-Glo Microbial Cell Viability Assay, Promega). Data are means ± standard deviation of the results from three independent experiments, (performed in triplicates with three individual cultures per strain). $^*P < 0.05$; $^{**}P < 0.01$; $^{***}P < 0.001$; two-tailed, unpaired Student's t test.

4.7.3 Effect of DETA/NO on the growth and viability of Porin KO and PpiA KO mutants in *M. abscessus*

The sensitivity of the strains MABS 40/14-3 (pSAK14) (control), MABS 40/14-3 (pLH1) Porin KO, and MABS 40/14-3 (pSAK43) PpiA KO was also tested with a NO donor (25 mM DETA/NO) treatment for 4 hours incubation. Three independent experiments were normalized for 0 mM DETA/NO (expression ratio 100 %) to determine the % of RLU ratio for the mutants in comparison to MABS 40/14-3 (pSAK14) (control). The ATP quantification showed a significant difference between the strains MABS 40/14-3 (pSAK14) (control) and MABS 40/14-3 (pLH1) Porin KO exhibiting a decrease to 58 % and 32 %, respectively (Figure 26 A). On the other hand, The ATP quantification only showed a minor difference between the control strains MABS 40/14-3(pSAK14) and MABS 40/14-3 (pSAK43) PpiA KO mutant strain (a decrease to 58 % and 68 %, respectively), which was not significant (Figure 26 B).

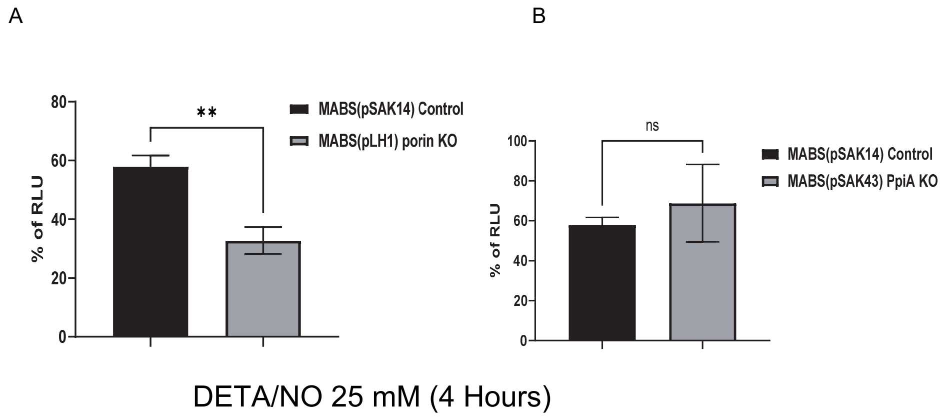

Figure 26 Effect of NO stress on survival of the *M. abscessus* strains.

To assess the sensitivity of different strains, including MABS 40/14-3(pSAK14) (control), MABS 40/14-3 (pLH1) Porin KO, and MABS 40/14-3 (pSAK43) PpiA KO, were exposed to 25 mM DETA/NO for a duration of 4 hours. The survival percentage under this stress conditions was determined by measuring ATP production using a luminescence assay kit (BacTiter-Glo Microbial Cell Viability Assay, Promega). Data are means ± standard deviation of the results from three independent experiments, (performed in triplicates with three individual cultures per strain). *P < 0.05; **P < 0.01; *** P < 0.001; two-tailed, unpaired Student's t test.

4.7.4 Antibiotic Sensitivity test of Porin KO and PpiA KO mutants in *M. abscessus* using Sensititre^{TM}

The MIC of the mutants MABS 40/14-3 (pLH1) Porin KO and PpiA mutant MABS 40/14-3 (pSAK43) PpiA KO and MABS (pSAK14) as control was determined using Sensititre^{TM} RAPMYCOI plates (Table 28). Each mutant was inoculated in two independent experiments at an OD_{600} of 0.08 to 0.10, and the growth was tracked for 14 days. The MIC levels after 5 days are displayed in Table 28. A substantial or significant difference was defined as a two 2 fold dilution steps or more.

Table 28 Sensititre^{TM} results of MABS 40/14-3 (pSAK14) (control) with mutated MABS 40/14-3 (pLH1) Porin KO and MABS 40/14-3 (pSAK43) PpiA KO after 5 days of incubation from two independent experiments.

Antibiotic (µg/ml)	MABs. 40/14 -3(pSAK14) Control	MABs. 40/14 -3(pLH1) Porin KO	MABs. 40/14 -3(pSAK43) PpiA KO
Amikacin	8;8	16;32	8;16
Amoxicillin/ Clavulanic Acid	64/32;64/32	64/32;64/32	64/32;64/32
Cefepime	>32;>32	>32;>32	>32;>32
Cefoxitin	16;32	32;64	32;64
Ceftriaxone	>64;>64	64;64	>64;>64
Ciprofloxacin	4;4	4;4	2;4
Clarithromycin	0,25;0,25	0.25;0,5	0.25;1
Doxycycline	>16;>16	>16;>16	>16;>16
Imipenem	16;64	8;64	32;64
Linezolid	2;32	2;4	2;32
Minocycline	>8;>8	>8;>8	>8;>8
Moxifloxacin	2;4	1;8	2;8
Tigecycline	0,25;0,25	0,5;0,5	0,5;0,5
Tobramycin	16;16	>16;>16	>8;16
Trimethoprim/ Sulfamethoxazole	8/152; 8/152	8/152;8/152	8/152;8/152

No consistent difference in MIC of two 2-dilution steps or more between the *porin* mutants MABS 40/14-3 (pLH1) Porin KO and MABS 40/14-3 (pSAK43) PpiA KO compared with MABS 40/14-3 (pSAK14) against any of the tested antibiotics could be found.

4.7.5 Cytokine responses of THP-1 cell line infected with Porin KO and PpiA KO mutants in *M. abscessus*

Mycobacterial infections induce the host immune cells to produce inflammatory cytokines such as tumor necrosis factor-alpha (TNF-α), IL-6, and IL-1ß. To evaluate the ability of the control strain MABS (pSAK14) and the two mutants MABS (pLH1) Porin KO and the MABS (pSAK43) PpiA KO to stimulate the immune signaling in THP-1 macrophages, the secretion of the pro-inflammatory cytokines TNF-α and IL-1β, and the anti-inflammatory cytokine IL-10 was quantified 24 hours after infection. For positive control, INF-γ and Lipopolysaccharide (LPS) were used and for negative control, we used uninfected THP-1 cells. Two independent experiments were performed. No significant differences could be found between the mutants and the control strain with any of the three tested cytokines (Figure 27).

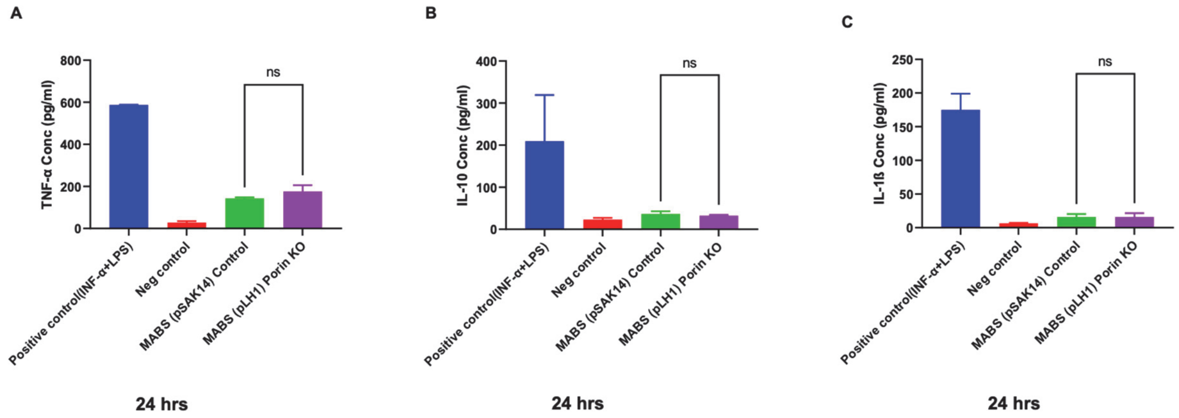

Figure 27 Induction of cytokine secretion by THP1 macrophage after infection with the Porin KO MABS strain and the control *M. abscessus* strain.

Induction of cytokine secretion by THP1 macrophage after infection with the MABS strains (MOI 1) MABS (pSAK14) (control) (green bar), and MABS (pLH1) Porin KO (violet bar). Cytokines TNF-α (A), IL-1β (B), and IL-10 (C), were quantified from supernatants collected 24 hours after infection. The measurements were performed using ELISA kits specifically designed for each cytokine (ELISA Ready-SET-Go! Kit, Thermo Fisher Scientific).

THP1 cells were either infected (MOI 1) or treated with LPS (250 ng/ml) and IFN-γ (400 u/ml) as positive controls (blue bars), and uninfected cells were used as negative control (red bars).

The presented data represent the mean values ± standard deviation obtained from two independent experiments. Statistical significance was determined using a two-tailed, unpaired Mann-Whitney U test.

Also, the MABS (pSAK43) PpiA KO mutant showed no significance for pro-inflammatory cytokine secretion when compared to the control MABS (pSAK14) (Figure 28 A-C).

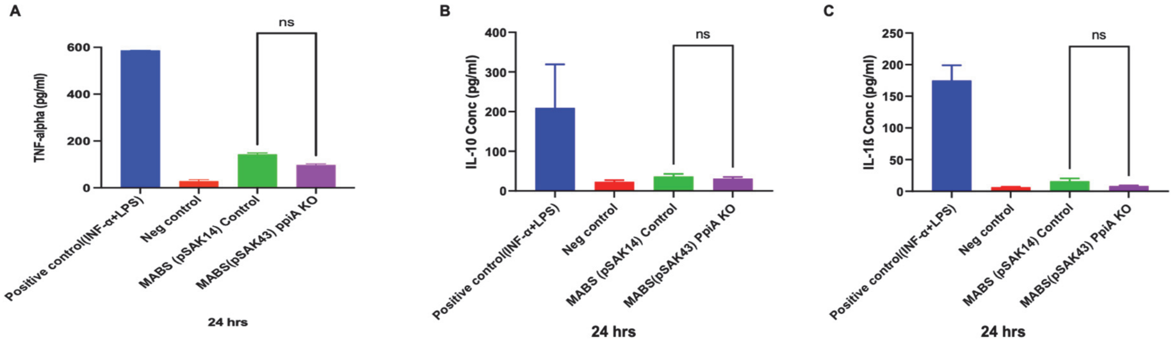

Figure 28 Induction of cytokine secretion by THP1 macrophage after infection with the PpiA KO *M. abscessus* strains.

Induction of cytokine secretion by THP1 macrophage after infection with the MABS strains MABS (pSAK14) (control) (Green bar) and MABS (pSAK43) PpiA KO mutant (Violet bar). At 24 hours post-infection, the levels of TNF-α (A), IL-1β (B), and IL-10 (C) cytokines were measured from the supernatants using ELISA kits (ELISA Ready-SET-Go! Kit, Thermo Fisher Scientific). THP1 cells were either infected (MOI 1), or INF-γ (400 u) and LPS (250 ng) were used as the positive control (represented by the blue bar), while uninfected cells served as the negative control (represented by the red bar). The data presented represents the mean values ± standard deviation obtained from two independent experiments. Statistical significance was determined using a two-tailed, unpaired Mann-Whitney U test, "ns" indicating non-significant differences.

4.7.6 Intracellular survival in THP-1 cell line of Porin KO and PpiA KO mutants in *M. abscessus*

The MABS (pLH1) Porin KO, MABS (pSAK43) PpiA KO, and MABS (pSAK14) Control were all individually infected into the THP-1 cell lines. Quantitative real-time PCR was used to quantify intracellular mycobacteria. In two biological replicates, none of the two mutants' survival rates in THP-1 significantly differed from the MABS (pSAK14) Control (Figure 29).

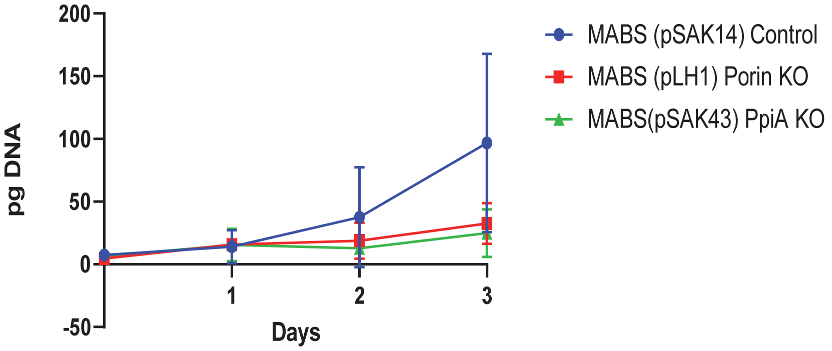

Figure 29 Intracellular survival of *M. abscessus* mutants compared to wild-type in THP-1 cell line.

THP-1 cells (250,000 cells) were infected (MOI 1) with mutants and control. Intracellular bacteria were quantified after 4 hours of infection, and after 1, 2, & 3 days. The monocytes were lysed and quantified by real-time PCR. MABS (pSAK14) Control (blue line), MABS (pLH1) Porin KO (red line), and MABS (pSAK43) PpiA KO mutant (green line) were used. The presented data represent the mean values ± standard deviation obtained from two separate and independent experiments. Two-tailed, unpaired Mann-Whitney U test was used for statistical analysis. Both PpiA and Porin KO MABS strains did not show any significant effect at 1, 2, and 3 days.

5 Discussion and Outlook

5.1 Discussion

Non-tuberculous mycobacteria (NTM) infections are a concerning public health issue due to their ability to cause severe illness and their resistance to antibiotics. The incidence of NTM infections has been on the rise in recent years. Some strains of NTM have developed resistance to antibiotics, making treatment challenging (Hoefsloot et al., 2013). Individuals with weakened immune systems, such as those with HIV/AIDS or who have undergone organ transplants, are at a higher risk of developing NTM infections. While NTM infections can also affect healthy individuals, preventive measures like avoiding contact with contaminated water or soil are crucial. The role of NTM genes involved in virulence and antibiotic resistance in the host remains largely unknown. Mutagenesis techniques can help identify these genes, allowing for a better understanding of NTM biology, potential drug targets, and the development of new treatments and vaccines to prevent NTM infections. Ongoing research and public health efforts are necessary to address this growing public health concern.

Mutagenesis in non-tuberculous mycobacteria (NTM) is challenging due to their slow growth rate, high genetic stability, and thick cell wall. The slow growth rate hinders obtaining sufficient bacterial numbers for mutagenesis experiments (Stout et al., 2016), while the thick cell wall hampers the isolation of DNA and may promote genetic stability (Dheda et al., 2017). The high genetic stability of NTM makes it difficult to introduce and maintain mutations, potentially influenced by efficient DNA repair mechanisms (Brennan & Nikaido, 1995; Gomez-Valero et al., 2011). However, recent advances in molecular tools, such as CRISPRi and CRISPR/Cas9-based methods, offer promising avenues for precise and efficient genetic manipulation of NTM (N. M. Chimukuche & M. J. Williams, 2021). These advancements hold the potential to enhance our understanding of NTM biology and facilitate the development of new treatments for NTM infections.

The development of CRISPR/Cas9 technology in mycobacteria, including MTB and Msmeg, has provided valuable tools for genetic manipulation and understanding the pathogenicity of these bacteria. CRISPR interference (CRISPRi) was developed as a method to prevent transcriptional activity in mycobacteria, and dCas9Sth1 was identified as an effective enzyme for gene knockdown in MTB (Rock et al., 2017). A vector called pLJR965 was created for high-efficiency CRISPRi in MTB and successfully modified for CRISPRi in MABS (Kurepina et al., 2022). Additionally, CRISPR/Cas9-mediated knockout using a derived vector showed high success rates in deleting genes in both Msmeg and MTB species (Yan et al., 2020). However, the challenge of the mycobacteria's cell wall, which limits electroporation effectiveness, remains an obstacle to introducing site-directed mutations. Despite this, the establishment of CRISPRi and CRISPR/Cas9 technologies in NTM holds promise for studying their pathogenicity and developing new therapies.

CRISPRi, particularly useful for gene knockdown rather than complete knockout, allows for the study of gene expression reduction without completely eliminating gene function.

One of the aims of this study was to establish CRISPRi in two clinically important NTM species, MABS and MAH. To this aim, reporter NTM strains containing the *eGFP* gene were constructed. Plasmids containing the dCas9 protein under an inducible promoter and a sgRNA targeting the *eGFP* gene were constructed using the backbone plasmids pLJR962 for rapid-growing NTM and pLJR965 for slow-growing NTM.

Flow cytometry was used to measure the knockdown efficiency of the *eGFP* gene expression through CRISPRi in reporter NTM species Msmeg, MAH, and MABS indicated successful knockdown of *eGFP* gene expression.

In reporter Msmeg, successful fluorescence reduction of the *eGFP* gene was observed with two sgRNAs inserted in vector pLJR962 and two different concentrations of anhydrotetracycline (ATc) 50 ng/ml and 100 ng/ml. A decline in *eGFP* expression was observed using pSAK9 and a concentration of 100 ng/ml ATc at 8 days.

In reporter MAH, a similar decline in *eGFP* fluorescence expression was observed with two sgRNAs inserted in vector pLJR965 and two different concentrations of anhydrotetracycline (ATc) 100 ng/ml and 500 ng/ml, and the highest reduction of fluorescence was achieved with pSAK7 and a concentration of 500 ng/ml ATc at 12 days. It is important to highlight that the vector pLJR965 already had an impact on *eGFP* expression. In conclusion, this system is of limited use in MAH.

In reporter MABS, successful fluorescence reduction of the *eGFP* gene was achieved with two ATc concentrations of 50 ng/ml and 100 ng/ml using the same recommended plasmid construct, pLJR962, as in Msmeg. The highest induction of dcas9 was achieved using a concentration of 100 ng/ml ATc at 8 days, resulting in an expression reduction of approximately

22.7 % compared to the control. This suggests that the plasmid construct pLJR962 is also effective as a CRISPRi/dCas9 system for MABS.
In conclusion, the study highlights the high effectiveness of the recommended plasmid constructs as CRISPRi/dCas9 systems for the NTM species Msmeg and MABS, while the system is of limited benefit for MAH due to the effect on the expression reduction of *eGFP* by the vector containing no sgRNA.

The use of CRISPR/dCas9-mediated gene knockdown has been demonstrated in various bacterial species, including MTB and *Pseudomonas putida*. In the study by (Singh et al., 2016), the *eGFP* gene expression was successfully reduced in MTB by introducing a sgRNA targeting the *eGFP* gene along with the dCas9 enzyme. This knockdown strain proved useful for studying gene function and drug discovery. Similarly, (Kim et al., 2020) achieved *eGFP* gene knockdown in *Pseudomonas putida* using a plasmid-based system with a sgRNA targeting the *eGFP* gene. The fluorescence of the *eGFP* gene was significantly reduced in the treated cells, confirming successful knockdown.

One of the significant advantages of CRISPRi is its ability to simultaneously regulate the expression of multiple genes. This has been demonstrated by (Qi et al., 2013) and (Kim et al., 2017), who successfully regulated multiple genes using the CRISPRi system. In Kim et al.'s study, the adaptable CRISPRi system was employed to increase n-butanol yield and productivity in recombinant *E. coli* by suppressing the expression of various genes. These findings highlight the broad potential and versatility of CRISPRi in gene regulation and biotechnological applications.

CRISPRi offers the advantage of inducible and reversible knockdown of genes, allowing for dynamic and temporal regulation. The tight control of ATc-inducible promoters enables the induction or reversal of gene knockdown through the regulation of dCas9, as demonstrated by (Qi et al., 2013). Additionally, the use of arabinose as an inducer can activate dCas9 expression from the PBAD promoter, leading to CRISPRi-based knockdown, which can be reversed by removing the inducer from the media. Studies by (Li et al., 2016; Wang et al., 2019) showed successful reversibility of CRISPRi-mediated gene silencing in actively replicating *Yersinia pestis* by simply washing away the inducer. This reversible control of gene expression provides researchers with a powerful tool to precisely manipulate gene activity as needed.

Despite its advantages, CRISPRi also has several disadvantages, such as the polar effect, reverse polar effect, toxicity, and off-target effects, as noted by (Cui et al., 2018) and (Peters et al., 2016). Similar to Cas9, dCas9 has been shown to have varying degrees of toxicity in different bacterial strains. (Lee et al., 2019) observed that dCas9 caused a longer lag phase in *Vibrio natriegens*, indicating its marginal toxicity. MTB was killed by high doses of dCas9Spy in the absence of a specific sgRNA (Rock et al., 2017) To mitigate the risk of off-target effects, Zhang and Voigt developed a non-toxic version of dCas9 (dCas9∗_PhlF) that binds to DNA through PhlF instead of dCas9 (Zhang & Voigt, 2018). Also, the potential leakiness of promotor activity without induction should be taken into consideration.

(Chhotaray et al., 2018; Meijers et al., 2020) both researchers developed CRISPR-knockout for the bacteria *M. marinum* and MTB to knock out gene functions. They used modified versions of the CRISPR/Cas9 backbone vector pLJR965 and achieved successful gene deletions and frameshift mutations in these bacterial species. The CRISPR-Cas9 system allowed for efficient and precise genome engineering without adverse effects on non-targeted regions.

In the present study, a method for introducing mutations in specific target genes in the NTM species MAH and MABS using CRISPR should be developed. By reconstituting the Cas9 activity in pLJR965 by site-directed mutagenesis, the *eGFP* gene was successfully mutated in Msmeg (83 % mutants among obtained colonies) and MAH (3 % mutants among obtained colonies), but no mutations were observed in MABS.

A previous study by (Jiang et al., 2013) successfully knocked out the *eGFP* gene in *E. coli* using a plasmid-based CRISPR/Cas9 method, resulting in a significant loss of *eGFP* fluorescence. Another recent study by (Zou et al., 2022) targeted the *eGFP* gene in *Bacillus subtilis* using a CRISPR/Cas9 system with two single guide RNAs (sgRNAs), leading to the complete loss of *eGFP* fluorescence in the knockout strain.

To further investigate the potential to mutate MABS with CRISPR/Cas9, we then applied the method to intrinsic MABS genes. We selected a MABS CF patient isolate to mutate the *mps1* gene involved in the GPL synthesis and colony morphology using CRISPR/Cas9 technology andobtained a variety of mutants with deletions of different sizes and small insertions.
We also aimed to determine if off-target mutations occurred in *mps1* knock-out mutants. WGS was performed on *mps1* knock-out mutants, along with control strains and the wild-type strain of MABS.

By analyzing and comparing the mutant and control sequences with the wild-type strain, we observed genetic modification in the targeted *mps1* gene. These changes encompassed various types of alterations, including deletions ranging from 4 base pairs to 4757 bp in length, and insertions involving a single bp. These modifications were specifically localized within the *mps1* gene, indicating that it was the primary site of genetic modification. One mutant had an additional modification in another gene.

We thus demonstrated the effectiveness and specificity of the CRISPR approach using pSAK14 for generating *mps1* knock-out mutants, as only one mutant had an additional mutation observed in a non-target gene. Surprisingly, a mutation in the *rrs* gene was found in the control strains, which was unrelated to the *mps1* gene knock-out mutation analysis.

We chose one *mps1* mutant that had a 55 bp deletion in the target gene for further analysis and used the isolate containing the vector without sgRNA as a control. The deletion in the *mps1* gene, which is normally 10365 bp long, was expected to result in a non-functional mutant protein.

We showed that the mutations of the *mps1* gene in MABS led to a transition from S to R morphotype and a significant decrease in GPL production. Although the *mps1* mutant displayed only minor changes in antimicrobial drug susceptibility, it showed increased susceptibility to Amikacin, possibly due to alterations in the permeability barrier of the outer membrane caused by the absence of GPLs. These findings highlight the impact of GPLs on colony morphology and antibiotic susceptibility. Further analysis at the transcriptomic and proteomic levels is necessary to fully understand the functional consequences of the *mps1* gene mutation.

Previous studies have highlighted the association between GPL expression on the cell surface of MABS and the morphological characteristics of S and R morphotypes (Nessar et al., 2012). Similarly, (Ripoll et al., 2007) demonstrated the involvement of the *mps1* gene in the regulation of GPL production in other mycobacterial species like Msmeg and *M. chelonae*. A mutation in one of the genes in the GPL locus, such as the *mps1* gene, is known to cause a transition from the S to the R morphotype in mycobacteria (Ferrell et al., 2022). Previous research by (Pawlik et al., 2013) has identified the *mps1* gene within the GPL locus of MABS.

The successful CRISPR/Cas9 knockout of the *mps1* gene in MABS 09/13-3 prompted the investigation of other genes using the same technique. The *porin* gene, *ppiA* gene, *erm-41* gene, and *whiB7* gene were targeted for editing. The CRISPR/Cas9 knockout approach was successfully applied to the target and mutated the *porin* gene and *ppiA* gene in MABS. The *porin* gene editing resulted in mutations in a significant proportion of transformants, even in the absence of ATc induction. The *ppiA* gene was efficiently deleted in the two colonies obtained, with two different deletions observed. *erm-41* gene and *whiB7* were not successfully mutated, which may be explained by the choice of PAM sites present in the genes.

(Rock et al., 2017) investigated the impact of PAM site availability on the efficiency of CRISPR-Cas9-mediated genome editing. It was observed that the presence of PAM sites 5´ NNAGAAG 3´ and 5´NNGGAAG 3´ were important for the successful generation of mutants using Sth1Cas9. In the *mps1* gene, and *porin* gene, the PAM site is 5´NNAGAAG 3´and *ppiA* gene the PAM site is 5´NNGGAAG 3´ present, which helps the generation of a mutant on target sites. For the *erm-41* and *whiB7* genes, we did not find these 5´ NNAGAAG 3´ and 5´NNGGAAG 3´ PAM sites. For that reason, we used alternate other PAM sites. For the *erm-41* gene, we used 5´ NNGGAAA 3´ and 5´ NNAGCAG 3´, and for *whiB7* genes 5´ NNAGAAT 3´, but did not get any mutant. This highlights the importance of having compatible PAM sites for the successful activation of the CRISPR machinery with Sth1Cas9.

Overall, as three out of five target genes were successfully mutated, these results demonstrate the potential of CRISPR/Cas9-mediated gene editing to investigate gene function in MABS.

For the *porin* gene, introducing ATc to the selective medium resulted in mutations in up to 62 % of the MABS transformants. Surprisingly, even in colonies selected without ATc, 39 % of them showed mutations, indicating that the CRISPR/Cas9 system remained active in the absence of induction. Mutations were observed in 4 to 6 base pairs upstream of the PAM site, with deletions ranging from 1 to 403 base pairs and an insertion of 1 base pair. These findings align with a study by (Yan et al., 2020) in which deletions in MTB occurred 3 base pairs upstream of the PAM site and varied in length from 1 to 324 base pairs. Mutation of the *ppiA* gene resulted in only two colonies from the plate containing 100 µg/ml of ATc. Both colonies were subjected to PCR and Sanger sequencing and showed mutations in the *ppiA* gene. One colony had a 14-base pair deletion, while the other had a 17-base pair deletion.

The successful site-directed mutagenesis of MABS using CRISPR/Cas9 opens possibilities for investigating gene functions in the cellular environment and their impact on phenotypic characteristics. The mutants of the *porin* gene and *ppiA* gene in MABS were used for further phenotypic characterization. Several assays were performed to assess the potential roles of these genes in virulence and antibiotic resistance. The assays included testing for resistance to low pH, H_2O_2, and DETA-NO, determining antibiotic resistance/susceptibility, evaluating cytokine secretion by infected THP-1 macrophages, and examining intracellular survival and growth in THP-1 macrophages.

Upon host infection, mycobacteria encounter a hostile macrophage environment containing various stressors such as antimicrobial peptides, reactive oxygen and nitrogen species (ROS, RNS), and acidic pH. These stressors, particularly ROS and RNS, can promote the death of pathogens by damaging their DNA, lipids, and proteins. To survive in this challenging environment, mycobacteria have evolved diverse stress tolerance mechanisms (Tischler & McKinney, 2010).

A function in growth regulation of MABS *porin* genes was shown by (de Moura et al., 2021), who highlighted the role of the *porin* genes MAB_1080 (*mmpA*) and MAB_1081 (*mmpB*) in the growth and glucose uptake of MABS subspecies *massiliense*, with *mmpA* deletion affecting growth rate and glucose accumulation, and *mmpB* deletion influencing the expression levels of *mmpA*. The porin mutated in the present study was *mmpA*. Mutants did not show significant differences in growth compared to the control strain under acidic and neutral pH conditions. The same was observed for the *ppiA* mutants.

Multiple studies have highlighted the differences in survival strategies and susceptibility to host-mediated stresses among different Mycobacterium species. MTB has been found to be more susceptible to nitric oxide and other bactericidal compounds compared to *M. avium* (Gomes et al., 1999).

Msmeg possesses pore-forming proteins that regulate nutrient uptake, which is vital for maintaining normal growth rates. Deletion of MspA, MspC, and MspD in Msmeg has been found to increase its resistance to nitric oxide produced by the host, resulting in longer survival within macrophages (Fabrino et al., 2009).

The MABS porin knockout (KO) mutant was more sensitive to H_2O_2 and DETA-NO in the extracellular state compared to the control strain (without sgRNA). However, the MABS *ppiA* KO mutant showed no effect when exposed to H_2O_2 and DETA-NO in comparison to the control strain.

The Sensititre^{TM} method was employed to assess the antibiotic resistance/sensitivity of the CRISPR/Cas9-mediated knockout *porin* and *ppiA* mutants. After 5 days of inoculation, no significant differences in antibiotic response were observed compared to the control.

In other mycobacteria, the presence of MspA-type porins has been associated with antibiotic resistance. For instance, cloning MspA from Msmeg into *M. bovis* BCG and MTB increased resistance to ß-lactam antibiotics, isoniazid, ethambutol, and streptomycin. Overexpression of MspA-type porins PorM1 and PorM2 in *M. fortuitum* facilitated the diffusion of kanamycin

(Sharbati et al., 2009). However, (de Moura et al., 2021) found that in MABS subspecies massiliense, knockout of *mmpA* and/or *mmpB* did not result in changes in antibiotic resistance for the tested antibiotics, including amikacin, apramycin, azithromycin, cefoxitin, ciprofloxacin, erythromycin, imipenem, kanamycin, and linezolid. (Danilchanka et al., 2008) demonstrated that erythromycin, a larger molecule, cannot enter Msmeg cells via MspA, suggesting that clarithromycin, a derivative of erythromycin, may encounter the same limitation.

The innate immune system recognizes pathogens through phagocytic cells, which activate and produce cytokines that regulate macrophage activation and granuloma formation (Gomes et al., 2008), leading to the activation of the adaptive immune system. Therefore, one of the aims of the study was to investigate the impact of mutations in *porin* and *ppiA* genes on cytokine expression of infected THP-1 cells. The study found that there was no significant difference in cytokine induction in THP-1 cells infected with the mutant strains compared to those infected with the control strain. This suggests that the mutated genes did not affect the synthesis of components that bind to TLR2 or that the THP-1 cells used in the experiments may not have been appropriate for cytokine testing due to their age and passage history.

The study involved infecting THP-1 cells to investigate the intracellular survival of MABS mutants and control strains by measuring intracellular mycobacterial growth using real-time PCR. However, the results showed no significant differences in intracellular survival between the mutants and the control strain. This suggests that the knockout of the targeted genes (*porin* and *ppiA*) did not have a significant impact on the ability of MABS to survive and replicate inside macrophage phagosomes, at least in the context of the THP-1 cell line used in this study. Although THP-1 cells have been considered a suitable alternative to blood monocytes and have been widely used for assessing mycobacterial virulence, the findings of this investigation did not yield promising results. The study highlights the complexity of the host-pathogen interaction and the need for further research to fully understand the mechanisms underlying mycobacterial virulence and intracellular survival.

(Sharbati-Tehrani et al., 2005) used mouse macrophages to investigate, if the permeability of the outer membrane of mycobacteria plays a crucial role in their intracellular persistence within eukaryotic cells, highlighting the importance of porins in this process. He showed that the deletion of *mspA* together with *mspC* significantly increased the intracellular survival of Msmeg in various host cells, including murine bone marrow macrophages, the mouse macrophage cell line J774A.1, and *Acanthamoeba castellanii*. To investigate if the loss of *mmpA* and *mmpB* in MABS affects intracellular survival similarly to the deletion of *mspA* and *mspC* in Msmeg, both *mmpA*, and *mmpB* should be removed.

Overall, the findings suggest that Sth1Cas9 can be a valuable tool for precise genome editing in NTM such as MABS. For MABS we have shown by whole genome sequencing that the method is specific and off-target effects were rare to absent. We showed that a gene of interest can be altered distally to the PAM sites NNAGAAG, and NNGGAAG, significantly increasing the overall number of possible target sites in mycobacterial genomes. Compared to SpCas9, Sth1Cas9 recognizes an extended range or PAM sequence, and Sth1Cas9 was hypothesized to produce fewer off-target effects (Meijers et al., 2020). (Yan et al., 2020) found no (or just one) off-target alteration when using Sth1Cas9 in MTB, which is consistent with the observation from (Meijers et al., 2020) as well as the results from the present study. The study also investigated the impact of PAM site availability on the efficiency of CRISPR-Cas9-mediated genome editing. It was observed that the absence of PAM sites NNAGAAG and NNGGAAG in the *erm-41* and *whiB7* genes of MABS hindered the generation of mutants using Sth1Cas9. This highlights the importance of having compatible PAM sites for the successful activation of the CRISPR machinery with Sth1Cas9.

In conclusion, the CRISPR/Cas9 system established for different NTM provides a powerful and versatile tool for NTM research, allowing for targeted genetic manipulations and providing insights into the biology of these bacteria. It holds promise for advancing our understanding of NTM infections and for the development of improved diagnostic and therapeutic strategies in the future.

5.2 Outlook

The establishment of CRISPRi and CRISPR/Cas9 technology in NTM opens new avenues for research in this important group of bacteria. These technologies provide powerful tools for the study of gene function in NTM.

One potential application of CRISPR/Cas9 technology in NTM is the development of new diagnostic tools.

Another potential application is the development of new treatments for NTM infections. By identifying and targeting key genes involved in NTM pathogenesis or drug resistance, CRISPR/Cas9 technology could be used to develop new antimicrobial therapies that are more effective and less prone to the development of resistance.

6 Zusammenfassung

Etablierung und Anwendung der CRISPR/Cas-Technologie in nicht-tuberkulösen Mykobakterien (NTM)

Nicht-tuberkulöse Mykobakterien (NTM) werden zunehmend für ihre Auswirkungen auf die menschliche Gesundheit erkannt, da sie Infektionen verursachen, insbesondere bei Personen mit geschwächtem Immunsystem oder zugrunde liegenden Lungenerkrankungen. Im Gegensatz zum bekannten *Mycobacterium tuberculosis* (MTB) stellt die intrinsische Resistenz von NTM gegen gängige Antibiotika eine Herausforderung für die Behandlung dar. Die Diagnose von NTM-Infektionen ist aufgrund unspezifischer Symptome, die häufig mit anderen Krankheiten verwechselt werden, kompliziert.

Das Verständnis der NTM-Biologie ist für eine verbesserte Diagnose und Behandlung von entscheidender Bedeutung. Die Einführung von CRISPRi (Clustered Regularly Interspaced Short Palindromic Repeats Interference) und CRISPR/Cas9 bei NTM stellt einen bedeutenden Durchbruch für die Weiterentwicklung der NTM-Forschung und -Behandlung dar.

Die Studie wendete das CRISPRi/dCas9-System auf NTM-Arten (*M. smegmatis*, *M. abscessus* und *M. avium*) an und verwendete ein Reporter-*eGFP*-Gen für die Funktionsanalyse. CRISPRi führte zu einer signifikanten Herunterregulierung von *eGFP* bei *M. smegmatis* und *M. abscessus*. Bei *M. avium* deutete die verringerte Fluoreszenz, auch ohne sgRNA, auf die Notwendigkeit einer weiteren Optimierung hin. CRISPRi erwies sich als wirksam für den Gen-Knockdown bei *M. abscessus*.

CRISPR/Cas9 wurde eingesetzt, um das *eGFP*-Gen auszuschalten, was zu einem Fluoreszenzverlust bei *M. smegmatis* und *M. avium* führte, nicht jedoch bei *M. abscessus*. Die Untersuchung des Systems auf dem *mps1*-Gen in *M. abscessus* ergab Defekte in der Glycopeptidolipid-Synthese, die einen Morphotypübergang verursachten.

Die erfolgreiche Etablierung von CRISPRi und CRISPR/Cas9 in der NTM stellt einen Meilenstein dar und eröffnet neue Wege für die Forschung und mögliche Therapien. Diese Technologien ermöglichen eine präzise Genommanipulation, verbessern unser Verständnis der NTM-Biologie und erleichtern die Entwicklung wirksamerer NTM-Infektionsbehandlungen.

7 Summary

Establishment and Application of CRISPR/Cas Technology in Non-Tuberculous Mycobacteria (NTM)

Non-tuberculous mycobacteria (NTM) are increasingly recognized for their impact on human health, causing infections, especially in individuals with compromised immune systems or underlying lung conditions. Unlike the well-known *Mycobacterium tuberculosis* (MTB), NTM's intrinsic resistance to common antibiotics poses treatment challenges. Diagnosing NTM infections is complicated due to nonspecific symptoms, often confused with other diseases.
Understanding NTM biology is crucial for improved diagnostics and treatments. The adoption of CRISPRi (Clustered Regularly Interspaced Short Palindromic Repeats interference) and CRISPR/Cas9 in NTM represents a significant breakthrough for advancing NTM research and treatment.

The study applied the CRISPRi/dCas9 system to NTM species (*M. smegmatis*, *M. abscessus*, and *M. av*ium), using a reporter *eGFP* gene for functional analysis. CRISPRi led to significant downregulation of *eGFP* in *M. smegmatis* and M. *abscessus*. In *M. avium*, reduced fluorescence, even without sgRNA, suggested the need for further optimization. CRISPRi proved effective for gene knockdown in *M. abscessus*.

CRISPR/Cas9 was employed to knockout the *eGFP* gene, resulting in loss of fluorescence in *M. smegmatis* and *M. avium* but not in *M. abscessus*. Assessing the system on the *mps*1 gene in *M. abscessus* revealed defects in Glycopeptidolipid synthesis, causing morphotype transition.
Evaluation on endogenous genes (*porin, ppiA, erm*-41, and *whiB7*) showed successful knockout for *porin* and *ppiA*. However, targeting *erm-41* and *whiB7* indicated the need for system optimization.

The successful establishment of CRISPRi and CRISPR/Cas9 in NTM signifies a milestone, offering new avenues for research and potential therapies. These technologies enable precise genomic manipulation, enhancing our understanding of NTM biology and facilitating the development of more effective NTM infection treatments.

8 References

Adjemian, J., Olivier, K. N., Seitz, A. E., Falkinham, J. O., 3rd, Holland, S. M., & Prevots, D. R. (2012). Spatial clusters of nontuberculous mycobacterial lung disease in the United States. *Am J Respir Crit Care Med*, *186*(6), 553-558. https://doi.org/10.1164/rccm.201205-0913OC

Bernut, A., Viljoen, A., Dupont, C., Sapriel, G., Blaise, M., Bouchier, C., Brosch, R., de Chastellier, C., Herrmann, J. L., & Kremer, L. (2016). Insights into the smooth-to-rough transitioning in Mycobacterium bolletii unravels a functional Tyr residue conserved in all mycobacterial MmpL family members. *Mol Microbiol*, *99*(5), 866-883. https://doi.org/10.1111/mmi.13283

Bikard, D., Jiang, W., Samai, P., Hochschild, A., Zhang, F., & Marraffini, L. A. (2013). Programmable repression and activation of bacterial gene expression using an engineered CRISPR-Cas system. *Nucleic Acids Res*, *41*(15), 7429-7437. https://doi.org/10.1093/nar/gkt520

Bortesi, L., & Fischer, R. (2015). The CRISPR/Cas9 system for plant genome editing and beyond. *Biotechnol Adv*, *33*(1), 41-52. https://doi.org/10.1016/j.biotechadv.2014.12.006

Brennan, P. J., & Nikaido, H. (1995). The envelope of mycobacteria. *Annu Rev Biochem*, *64*, 29-63. https://doi.org/10.1146/annurev.bi.64.070195.000333

Brown-Elliott, B. A., Nash, K. A., & Wallace, R. J., Jr. (2012). Antimicrobial susceptibility testing, drug resistance mechanisms, and therapy of infections with nontuberculous mycobacteria. *Clin Microbiol Rev*, *25*(3), 545-582. https://doi.org/10.1128/cmr.05030-11

Bryant, J. M., Grogono, D. M., Rodriguez-Rincon, D., Everall, I., Brown, K. P., Moreno, P., Verma, D., Hill, E., Drijkoningen, J., Gilligan, P., Esther, C. R., Noone, P. G., Giddings, O., Bell, S. C., Thomson, R., Wainwright, C. E., Coulter, C., Pandey, S., Wood, M. E., . . . Floto, R. A. (2016). Emergence and spread of a human-transmissible multidrug-resistant nontuberculous mycobacterium. *science*, *354*(6313), 751-757. https://doi.org/10.1126/science.aaf8156

Burian, J., Ramón-García, S., Sweet, G., Gómez-Velasco, A., Av-Gay, Y., & Thompson, C. J. (2012). The mycobacterial transcriptional regulator whiB7 gene links redox homeostasis and intrinsic antibiotic resistance. *J Biol Chem*, *287*(1), 299-310. https://doi.org/10.1074/jbc.M111.302588

Catherinot, E., Roux, A. L., Macheras, E., Hubert, D., Matmar, M., Dannhoffer, L., Chinet, T., Morand, P., Poyart, C., Heym, B., Rottman, M., Gaillard, J. L., & Herrmann, J. L. (2009). Acute respiratory failure involving an R variant of Mycobacterium abscessus. *J Clin Microbiol*, *47*(1), 271-274. https://doi.org/10.1128/jcm.01478-08

Chedore, P., Th'ng, C., Nolan, D. H., Churchwell, G. M., Sieffert, D. E., Hale, Y. M., & Jamieson, F. (2002). Method for inactivating and fixing unstained smear preparations of mycobacterium tuberculosis for improved laboratory safety. *J Clin Microbiol*, *40*(11), 4077-4080. https://doi.org/10.1128/jcm.40.11.4077-4080.2002

Chhotaray, C., Tan, Y., Mugweru, J., Islam, M. M., Adnan Hameed, H. M., Wang, S., Lu, Z., Wang, C., Li, X., Tan, S., Liu, J., & Zhang, T. (2018). Advances in the development of molecular genetic tools for Mycobacterium tuberculosis. *J Genet Genomics*. https://doi.org/10.1016/j.jgg.2018.06.003

Chimukuche, N. M., & Williams, M. J. (2021). Genetic Manipulation of Non-tuberculosis Mycobacteria. *Front Microbiol*, *12*, 633510. https://doi.org/10.3389/fmicb.2021.633510

Chimukuche, N. M., & Williams, M. J. (2021). Genetic Manipulation of Non-tuberculosis Mycobacteria [Review]. *Frontiers in microbiology*, *12*. https://doi.org/10.3389/fmicb.2021.633510

Cho, S. W., Kim, S., Kim, J. M., & Kim, J. S. (2013). Targeted genome engineering in human cells with the Cas9 RNA-guided endonuclease. *Nat Biotechnol*, *31*(3), 230-232. https://doi.org/10.1038/nbt.2507

Choudhary, E., Thakur, P., Pareek, M., & Agarwal, N. (2015). Gene silencing by CRISPR interference in mycobacteria. *Nat Commun*, *6*, 6267. https://doi.org/10.1038/ncomms7267

Cong, L., Ran, F. A., Cox, D., Lin, S., Barretto, R., Habib, N., Hsu, P. D., Wu, X., Jiang, W., Marraffini, L. A., & Zhang, F. (2013). Multiplex genome engineering using CRISPR/Cas systems. *science*, *339*(6121), 819-823. https://doi.org/10.1126/science.1231143

Conn, H. J., & Dimmick, I. (1947). Soil Bacteria Similar in Morphology to Mycobacterium and Corynebacterium. *J Bacteriol*, *54*(3), 291-303. https://doi.org/10.1128/jb.54.3.291-303.1947

Cui, L., Vigouroux, A., Rousset, F., Varet, H., Khanna, V., & Bikard, D. (2018). A CRISPRi screen in E. coli reveals sequence-specific toxicity of dCas9. *Nature communications*, *9*(1), 1912.

Danilchanka, O., Mailaender, C., & Niederweis, M. (2008). Identification of a novel multidrug efflux pump of Mycobacterium tuberculosis. *Antimicrob Agents Chemother*, *52*(7), 2503-2511. https://doi.org/10.1128/aac.00298-08

de Moura, V. C. N., Verma, D., Everall, I., Brown, K. P., Belardinelli, J. M., Shanley, C., Stapleton, M., Parkhill, J., Floto, R. A., Ordway, D. J., & Jackson, M. (2021). Increased Virulence of Outer Membrane Porin Mutants of Mycobacterium abscessus. *Front Microbiol*, *12*, 706207. https://doi.org/10.3389/fmicb.2021.706207

Degiacomi, G., Sammartino, J. C., Chiarelli, L. R., Riabova, O., Makarov, V., & Pasca, M. R. (2019). Mycobacterium abscessus, an Emerging and Worrisome Pathogen among Cystic Fibrosis Patients. *Int J Mol Sci*, *20*(23). https://doi.org/10.3390/ijms20235868

Dheda, K., Chang, K. C., Guglielmetti, L., Furin, J., Schaaf, H. S., Chesov, D., Esmail, A., & Lange, C. (2017). Clinical management of adults and children with multidrug-resistant and extensively drug-resistant tuberculosis. *Clin Microbiol Infect*, *23*(3), 131-140. https://doi.org/10.1016/j.cmi.2016.10.008

DiCarlo, J. E., Norville, J. E., Mali, P., Rios, X., Aach, J., & Church, G. M. (2013). Genome engineering in Saccharomyces cerevisiae using CRISPR-Cas systems. *Nucleic Acids Res*, *41*(7), 4336-4343. https://doi.org/10.1093/nar/gkt135

Ding, X. Y., Li, S. S., Geng, Y. M., Yan, M. Y., Li, G. B., Zhang, G. L., & Sun, Y. C. (2021). Programmable Base Editing in Mycobacterium tuberculosis Using an Engineered CRISPR RNA-Guided Cytidine Deaminase. *Front Genome Ed*, *3*, 734436. https://doi.org/10.3389/fgeed.2021.734436

Doudna, J. A., & Charpentier, E. (2014). Genome editing. The new frontier of genome engineering with CRISPR-Cas9. *science*, *346*(6213), 1258096. https://doi.org/10.1126/science.1258096

Dubée V, T. S., Mainardi JL, et al. (2017). MmpS6/MmpL6 Mycolic Acid Transporter of Mycobacterium abscessus Is Upregulated by Antimicrobials, Including Ethambutol. . *Antimicrob Agents Chemother 61(1)*, e01020-01016.

Fabrino, D. L., Bleck, C. K., Anes, E., Hasilik, A., Melo, R. C., Niederweis, M., Griffiths, G., & Gutierrez, M. G. (2009). Porins facilitate nitric oxide-mediated killing of mycobacteria. *Microbes Infect*, *11*(10-11), 868-875. https://doi.org/10.1016/j.micinf.2009.05.007

Falkinham, J. O., 3rd. (1996). Epidemiology of infection by nontuberculous mycobacteria. *Clin Microbiol Rev*, *9*(2), 177-215. https://doi.org/10.1128/cmr.9.2.177

Falkinham, J. O., 3rd. (2009). Surrounded by mycobacteria: nontuberculous mycobacteria in the human environment. *J Appl Microbiol*, *107*(2), 356-367. https://doi.org/10.1111/j.1365-2672.2009.04161.x

Falkinham, J. O., 3rd. (2016). Current Epidemiologic Trends of the Nontuberculous Mycobacteria (NTM). *Curr Environ Health Rep*, *3*(2), 161-167. https://doi.org/10.1007/s40572-016-0086-z

Ferrell, K. C., Johansen, M. D., Triccas, J. A., & Counoupas, C. (2022). Virulence Mechanisms of Mycobacterium abscessus: Current Knowledge and Implications for Vaccine Design. *Front Microbiol*, *13*, 842017. https://doi.org/10.3389/fmicb.2022.842017

Forbes, B. A., Hall, G. S., Miller, M. B., Novak, S. M., Rowlinson, M. C., Salfinger, M., Somoskövi, A., Warshauer, D. M., & Wilson, M. L. (2018). Practical Guidance for Clinical Microbiology Laboratories: Mycobacteria. *Clin Microbiol Rev*, *31*(2). https://doi.org/10.1128/cmr.00038-17

Fowler, J., & Mahlen, S. D. (2014). Localized cutaneous infections in immunocompetent individuals due to rapidly growing mycobacteria. *Arch Pathol Lab Med*, *138*(8), 1106-1109. https://doi.org/10.5858/arpa.2012-0203-RS

Franco-Paredes, C., Marcos, L. A., Henao-Martínez, A. F., Rodríguez-Morales, A. J., Villamil-Gómez, W. E., Gotuzzo, E., & Bonifaz, A. (2018). Cutaneous Mycobacterial Infections. *Clin Microbiol Rev*, *32*(1). https://doi.org/10.1128/cmr.00069-18

Friedland, A. E., Tzur, Y. B., Esvelt, K. M., Colaiácovo, M. P., Church, G. M., & Calarco, J. A. (2013). Heritable genome editing in C. elegans via a CRISPR-Cas9 system. *Nat Methods*, *10*(8), 741-743. https://doi.org/10.1038/nmeth.2532

Gokhale, R. S., Saxena, P., Chopra, T., & Mohanty, D. (2007). Versatile polyketide enzymatic machinery for the biosynthesis of complex mycobacterial lipids. *Nat Prod Rep*, *24*(2), 267-277. https://doi.org/10.1039/b616817p

Gomes, M. S., Flórido, M., Pais, T. F., & Appelberg, R. (1999). Improved clearance of Mycobacterium avium upon disruption of the inducible nitric oxide synthase gene. *J Immunol*, *162*(11), 6734-6739.

Gomez-Valero, L., Rusniok, C., Jarraud, S., Vacherie, B., Rouy, Z., Barbe, V., Medigue, C., Etienne, J., & Buchrieser, C. (2011). Extensive recombination events and horizontal gene transfer shaped the Legionella pneumophila genomes. *BMC Genomics*, *12*(1), 536. https://doi.org/10.1186/1471-2164-12-536

Gopinath, K., & Singh, S. (2010). Non-tuberculous mycobacteria in TB-endemic countries: are we neglecting the danger? *PLoS Negl Trop Dis*, *4*(4), e615. https://doi.org/10.1371/journal.pntd.0000615

Griffith, D. E., Aksamit, T., Brown-Elliott, B. A., Catanzaro, A., Daley, C., Gordin, F., Holland, S. M., Horsburgh, R., Huitt, G., Iademarco, M. F., Iseman, M., Olivier, K., Ruoss, S., von Reyn, C. F., Wallace, R. J., Jr., & Winthrop, K. (2007). An official ATS/IDSA statement: diagnosis, treatment, and prevention of nontuberculous mycobacterial diseases. *Am J Respir Crit Care Med*, *175*(4), 367-416. https://doi.org/10.1164/rccm.200604-571ST

Gutiérrez, A. V., Viljoen, A., Ghigo, E., Herrmann, J. L., & Kremer, L. (2018). Glycopeptidolipids, a Double-Edged Sword of the Mycobacterium abscessus Complex. *Front Microbiol*, *9*, 1145. https://doi.org/10.3389/fmicb.2018.01145

Heifets, L. (2004). Mycobacterial infections caused by nontuberculous mycobacteria. *Semin Respir Crit Care Med*, *25*(3), 283-295. https://doi.org/10.1055/s-2004-829501

Hoefsloot, W., van Ingen, J., Andrejak, C., Angeby, K., Bauriaud, R., Bemer, P., Beylis, N., Boeree, M. J., Cacho, J., Chihota, V., Chimara, E., Churchyard, G., Cias, R., Daza, R., Daley, C. L., Dekhuijzen, P. N., Domingo, D., Drobniewski, F., Esteban, J., . . . Wagner, D. (2013). The geographic diversity of nontuberculous mycobacteria isolated from pulmonary samples: an NTM-NET collaborative study. *Eur Respir J*, *42*(6), 1604-1613. https://doi.org/10.1183/09031936.00149212

Howard, S. T., Rhoades, E., Recht, J., Pang, X., Alsup, A., Kolter, R., Lyons, C. R., & Byrd, T. F. (2006). Spontaneous reversion of Mycobacterium abscessus from a smooth to a rough morphotype is associated with reduced expression of glycopeptidolipid and reacquisition of an invasive phenotype. *Microbiology (Reading)*, *152*(Pt 6), 1581-1590. https://doi.org/10.1099/mic.0.28625-0

Hurst-Hess, K., Rudra, P., & Ghosh, P. (2017). Mycobacterium abscessus WhiB7 Regulates a Species-Specific Repertoire of Genes To Confer Extreme Antibiotic Resistance. *Antimicrob Agents Chemother*, *61*(11). https://doi.org/10.1128/aac.01347-17

Ishino, Y., Shinagawa, H., Makino, K., Amemura, M., & Nakata, A. (1987). Nucleotide sequence of the iap gene, responsible for alkaline phosphatase isozyme conversion in Escherichia coli, and identification of the gene product. *J Bacteriol*, *169*(12), 5429-5433. https://doi.org/10.1128/jb.169.12.5429-5433.1987

Jarlier, V., & Nikaido, H. (1994). Mycobacterial cell wall: structure and role in natural resistance to antibiotics. *FEMS Microbiol Lett*, *123*(1-2), 11-18. https://doi.org/10.1111/j.1574-6968.1994.tb07194.x

Jiang, F., & Doudna, J. A. (2017). CRISPR-Cas9 Structures and Mechanisms. *Annu Rev Biophys*, *46*, 505-529. https://doi.org/10.1146/annurev-biophys-062215-010822

Jiang, W., Bikard, D., Cox, D., Zhang, F., & Marraffini, L. A. (2013). RNA-guided editing of bacterial genomes using CRISPR-Cas systems. *Nat Biotechnol*, *31*(3), 233-239. https://doi.org/10.1038/nbt.2508

Jinek, M., Chylinski, K., Fonfara, I., Hauer, M., Doudna, J. A., & Charpentier, E. (2012). A programmable dual-RNA-guided DNA endonuclease in adaptive bacterial immunity. *Science*, *337*(6096), 816-821. https://doi.org/10.1126/science.1225829

Johansen, M. D., Herrmann, J. L., & Kremer, L. (2020). Non-tuberculous mycobacteria and the rise of Mycobacterium abscessus. *Nat Rev Microbiol*, *18*(7), 392-407. https://doi.org/10.1038/s41579-020-0331-1

Kanchiswamy, C. N. (2016). DNA-free genome editing methods for targeted crop improvement. *Plant Cell Rep*, *35*(7), 1469-1474. https://doi.org/10.1007/s00299-016-1982-2

Kim, S. K., Seong, W., Han, G. H., Lee, D. H., & Lee, S. G. (2017). CRISPR interference-guided multiplex repression of endogenous competing pathway genes for redirecting metabolic flux in Escherichia coli. *Microb Cell Fact*, *16*(1), 188. https://doi.org/10.1186/s12934-017-0802-x

Kim, S. K., Yoon, P. K., Kim, S. J., Woo, S. G., Rha, E., Lee, H., Yeom, S. J., Kim, H., Lee, D. H., & Lee, S. G. (2020). CRISPR interference-mediated gene regulation in Pseudomonas putida KT2440. *Microb Biotechnol*, *13*(1), 210-221. https://doi.org/10.1111/1751-7915.13382

Koh, W. J., Chang, B., Jeong, B. H., Jeon, K., Kim, S. Y., Lee, N. Y., Ki, C. S., & Kwon, O. J. (2013). Increasing Recovery of Nontuberculous Mycobacteria from Respiratory Specimens over a 10-Year Period in a Tertiary Referral Hospital in South Korea. *Tuberc Respir Dis (Seoul)*, *75*(5), 199-204. https://doi.org/10.4046/trd.2013.75.5.199

Kurepina, N., Chen, L., Composto, K., Rifat, D., Nuermberger, E. L., & Kreiswirth, B. N. (2022). CRISPR Inhibition of Essential Peptidoglycan Biosynthesis Genes in Mycobacterium abscessus and Its Impact on β-Lactam Susceptibility. *Antimicrob Agents Chemother*, *66*(4), e0009322. https://doi.org/10.1128/aac.00093-22

Lahiri, A., Sanchini, A., Semmler, T., Schäfer, H., & Lewin, A. (2014). Identification and comparative analysis of a genomic island in Mycobacterium avium subsp. hominissuis. *FEBS Lett*, *588*(21), 3906-3911. https://doi.org/10.1016/j.febslet.2014.08.037

Lee, H. H., Ostrov, N., Wong, B. G., Gold, M. A., Khalil, A. S., & Church, G. M. (2019). Functional genomics of the rapidly replicating bacterium Vibrio natriegens by CRISPRi. *Nature microbiology*, *4*(7), 1105-1113.

Lemay, M. L., Tremblay, D. M., & Moineau, S. (2017). Genome Engineering of Virulent Lactococcal Phages Using CRISPR-Cas9. *ACS Synth Biol*, *6*(7), 1351-1358. https://doi.org/10.1021/acssynbio.6b00388

Lévy-Frébault, V. V., & Portaels, F. (1992). Proposed minimal standards for the genus Mycobacterium and for description of new slowly growing Mycobacterium species. *Int J Syst Bacteriol*, *42*(2), 315-323. https://doi.org/10.1099/00207713-42-2-315

Lewin, A., Kamal, E., Semmler, T., Winter, K., Kaiser, S., Schäfer, H., Mao, L., Eschenhagen, P., Grehn, C., Bender, J., & Schwarz, C. (2021). Genetic diversification of persistent Mycobacterium abscessus within cystic fibrosis patients. *Virulence*, *12*(1), 2415-2429. https://doi.org/10.1080/21505594.2021.1959808

Li, X.-t., Jun, Y., Erickstad, M. J., Brown, S. D., Parks, A., Court, D. L., & Jun, S. (2016). tCRISPRi: tunable and reversible, one-step control of gene expression. *Scientific Reports*, *6*(1), 39076. https://doi.org/10.1038/srep39076

LoBue, P. A., Enarson, D. A., & Thoen, T. C. (2010). Tuberculosis in humans and its epidemiology, diagnosis and treatment in the United States. *Int J Tuberc Lung Dis*, *14*(10), 1226-1232.

Ma, X., Zhu, Q., Chen, Y., & Liu, Y. G. (2016). CRISPR/Cas9 Platforms for Genome Editing in Plants: Developments and Applications. *Mol Plant*, *9*(7), 961-974. https://doi.org/10.1016/j.molp.2016.04.009

Meijers, A. S., Troost, R., Ummels, R., Maaskant, J., Speer, A., Nejentsev, S., Bitter, W., & Kuijl, C. P. (2020). Efficient genome editing in pathogenic mycobacteria using Streptococcus thermophilus CRISPR1-Cas9. *Tuberculosis (Edinb)*, *124*, 101983. https://doi.org/10.1016/j.tube.2020.101983

Mijs, W., de Haas, P., Rossau, R., Van der Laan, T., Rigouts, L., Portaels, F., & van Soolingen, D. (2002). Molecular evidence to support a proposal to reserve the designation Mycobacterium avium subsp. avium for bird-type isolates and 'M. avium subsp. hominissuis' for the human/porcine type of M. avium. *Int J Syst Evol Microbiol*, *52*(Pt 5), 1505-1518. https://doi.org/10.1099/00207713-52-5-1505

Moscou, M. J., & Bogdanove, A. J. (2009). A simple cipher governs DNA recognition by TAL effectors. *science*, *326*(5959), 1501. https://doi.org/10.1126/science.1178817

Namkoong, H., Kurashima, A., Morimoto, K., Hoshino, Y., Hasegawa, N., Ato, M., & Mitarai, S. (2016). Epidemiology of Pulmonary Nontuberculous Mycobacterial Disease, Japan. *Emerg Infect Dis*, *22*(6), 1116-1117. https://doi.org/10.3201/eid2206.151086

Nash, K. A., Brown-Elliott, B. A., & Wallace, R. J., Jr. (2009). A novel gene, erm(41), confers inducible macrolide resistance to clinical isolates of Mycobacterium abscessus but is absent from Mycobacterium chelonae. *Antimicrob Agents Chemother*, *53*(4), 1367-1376. https://doi.org/10.1128/aac.01275-08

Nessar, R., Cambau, E., Reyrat, J. M., Murray, A., & Gicquel, B. (2012). Mycobacterium abscessus: a new antibiotic nightmare. *J Antimicrob Chemother*, *67*(4), 810-818. https://doi.org/10.1093/jac/dkr578

Nielsen, A. A., & Voigt, C. A. (2014). Multi-input CRISPR/Cas genetic circuits that interface host regulatory networks. *Mol Syst Biol*, *10*(11), 763. https://doi.org/10.15252/msb.20145735

Ovrutsky, A. R., Chan, E. D., Kartalija, M., Bai, X., Jackson, M., Gibbs, S., Falkinham, J. O., 3rd, Iseman, M. D., Reynolds, P. R., McDonnell, G., & Thomas, V. (2013). Cooccurrence of free-living amoebae and nontuberculous Mycobacteria in hospital water networks, and preferential growth of Mycobacterium avium in Acanthamoeba lenticulata. *Appl Environ Microbiol*, *79*(10), 3185-3192. https://doi.org/10.1128/aem.03823-12

Pandey, S., Sharma, A., Tripathi, D., Kumar, A., Khubaib, M., Bhuwan, M., Chaudhuri, T. K., Hasnain, S. E., & Ehtesham, N. Z. (2016). Mycobacterium tuberculosis Peptidyl-Prolyl Isomerases Also Exhibit Chaperone like Activity In-Vitro and In-Vivo. *PLoS One*, *11*(3), e0150288. https://doi.org/10.1371/journal.pone.0150288

Pandey, S., Tripathi, D., Khubaib, M., Kumar, A., Sheikh, J. A., Sumanlatha, G., Ehtesham, N. Z., & Hasnain, S. E. (2017). Mycobacterium tuberculosis Peptidyl-Prolyl Isomerases Are Immunogenic, Alter Cytokine Profile and Aid in Intracellular Survival. *Front Cell Infect Microbiol*, *7*, 38. https://doi.org/10.3389/fcimb.2017.00038

Parte, A. C., Sardà Carbasse, J., Meier-Kolthoff, J. P., Reimer, L. C., & Göker, M. (2020). List of Prokaryotic names with Standing in Nomenclature (LPSN) moves to the DSMZ. *International journal of systematic and evolutionary microbiology*, *70(11)*, 5607-5612. https://doi.org/doi:https://doi.org/10.1099/ijsem.0.004332

Paustian, M. L., Kapur, V., & Bannantine, J. P. (2005). Comparative genomic hybridizations reveal genetic regions within the Mycobacterium avium complex that are divergent from Mycobacterium avium subsp. paratuberculosis isolates. *J Bacteriol*, *187*(7), 2406-2415. https://doi.org/10.1128/jb.187.7.2406-2415.2005

Pawlik, A., Garnier, G., Orgeur, M., Tong, P., Lohan, A., Le Chevalier, F., Sapriel, G., Roux, A. L., Conlon, K., Honoré, N., Dillies, M. A., Ma, L., Bouchier, C., Coppée, J. Y., Gaillard, J. L., Gordon, S. V., Loftus, B., Brosch, R., & Herrmann, J. L. (2013). Identification and characterization of the genetic changes responsible for the characteristic smooth-to-rough morphotype alterations of clinically persistent Mycobacterium abscessus. *Mol Microbiol*, *90*(3), 612-629. https://doi.org/10.1111/mmi.12387

Peters, J. M., Colavin, A., Shi, H., Czarny, T. L., Larson, M. H., Wong, S., Hawkins, J. S., Lu, C. H. S., Koo, B. M., Marta, E., Shiver, A. L., Whitehead, E. H., Weissman, J. S., Brown, E. D., Qi, L. S., Huang, K. C., & Gross, C. A. (2016). A Comprehensive, CRISPR-based Functional Analysis of Essential Genes in Bacteria. *Cell*, *165*(6), 1493-1506. https://doi.org/10.1016/j.cell.2016.05.003

Porvaznik, I., Solovič, I., & Mokrý, J. (2017). Non-Tuberculous Mycobacteria: Classification, Diagnostics, and Therapy. *Adv Exp Med Biol*, *944*, 19-25. https://doi.org/10.1007/5584_2016_45

Prevots, D. R., & Marras, T. K. (2015). Epidemiology of human pulmonary infection with nontuberculous mycobacteria: a review. *Clin Chest Med*, *36*(1), 13-34. https://doi.org/10.1016/j.ccm.2014.10.002

Qi, L. S., Larson, M. H., Gilbert, L. A., Doudna, J. A., Weissman, J. S., Arkin, A. P., & Lim, W. A. (2013). Repurposing CRISPR as an RNA-guided platform for sequence-specific control of gene expression. *Cell*, *152*(5), 1173-1183. https://doi.org/10.1016/j.cell.2013.02.022

Ramirez, C. L., Foley, J. E., Wright, D. A., Müller-Lerch, F., Rahman, S. H., Cornu, T. I., Winfrey, R. J., Sander, J. D., Fu, F., Townsend, J. A., Cathomen, T., Voytas, D. F., & Joung, J. K. (2008). Unexpected failure rates for modular assembly of engineered zinc fingers. *Nat Methods*, *5*(5), 374-375. https://doi.org/10.1038/nmeth0508-374

Reis A, H. B., Tzertzinis G (2014). CRISPR/Cas9 and Targeted Genome Editing: A New Era in Molecular Biology. *https://www.neb.com/toolsand-resources/featurearticles/*.

Ripoll, F., Deshayes, C., Pasek, S., Laval, F., Beretti, J. L., Biet, F., Risler, J. L., Daffé, M., Etienne, G., Gaillard, J. L., & Reyrat, J. M. (2007). Genomics of glycopeptidolipid biosynthesis in Mycobacterium abscessus and M. chelonae. *BMC Genomics*, *8*, 114. https://doi.org/10.1186/1471-2164-8-114

Rock, J. M., Hopkins, F. F., Chavez, A., Diallo, M., Chase, M. R., Gerrick, E. R., Pritchard, J. R., Church, G. M., Rubin, E. J., Sassetti, C. M., Schnappinger, D., & Fortune, S. M. (2017). Programmable transcriptional repression in mycobacteria using an orthogonal CRISPR interference platform. *Nat Microbiol*, *2*, 16274. https://doi.org/10.1038/nmicrobiol.2016.274

Rodgers, M. R., Blackstone, B. J., Reyes, A. L., & Covert, T. C. (1999). Colonisation of point of use water filters by silver resistant non-tuberculous mycobacteria. *J Clin Pathol*, *52*(8), 629. https://doi.org/10.1136/jcp.52.8.629a

Rominski, A., Selchow, P., Becker, K., Brülle, J. K., Dal Molin, M., & Sander, P. (2017). Elucidation of Mycobacterium abscessus aminoglycoside and capreomycin resistance by targeted deletion of three putative resistance genes. *J Antimicrob Chemother*, *72*(8), 2191-2200. https://doi.org/10.1093/jac/dkx125

Rüger, K., Hampel, A., Billig, S., Rücker, N., Suerbaum, S., & Bange, F. C. (2014). Characterization of rough and smooth morphotypes of Mycobacterium abscessus isolates from clinical specimens. *J Clin Microbiol*, *52*(1), 244-250. https://doi.org/10.1128/jcm.01249-13

Sanchini, A., Dematheis, F., Semmler, T., & Lewin, A. (2017). Metabolic phenotype of clinical and environmental Mycobacterium avium subsp. hominissuis isolates. *PeerJ*, *5*, e2833. https://doi.org/10.7717/peerj.2833

Shah, N. M., Davidson, J. A., Anderson, L. F., Lalor, M. K., Kim, J., Thomas, H. L., Lipman, M., & Abubakar, I. (2016). Pulmonary Mycobacterium avium-intracellulare is the main driver of the rise in non-tuberculous mycobacteria incidence in England, Wales and

Northern Ireland, 2007-2012. *BMC Infect Dis*, *16*, 195. https://doi.org/10.1186/s12879-016-1521-3

Sharbati, S., Schramm, K., Rempel, S., Wang, H., Andrich, R., Tykiel, V., Kunisch, R., & Lewin, A. (2009). Characterisation of porin genes from Mycobacterium fortuitum and their impact on growth. *BMC Microbiol*, *9*, 31. https://doi.org/10.1186/1471-2180-9-31

Sharbati-Tehrani, S., Stephan, J., Holland, G., Appel, B., Niederweis, M., & Lewin, A. (2005). Porins limit the intracellular persistence of Mycobacterium smegmatis. *Microbiology (Reading)*, *151*(Pt 7), 2403-2410. https://doi.org/10.1099/mic.0.27969-0

Singh, A. K., Carette, X., Potluri, L. P., Sharp, J. D., Xu, R., Prisic, S., & Husson, R. N. (2016). Investigating essential gene function in Mycobacterium tuberculosis using an efficient CRISPR interference system. *Nucleic Acids Res*, *44*(18), e143. https://doi.org/10.1093/nar/gkw625

Snapper, S. B., Melton, R. E., Mustafa, S., Kieser, T., & Jacobs, W. R., Jr. (1990). Isolation and characterization of efficient plasmid transformation mutants of Mycobacterium smegmatis. *Mol Microbiol*, *4*(11), 1911-1919. https://doi.org/10.1111/j.1365-2958.1990.tb02040.x

Sorek, R., Kunin, V., & Hugenholtz, P. (2008). CRISPR--a widespread system that provides acquired resistance against phages in bacteria and archaea. *Nat Rev Microbiol*, *6*(3), 181-186. https://doi.org/10.1038/nrmicro1793

Sousa, S., Borges, V., Joao, I., Gomes, J. P., & Jordao, L. (2019). Nontuberculous Mycobacteria Persistence in a Cell Model Mimicking Alveolar Macrophages. *Microorganisms*, *7*(5). https://doi.org/10.3390/microorganisms7050113

Stout, J. E., Koh, W. J., & Yew, W. W. (2016). Update on pulmonary disease due to non-tuberculous mycobacteria. *Int J Infect Dis*, *45*, 123-134. https://doi.org/10.1016/j.ijid.2016.03.006

Tabarsi, P., Baghaei, P., Farnia, P., Mansouri, N., Chitsaz, E., Sheikholeslam, F., Marjani, M., Rouhani, N., Mirsaeidi, M., Alipanah, N., Amiri, M., Masjedi, M. R., & Mansouri, D. (2009). Nontuberculous mycobacteria among patients who are suspected for multidrug-resistant tuberculosis-need for earlier identification of nontuberculosis mycobacteria. *Am J Med Sci*, *337*(3), 182-184. https://doi.org/10.1097/maj.0b013e318185d32f

Taylor, R. H., Falkinham, J. O., 3rd, Norton, C. D., & LeChevallier, M. W. (2000). Chlorine, chloramine, chlorine dioxide, and ozone susceptibility of Mycobacterium avium. *Appl Environ Microbiol*, *66*(4), 1702-1705. https://doi.org/10.1128/aem.66.4.1702-1705.2000

TD, L. (2012). *CRISPR systems in prokaryotic immunity,The Doudna Lab* http://rna.berkeley.edu/crispr.html.

Thomson, R. M. (2010). Changing epidemiology of pulmonary nontuberculous mycobacteria infections. *Emerg Infect Dis*, *16*(10), 1576-1583. https://doi.org/10.3201/eid1610.091201

Thurtle-Schmidt, D. M., & Lo, T. W. (2018). Molecular biology at the cutting edge: A review on CRISPR/CAS9 gene editing for undergraduates. *Biochem Mol Biol Educ*, *46*(2), 195-205. https://doi.org/10.1002/bmb.21108

van Ingen, J., Egelund, E. F., Levin, A., Totten, S. E., Boeree, M. J., Mouton, J. W., Aarnoutse, R. E., Heifets, L. B., Peloquin, C. A., & Daley, C. L. (2012). The pharmacokinetics and pharmacodynamics of pulmonary Mycobacterium avium complex disease treatment. *Am J Respir Crit Care Med*, *186*(6), 559-565. https://doi.org/10.1164/rccm.201204-0682OC

Voskuil, M. I., Bartek, I. L., Visconti, K., & Schoolnik, G. K. (2011). The response of mycobacterium tuberculosis to reactive oxygen and nitrogen species. *Front Microbiol*, *2*, 105. https://doi.org/10.3389/fmicb.2011.00105

Wang, T., Wang, M., Zhang, Q., Cao, S., Li, X., Qi, Z., Tan, Y., You, Y., Bi, Y., Song, Y., Yang, R., & Du, Z. (2019). Reversible Gene Expression Control in Yersinia pestis by Using an Optimized CRISPR Interference System. *Appl Environ Microbiol*, *85*(12). https://doi.org/10.1128/aem.00097-19

WHO. (2022). *Global Tuberculosis Report 2022*.

Wiedenheft, B., Sternberg, S. H., & Doudna, J. A. (2012). RNA-guided genetic silencing systems in bacteria and archaea. *Nature*, *482*(7385), 331-338. https://doi.org/10.1038/nature10886

Woo, J. W., Kim, J., Kwon, S. I., Corvalán, C., Cho, S. W., Kim, H., Kim, S. G., Kim, S. T., Choe, S., & Kim, J. S. (2015). DNA-free genome editing in plants with preassembled CRISPR-Cas9 ribonucleoproteins. *Nat Biotechnol*, *33*(11), 1162-1164. https://doi.org/10.1038/nbt.3389

Wu, M. L., Aziz, D. B., Dartois, V., & Dick, T. (2018). NTM drug discovery: status, gaps and the way forward. *Drug Discov Today*, *23*(8), 1502-1519. https://doi.org/10.1016/j.drudis.2018.04.001

Wyman, C., & Kanaar, R. (2006). DNA double-strand break repair: all's well that ends well. *Annu Rev Genet*, *40*, 363-383. https://doi.org/10.1146/annurev.genet.40.110405.090451

Yan, M. Y., Li, S. S., Ding, X. Y., Guo, X. P., Jin, Q., & Sun, Y. C. (2020). A CRISPR-Assisted Nonhomologous End-Joining Strategy for Efficient Genome Editing in Mycobacterium tuberculosis. *mBio*, *11*(1). https://doi.org/10.1128/mBio.02364-19

Yan, M. Y., Yan, H. Q., Ren, G. X., Zhao, J. P., Guo, X. P., & Sun, Y. C. (2017). CRISPR-Cas12a-Assisted Recombineering in Bacteria. *Appl Environ Microbiol*, *83*(17). https://doi.org/10.1128/aem.00947-17

Yin, H., Kauffman, K. J., & Anderson, D. G. (2017). Delivery technologies for genome editing. *Nat Rev Drug Discov*, *16*(6), 387-399. https://doi.org/10.1038/nrd.2016.280

Zhang, S., & Voigt, C. A. (2018). Engineered dCas9 with reduced toxicity in bacteria: implications for genetic circuit design. *Nucleic acids research*, *46*(20), 11115-11125.

Zhang, Z. T., Jiménez-Bonilla, P., Seo, S. O., Lu, T., Jin, Y. S., Blaschek, H. P., & Wang, Y. (2018). Bacterial Genome Editing with CRISPR-Cas9: Taking Clostridium beijerinckii as an Example. *Methods Mol Biol*, *1772*, 297-325. https://doi.org/10.1007/978-1-4939-7795-6_17

Zou, Y., Qiu, L., Xie, A., Han, W., Zhang, S., Li, J., Zhao, S., Li, Y., Liang, Y., & Hu, Y. (2022). Development and application of a rapid all-in-one plasmid CRISPR-Cas9 system for iterative genome editing in Bacillus subtilis. *Microb Cell Fact*, *21*(1), 173. https://doi.org/10.1186/s12934-022-01896-0

9 Annex

9.1 List of publication

9.1.1 Scientific articles

9.1.2 Poster presentations at conferences

- RoKoCon2020, Robert Koch Doctoral Students Symposium

9.1.3 Scientific presentations at conferences

- RoKoCon2021, Robert Koch Doctoral Students Symposium

9.2 Acknowledgment

I am incredibly grateful to the All-Powerful Allah for giving me the stamina to complete this task.

My advisor, Dr. Astrid Lewin, for my doctoral thesis, has my sincere gratitude for allowing me to work at the esteemed Robert Koch Institute (RKI). I was able to complete this project because of her constant support, invaluable advice, never-ending encouragement, unending tolerance, and irreplaceable friendship during my thesis research and other projects. I appreciate everything she did to make my doctoral experience fruitful and engaging, including her time, ideas, and funding suggestions. I also want to thank her for being receptive to suggestions and for working with me to develop ideas for my projects. These efforts helped me think more critically and to be more creative. In addition, I must be a very fortunate student to have a mentor who allowed me the independence to experiment on my own while also providing me with the direction to backtrack when my plans fell through. My decision to pursue a doctoral thesis in accordance with her expertise and teachings is always inspired by her approach toward study and her never-ending passion for the creation of initiatives.

First and foremost, I want to thank my supervisor, Prof. Dr. Lothar Wieler, from the bottom of my heart for his perceptive criticism and insightful ideas throughout the writing of my thesis.

Elisabeth Kamal's superb technical assistance especially with cell culture experiments and attention to both my personal and experimental needs are also very appreciated. I am grateful to Lena Hümmler for her support in constructing plasmids for the generation of *porin* mutants. I would also want to thank Dr. Anton Aebischer for his insightful comments on my research project and his challenging inquiries that motivated me to broaden my research from a number of angles. I also value Dr. Hubert Schäfer and Barbara Kropp's assistance with the GPL experiments during my research, I am also grateful for his encouragement, local knowledge, and knowledge sharing.

I am grateful to Jeremy M Rock and Sarah Fortune for providing plasmids pLJR962 and pLJR965 and to Michael Niederweis for providing plasmid pMN437.

I am appreciative of the financing sources that made my doctoral studies feasible. I was fortunate to obtain the Georg & Agnes Blumenthal Stiftung in my finishing phase after being supported by the DAAD grant for my first four years.

The numerous friends and groups that I met throughout my stay at RKI, Berlin, helped to make it fun for me. I am appreciative of the FG16 division group at the RKI members who supported me and were always willing to assist. My stay was made unforgettable by the welcoming atmosphere that the lab members of our research team, Linus Fiedler, Anna Maria Oschmann, and Alexander Lüders, created. I'm grateful for the enjoyable times we had while working long hours and for our enjoyable excursions together.

Finally, I want to express my gratitude to my family for their support, love, and prayers. My parents, who encouraged me to pursue all my goals and instilled me a love for learning; for having my daughter Raya Akter stay with me for two years in Berlin. Most importantly, I'll never forget how God's grace enabled me to overcome every challenge and obstacle I encountered along this life's path.

Suriya Akter

9.3 Sources of funding-Funding Sources

The work was supported by DAAD Research Grants - Doctoral Programmes in Germany, 2017/18 and The Georg & Agnes Blumenthal Stiftung.

9.4 Conflicts of Interest

In the context of this work, there is no conflict of Interest due to financial support of the work.

10 Declaration of Independence

I hereby confirm that I have completed this work independently. I certify that I have only used the sources and aids indicated.

Berlin, 12.01.2024
Suriya Akter

9 783967 292374

mbvberlin mensch und buch verlag

49,90 Euro | ISBN: 978-3-96729-237-4